The role of subcellular plant carbohydrate metabolism in heat response and acclimation

Dissertation

der Fakultät für Biologie

der Ludwig-Maximilans-Universität München

zur Erlangung des Grades eines Doktors der Naturwissenschaften

Vorgelegt von

Charlotte Seydel

21. November 2025

Diese Dissertation wurde angefertigt
unter der Leitung von Prof. Dr. Thomas Nägele an der Fakultät für Biologie
an der Ludwig-Maximilians-Universität München

Erstgutachter: Prof. Dr. Thomas Nägele

Zweitgutachter: Prof. Dr. Martin Heß

Tag der Abgabe: 21.11.2025

Tag der mündlichen Prüfung: 17.02.2026

Statutory declaration and statement

Erklärung
Declaration

Hiermit erkläre ich, *
Hereby I declare

☒ dass die Dissertation nicht ganz oder in wesentlichen Teilen einer anderen Prüfungskommission vorgelegt worden ist.
that this work, complete or in parts, has not yet been submitted to another examination institution

☒ dass ich mich anderweitig einer Doktorprüfung ohne Erfolg **nicht** unterzogen habe.
*that I did **not** undergo another doctoral examination without success*

☐ dass ich mich mit Erfolg der Doktorprüfung im Hauptfach
that I successfully completed a doctoral examination in the main subject

und in den Nebenfächern
and in the minor subjects

bei der Fakultät für
at the faculty of _____

der
at _____
(Hochschule/*University*)

unterzogen habe.

☐ dass ich ohne Erfolg versucht habe, eine Dissertation einzureichen oder mich der Doktorprüfung zu unterziehen.
that I submitted a thesis or did undergo a doctoral examination without success

Munich, 21.11.2025 — Charlotte Seydel

Ort, Datum/*place, date* — Unterschrift/*signature*

*) Nichtzutreffendes streichen/
delete where not applicable

Eigenständigkeitserklärung

Hiermit versichere ich an Eides statt, dass die vorliegende Dissertation mit dem Titel

_____

von mir selbstständig verfasst wurde und dass keine anderen als die angegebenen Quellen und Hilfsmittel benutzt wurden. Die Stellen der Arbeit, die anderen Werken dem Wortlaut oder dem Sinne nach entnommen sind, wurden in jedem Fall unter Angabe der Quellen (einschließlich des World Wide Web und anderer elektronischer Text- und Datensammlungen) kenntlich gemacht. Weiterhin wurden alle Teile der Arbeit, die mit Hilfe von Werkzeugen der künstlichen Intelligenz de novo generiert wurden, durch Fußnote/Anmerkung an den entsprechenden Stellen kenntlich gemacht und die verwendeten Werkzeuge der künstlichen Intelligenz gelistet. Die genutzten Prompts befinden sich im Anhang. Diese Erklärung gilt für alle in der Arbeit enthaltenen Texte, Graphiken, Zeichnungen, Kartenskizzen und bildliche Darstellungen.

Munich, 21.11.2025

(Ort / Datum)

Charlotte Seydel — Charlotte Seydel

(Vor und Nachname in Druckbuchstaben) (Unterschrift)

Affidavit

Herewith I certify under oath that I wrote the accompanying Dissertation myself.

Title: _____

In the thesis no other sources and aids have been used than those indicated. The passages of the thesis that are taken in wording or meaning from other sources have been marked with an indication of the sources (including the World Wide Web and other electronic text and data collections). Furthermore, all parts of the thesis that were de novo generated with the help of artificial intelligence tools were identified by footnotes/annotations at the appropriate places and the artificial intelligence tools used were listed. The prompts used were listed in the appendix. This statement applies to all text, graphics, drawings, sketch maps, and pictorial representations contained in the Work.

Munich, 21.11.2025

(Location/date)

Charlotte Seydel — Charlotte Seydel

(First and last name in block letters) (Signature)

Regeln für den Einsatz von Werkzeugen der Künstlichen Intelligenz (KI) für prüfungsrelevante Tätigkeiten

1. Der Einsatz von KI-Werkzeugen für prüfungsrelevante Leistungen ist möglich.

2. Der Einsatz von KI-Werkzeugen zur Optimierung, Übersetzung, Korrektur von Rechtschreibung und Grammatik von selbstgenerierten Texten und zur Optimierung von Designaspekten selbstgenerierter Abbildungen ist ohne Kennzeichnung zulässig.

3. Von KI-Werkzeugen de novo generierte und in der Arbeit verwendete Textabschnitte und Abbildungen sind durch Fußnoten/Anmerkungen an den entsprechenden Stellen deutlich zu kennzeichnen und das KI-Tool ist analog zu Literaturquellen anzugeben. Die verwendeten Prompts sind im Anhang zu listen.

4. Textabschnitte, die durch den iterativen Einsatz von KI-Tools erzeugt wurden, sind zu kennzeichnen.

5. Die Autorin / der Autor ist für die Korrektheit und korrekte Darstellung in schriftlichen Leistungen und Präsentationen verantwortlich.

6. Quellen / Referenzen müssen nach den Regeln der guten wissenschaftlichen Praxis zitiert werden.

Rules for the use of artificial intelligence (AI) tools for examination-relevant activities

1. The use of AI tools for examination-relevant performances is possible.

2. The use of AI tools to optimize, translate and correct the spelling and grammar of self-generated texts and to optimize self-generated illustrations is permitted without indication.

3. Text sections and illustrations de novo generated by AI tools and used in the thesis must be clearly marked by footnotes/annotations at the appropriate places and the AI tool must be indicated analogously to literature sources. The prompts used have to be listed in the appendix.

4. Sections of the text generated through iterative use of AI tools should be marked.

5. The author is responsible for the correctness and proper presentation in written performances and presentations.

6. Sources / references must be cited in accordance with the rules of good scientific practice.

Contents

Abbreviations

Abbreviation	Definition
2D/ 3D	two-/ three-dimensional
Acetyl-CoA	Acetyl coenzyme A
ATP	Adenosine triphosphate
ADP	Adenosine diphosphate
$BE_{1/2}$	Balance equation 1/ 2
CBBC	Calvin-Benson-Bassham cycle
Col-0	Columbia-0
(v)EM	(Volume) electron microscope/ microscopy
ERDL	Early Response to Dehydration Like
ESL	Early Response to Dehydration Six-Like
ETC	Electron transport chain
ETR	Electron transport rate
F6P	Fructose-6-phosphate
FP	Fourier polynomial
Frc	Fructose
F_v/F_m	Maximum quantum yield of photosystem II
G6P	Glucose-6-phosphate
GEM	Genome-scale metabolic model
Glc	Glucose
HexP	Hexose phosphate
Inv_a	Acidic invertase
Inv_{cw}	Cell wall invertase
Inv_n	Neutral invertase
Inv_p	Plastidic invertase
NADP(H)	Nicotinamide adenine dinucleotide phosphate
NAF	Non-aqueous fractionation
NPS	Net photosynthesis
ODE	Ordinary differential equation
PDE	Partial differential equation
PGM	Phosphoglucomutase

Abbreviation	Definition
PHYB	Phytochrome B
PSI/ PSII	Photosystem I/ II
RFO	Raffinose family oligosaccharide
RNA	Ribonucleic acid
ROS	Reactive oxygen species
Rubisco	Ribulose-1,5-bisphosphate carboxylase/ oxygenase
S6P	Sucrose-6-phosphate
SAST	Senescence-Associated Sugar Transporter
SBF-SEM	Serial block-face scanning electron microscope/ microscopy
SEM	Scanning electron microscope/ microscopy
SPP	Sucrose phosphate phosphatase
SPS(A1)	Sucrose phosphate synthase (A1)
Suc	Sucrose
SUC4	Sucrose transporter 4
SWEET	Sugars Will Eventually be Exported Transporter
TCA cycle	Tricarboxylic acid cycle
TEM	Transmission electron microscope/ microscopy
Triose-P	Triose phosphates
TST	Tonoplast Sugar Transporter
UDPG	Uridine diphosphate glucose
VGT	Vacuolar glucose transporter

List of publications and contribution as co-author

All articles being published throughout the doctoral studies are collected in the following section. Contributions of Charlotte Seydel are underscored and highlighted in bold.

Seydel, C., Biener, J., Brodsky, V., Eberlein, S., & Nägele, T. (2022a). Predicting plant growth response under fluctuating temperature by carbon balance modelling. Commun Biol, 5(1), 164

> **C.S.**, J.B., V.B., S.E., and T.N. performed experiments. **C.S.** and T.N. performed statistics and modelling and wrote the paper. All authors approved the paper.

Seydel, C., Kitashova, A., Fürtauer, L., & Nägele, T. (2022b). Temperature-induced dynamics of plant carbohydrate metabolism. Physiol Plant, 174(1), e13602

> **C.S.** and A.K. contributed equally to writing and illustrating this review. A declaration of contribution as co-authors can be found at the end of this chapter. L.F. contributed to writing the paragraph on low temperature perception and regulation. T.N. conceived and wrote the review. All authors wrote and approved the review.

Vicente, A. M., Manavski, N., Rohn, P. T., Schmid, L. M., Garcia-Molina, A., Leister, D., Seydel, C., Bellin, L., Mohlmann, T., Ammann, G., Kaiser, S., & Meurer, J. (2023). The plant cytosolic m(6)a rna methylome stabilizes photosynthesis in the cold. Plant Commun, 4(6), 100634

> A.M.V., N.M., L.-M.S., P.T.R., **C.S.**, L.B., G.A., A.G.-M., and J.M. performed the research. A.M.V., N.M., T.M., D.L., S.K., and J.M. analysed the data. A.M.V. and J.M. designed the work and wrote the article with the contribution of all coauthors.

Hernandez, J. S., Dziubek, D., Schröder, L., Seydel, C., Kitashova, A., Brodsky, V., & Nägele, T. (2023). Natural variation of temperature acclimation of arabidopsis thaliana. Physiol Plant, 175(6), e14106

> J.H. performed experiments and data evaluation, developed the R app (NAFalyzer) and wrote the paper. D.D. performed experiments and supported data evaluation. L.S., **C.S.** and A.K. performed experiments. V.B. developed the R app (NAFalyzer). T.N. conceived the study, supported data evaluation and wrote the paper.

Ries, F., Gorlt, J., Kaiser, S., Scherer, V., Seydel, C., Nguyen, S., Klingl, A., Legen, J., Schmitz-Linneweber, C., Plaggenborg, H., Ng, J. Z. Y., Wiens, D., Hochberg, G. K. A., Raschle, M., Mohlmann, T., Scheuring, D., & Willmund, F. (2025). A truncated variant of the ribosome-associated trigger factor specifically contributes to plant chloroplast ribosome biogenesis. Nat Commun, 16(1), 629

F.R. performed and/or designed most of the experiments and wrote parts of the manuscript, J.G., S.N., S.K., V.S., H.P., and T.M. performed phenotypic analyses and created *Arabidopsis* lines. **C.S.** and A.K. conducted electron microscopy analyses and analysed data. J.L. and C.S.L. performed northern blot analyses and immunofluorescence. J.Z.Y.N., D.W., and G.K.A.H performed phylogeny and part of the AlphaFold prediction. M.R. did proteomic measurements. D.S. helped with mutant analyses, line generation and performed microscopy. F.W. designed experiments, analysed data, and wrote the manuscript.

Seydel, C., Heß, M., Schröder, L., Klingl, A., & Nägele, T. (2025). Subcellular plant carbohydrate metabolism under elevated temperature. Plant Physiol

C.S. performed leakage and PAM assay, NAF analysis, microscopy, data analysis, and wrote the paper. M.H. performed SBF-SEM microscopy. L.S. quantified enzyme activities. A.K. supervised and supported microscopy. T.N. conceived the study, analysed data, developed the R Shiny app, and wrote the paper.

Abstract

During exposure to elevated temperatures, plants employ various mechanisms to survive and maintain cellular functions, ultimately leading to increased thermotolerance. Heat affects membrane integrity, protein function, enzyme activity and transport processes, impacting photosynthesis and the primary carbohydrate metabolism. To adjust to the environmental conditions, plants regulate their metabolism to stabilise growth and development. Especially photosynthesis and the metabolism of carbohydrates, which are primary products of photosynthetic CO_2 fixation, need to be adjusted to prevent irreversible tissue damage.

The metabolic and photosynthetic response to transient heat exposure of differing severity was quantified in *Arabidopsis thaliana* accession Columbia-0 (Col-0), and two mutants deficient in enzyme activities of starch and sucrose biosynthesis, plastidial Phosphoglucomutase (PGM1) and Sucrose Phosphate Synthase A1 (SPSA1), respectively. A mathematical carbon balance model utilising Fourier polynomials was employed to analyse underlying dynamics of net carbon fluxes. Integrals and derivatives of the Fourier polynomials revealed a stabilising role of a lowered activity of SPS during transient heat exposure.

To further understand the effect of carbohydrates on heat response, the acclimation of *Arabidopsis* to elevated temperatures was analysed. Wild type Col-0 plants before and after 7 days of acclimation to heat, ranging from moderate to severe, were analysed by photosynthesis and electrolyte leakage measurements to assess their acclimation capability. Across a temperature range from 22°C to 40°C, it was found that *Arabidopsis* most efficiently increases its heat tolerance during acclimation at 34°C. Leaf tissue of non-acclimated and acclimated plants was analysed using the non-aqueous fractionation (NAF) technique, which enabled the quantification of subcellular sugar distribution. Ultrastructural 3D measurements by serial block-face scanning electron microscopy (SBF-SEM) resolved compartment volumes, which enabled estimations of effective sugar concentrations. The compartment-specific concentrations of the three sugars sucrose, glucose and fructose were quantified for vacuole, cytosol and chloroplasts. In acclimated plants, cytosolic sucrose levels were stabilised by shifting invertase-catalysed sucrose cleavage into the vacuole. Further, glucose and fructose concentrations were observed to peak in the cytosol of acclimated plants, indicating a heat-induced deregulation of dissimilatory pathways, e.g., glycolysis.

In summary, it is hypothesised that a coordinate heat response of sucrose transport into the vacuole and a hexose-induced inhibition of sucrose cleavage in the cytosol stabilises carbohydrate metabolism and photosynthesis.

Zusammenfassung

Pflanzen haben eine Vielzahl an zellulären Mechanismen entwickelt, um sich an erhöhte Temperaturen anzupassen. Hitze beeinträchtigt die Zusammensetzung und Funktion zellulärer Membransysteme, sowie die Funktion von Proteinen und Enzymen, die sowohl die Photosynthese als auch den Kohlenhydratstoffwechsel beeinflussen können. Um sich an dynamische Umweltbedingungen anzupassen, regulieren Pflanzen ihren Stoffwechsel, um Wachstum und Entwicklung zu stabilisieren und um irreversiblen Gewebeschaden abzuwenden.

In der vorliegenden Arbeit wurden Photosynthese und Kohlenhydratstoffwechsel in *Arabidopsis thaliana* während transient auftretender Hitzewellen untersucht. Dafür wurden Mutanten im genetischen Hintergrund der Akzession Columbia-0 (Col-0) analysiert, die entweder eine verringerte Aktivität der plastidären Phosphoglucomutase (PGM1) oder der cytosolischen Saccharose-Phosphat-Synthase A1 (SPSA1) aufwiesen. Ein mathematisches Bilanzmodell wurde unter Einbindung von Fourierpolynomen verwendet, um zugrundeliegende Dynamiken des Netto-Kohlenstoffflusses zu analysieren. Mit Hilfe von Integralen und Ableitungen der Polynome konnte ein stabilisierender Effekt von verminderter SPS-Aktivität während einer Hitzewelle aufgezeigt werden.

Um die Bedeutung des pflanzlichen Kohlenhydratstoffwechsels für die Anpassung an Hitze zu untersuchen, wurden Pflanzen der Akzession Col-0 zunächst vor und nach Hitzeakklimatisierung auf ihre Toleranz untersucht. Hierbei zeigte sich ein Optimum der Hitzeakklimatisierung bei 34°C über einen Zeitraum von sieben Tagen. Durch nichtwässrige Fraktionierung (NAF) wurden kompartimentspezifische Zuckerkonzentrationen ermittelt, unterstützt durch ultrastrukturelle 3D-Analysen mittels serieller Rasterelektronenmikroskopie (serial block-face scanning electron microscopy, SBF-SEM). In akklimatisierten Pflanzen zeigte sich eine stabilisierte Saccharosekonzentration, die in einem kinetischen Modell durch Verlagerung Invertase-katalysierter Saccharosehydrolyse aus dem Cytosol in die Vakuole erklärt wurde. Zudem stiegen die cytosolischen Konzentrationen der Hydrolyseprodukte Glukose und Fruktose in hitzeakklimatisierten Pflanzen deutlich an, was möglicherweise auf eine Regulation dissimilatorischer Stoffwechselwege, wie beispielsweise der Glykolyse, hindeutet.

Zusammenfassend lassen diese Befunde darauf schließen, dass die Stabilisierung der cytosolischen Saccharosekonzentration eine zentrale Rolle bei der Anpassung von Photosynthese und Stoffwechsel an erhöhte Umgebungstemperaturen spielt. Dabei scheint der Transport von Saccharose in die Vakuole an eine Hexose-vermittelte Produktinhibition der cytosolischen Saccharosespaltung gekoppelt zu sein.

1. Introduction

1.1. Elevated temperature – a challenge for plants

With climate change progressing, many organisms on Earth will be challenged to survive the ensuing changes to their habitat. From extreme weather events to precipitation and temperature, the changes can be manifold and encompass the entire globe. Changing climate already impacts agriculture and non-agricultural ecosystems alike and contributes to yield loss, insufficient food security, and to extinction of habitats and species (Lippmann et al., 2019; Gampe et al., 2021; Kumar et al., 2022; IPCC, 2023). Those problems will progress further, and many of the impacted organisms are already unable to fully compensate for the changing conditions by migration or other means (Thuiller et al., 2005; Wilczek et al., 2014; IPCC, 2023). One step in dealing with this global crisis is to understand the processes involved in it in order to take steps in alleviating the negative effects. A prominent symptom of climate change is the rise of annual mean temperature and the increasing number of high temperature extremes, such as heatwaves, being observed across the globe since the 1950s. As global mean temperatures have already risen 1.5°C above pre-industrial levels, a further increase of 1°C to 3.5°C is predicted to occur by the end of the 21st century (IPCC, 2023).

The response and survival of plants during elevated temperature differs greatly depending on the specific temperature resilience of a species, the severity of the heat, the duration of the temperature exposure, combination with other stresses and previously acquired thermotolerance (Mittler et al., 2012; Zhu et al., 2018; Xalxo et al., 2020; Samtani et al., 2022; Neuner & Buchner, 2023; Jiang et al., 2024). In general, a temperature rise to between 10°C and 15°C above the growth optimum can be considered heat stress (Wahid et al., 2007). Under natural growth conditions, a change in temperature is the norm for plants. The model organism *Arabidopsis thaliana* mostly grows in temperate zones, where, during the course of the day, temperature transiently increases and decreases, leading to a highly dynamic environment (see example given in Figure 1A). In temperate climate, also annual temperature fluctuations can easily span 20°C (see Figure 1B for reference). This shows the enormous variability in growth temperature that plants experience, even without taking into account the increasing occurrences of temperature extremes due to climate change. The capability to cope with those fluctuations is integral for plant survival.

When temperatures increase moderately above the optimum, the plants are able to continue growing and adjust physiological processes to maintain the equilibrium of their cellular reactions. They have to adjust for a change in the thermodynamics and structures of proteins, RNA

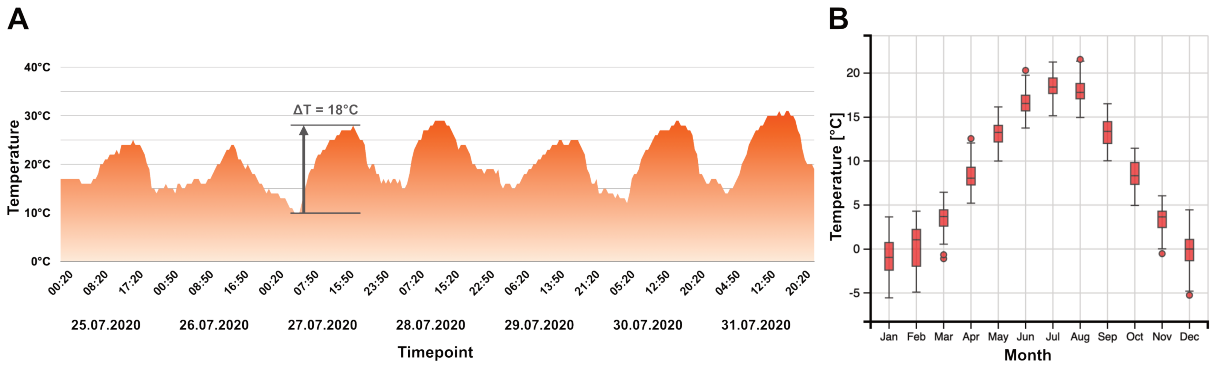

Figure 1. A: Temperatures recorded in 30-minute increments over the course of one week in July 2020 in Munich, Germany. The corresponding data is collected in Supplementary Table I. Exemplary temperature difference ΔT is indicated with a grey arrow. Data source: https://www.timeanddate.com/weather/germany/munich/historic?month=7&year=2020, accessed 25.03.2022. B: Distribution plot of mean monthly temperatures of the last 30 years (1992-2022) from the weather station in Kocelovice, Czech Republic, 49.47°N, 13.83°E, Elevation 521m, climate classification Cfb (warm temperate climate, fully humid, with warm summers) after Kottek et al. (2006). Chart created with ClimateCharts.net (Zepner et al., 2020), data provided by the Global Historical Climatology Network (https://www.ncdc.noaa.gov/ghcnm/).

species, components of the cytoskeleton and enzymatic reactions, as well as membrane fluidity, impacting membrane transport (Ruelland & Zachowski, 2010; Mittler et al., 2012). The severity of the temperature change is important for the response it elicits. Mild warming just a few degrees over the optimal growth temperature (for *Arabidopsis* 24°C to 30°C) is sensed by the photoreceptor Phytochrome B (PHYB) and leads to thermomorphogenesis, a growth response entailing hypocotyl elongation and early flowering (Jung et al., 2016; Samtani et al., 2022; Distéfano et al., 2024). Higher temperatures, between 30°C and 40°C, cause a change in membrane fluidity and the permeability of calcium channels, triggering calcium signalling cascades. The following responses encompass a heat shock response, aimed at protecting the organism from heat-induced damage, as well as a change in growth and development. Eventually, the plant can develop thermotolerance to deal with the increased ambient temperature. At over 40°C, extensive damage occurs, such as misfolded and denatured proteins, as well as lipid peroxidation, ultimately concluding in cell death (Samtani et al., 2022; Distéfano et al., 2024). A distinction between warming and heating can also be made based on the differentially induced genes during mild and more extreme temperature treatment at 27°C and 37°C, respectively (Mittler et al., 2012). But not only the temperature itself can impact the response of plants. It is also critical to observe the duration of the heat exposure, taking into account the heat dose. It was shown that in five alpine species and two Australian desert trees, increased heat duration lowered the threshold temperature for heat-induced damage to photosystem II (PSII) (Neuner & Buchner, 2023; Cook et al., 2024).

1.2. The importance of photosynthesis and carbohydrate metabolism for heat stress survival

In photoautotrophic organisms, growth and development depend on the availability of carbon in the form of carbohydrates and energy in the form of ATP and NADPH. Sugars are not only important as a source of energy, but also play central roles in signalling, influence germination and growth, can act as osmoprotectants, and are important precursors for polysaccharides such as cellulose and starch (Xalxo et al., 2020). Thus, photosynthesis and CO_2 fixation, as well as the downstream synthesis of carbohydrates, are of central importance for the survival of plants under adverse conditions (Herrmann et al., 2019). Increased energy requirements during a prolonged period of elevated temperature can also cause problems for the plant, like carbon depletion, especially during the night, and a decrease in net photosynthesis, carbon assimilation and biomass accumulation (Vasseur et al., 2011; Prasch & Sonnewald, 2013; Sharmin et al., 2013).

1.2.1. Photosynthesis and CO_2 uptake during heat exposure

Photosynthesis needs to be stabilised in the face of increasing temperatures, as it is the main energy source of the plant and can be severely affected by heat. Elevated temperatures can decrease the net photosynthetic rate and CO_2 uptake by impacting electron transport, the integrity of the photosystems, Rubisco activity, chlorophyll content and generation of reactive oxygen species (ROS) (Yamori et al., 2014; Ali et al., 2020; Sharma et al., 2020; Firmansyah & Argosubekti, 2020; Jagadish, 2020). Also, proteins involved in carbon assimilation and photosynthesis were found to be downregulated during the first 24 hours of heat exposure in soybean (Ahsan et al., 2010). Generally, the effects of heat on plant photosynthesis and CO_2 assimilation differ depending on the intensity of the heat. As long as the proteins of the photosynthetic apparatus are not denatured by extreme heat, there are several mechanisms compensating for the problems of elevated temperature, facilitating survival during such adverse conditions. Those problems are mostly an increased fluidity of the thylakoid membranes, leading to increased proton leakiness and a possible dislocation of PS II light-harvesting complexes, a reduced Rubisco activation state, stability of proteins and membranes and the higher temperature optimum of respiration, changing the balance between photosynthesis and respiration (Yamori et al., 2014; Sharma et al., 2020).

Temperatures between 35°C and 45°C can cause an increase in proton permeability of the thylakoid membranes, which impairs the connection between ATP synthesis and electron transport (Sharkey, 2005). However, it can be compensated for by an increase in cyclic electron

flux around PS I, allowing for unimpeded ATP synthesis and maintaining the energy gradient across the thylakoid membranes (Havaux, 1996; Bukhov et al., 1999, 2000; Yamori et al., 2014; Sharma et al., 2020). The proteins of PS II can not be damaged by moderate heat, as they only denature at temperatures of 45°C and above. Below this threshold, photosynthesis is rather limited within the Calvin-Benson-Bassham cycle (CBBC) by an inadequate Rubisco activation state. The speed of Rubisco deactivation can not be compensated by Rubisco activase, as its activity is decreasing due to heat, leading to a lower amount of active Rubisco (Law & Crafts-Brandner, 1999; Crafts-Brandner & Salvucci, 2000; Salvucci & Crafts-Brandner, 2004; Kumar et al., 2009; Yamori et al., 2014). Some species, for example spinach, can produce another isoform of Rubisco activase when they are subjected to elevated temperatures, increasing the thermostability of the enzyme, which results in higher amounts of active Rubisco during heat exposure and buffers the heat-induced decrease of photosynthetic efficiency (Crafts-Brandner et al., 1997; Yamori et al., 2014). Another limitation of the photosynthetic process due to heat is introduced by an increase in photorespiration, as the solubility of CO_2 decreases and Rubisco loses specificity to CO_2. This in turn favours oxygenation over carboxylation (Long, 1991). However, an increase in CO_2 levels was shown to counteract this process, leading to increased heat tolerance in several C_3 plants such as *Pisum sativum, Triticum aestivum* and *Glycine max* (Wang et al., 2008). It has also been shown that heat can impair the efficiency of light absorption by PS I and II by decreasing chlorophyll accumulation, either caused by lower biosynthesis due to damaged enzymes, by expedited degradation of the pigment, or a combination of both (Ashraf & Harris, 2013). Even though the light reaction of photosynthesis might not be impacted as severely during moderate heat below 35°C, the final rate of carbon fixation and many following steps of carbohydrate metabolism are affected. During prolonged heat exposure, it was observed that less biomass accumulated due to a reduced rate of net photosynthesis and carbon assimilation (Vasseur et al., 2011; Prasch & Sonnewald, 2013).

1.2.2. Carbohydrate metabolism during heat exposure

Various processes of the carbohydrate metabolism are impacted by heat. It has been shown that in soy bean, 15% of heat-responsive proteins are associated with the carbon and carbohydrate metabolism (Ahsan et al., 2010). In *Arabidopsis*, over 140 metabolites were identified that showed a response to increased temperatures, 85 of them showing either transient or lasting increase or decrease during treatment with 40°C, often within the first 30 minutes of heat exposure (Kaplan et al., 2004). This work focuses on the metabolism of the central carbohydrates starch, as the primary storage form of assimilated carbon, as well as the soluble sugars sucrose, glucose and fructose. When CO_2 is assimilated, it is stored as transitory starch in the chloroplast or exported either as maltose or as triose phosphates into the cytosol (see figure 2).

There, the triose phosphates are converted to hexose phosphates that, in turn, are the precursors for sucrose, whereas maltose is broken down into glucose. Sucrose can be imported into the vacuole and is converted to glucose and fructose either in the vacuole or in the cytosol. Hexoses can also be phosphorylated to hexose phosphates in the cytosol, closing the cyclic structure of cellular sucrose synthesis and breakdown. Transport processes of sucrose, glucose and fructose over the vacuolar membrane are helpful for keeping concentrations balanced according to the physiological requirements (Stitt et al., 2010; Nägele & Heyer, 2013; Kitashova et al., 2021; Nägele, 2022). Additionally, sucrose is imported into the chloroplast and the subsequent degradation into hexoses there is catalysed by plastidic invertase (Vargas et al., 2008; Nägele & Heyer, 2013).

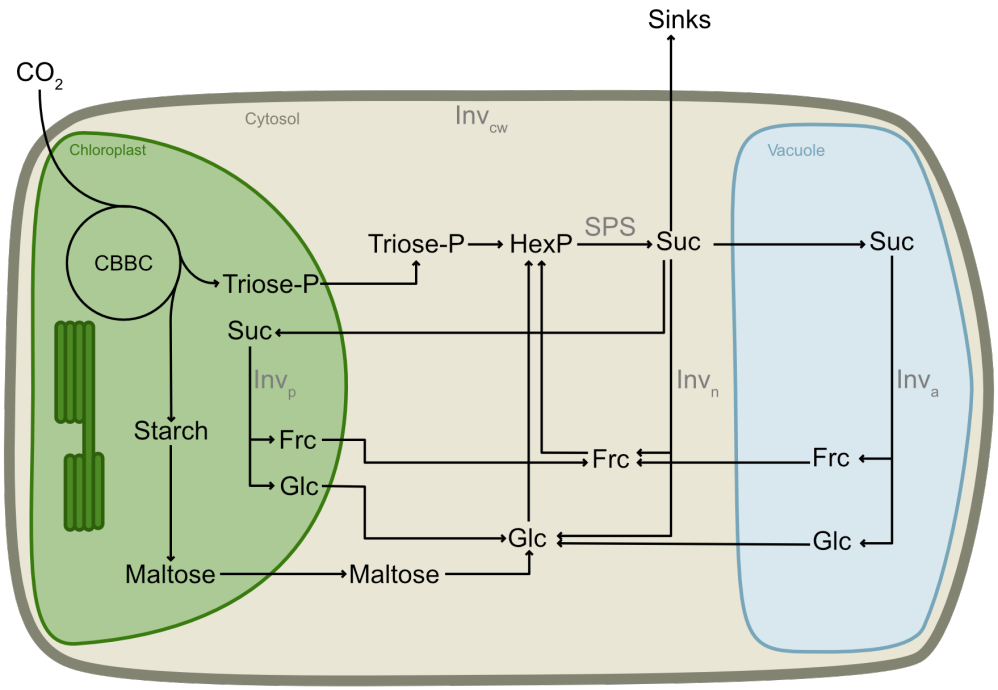

Figure 2. Simplified schematic overview of the central carbohydrate metabolism in leaf mesophyll cells of *Arabidopsis*. Substrates and products are written in black, enzymes are written in grey, CBBC: Calvin-Benson-Bassham cycle, Frc: fructose, Glc: glucose, HexP: hexose phosphates, Inv_a: acidic (vacuolar) invertase, Inv_{cw}: cell wall (apoplastic, acidic) invertase, Inv_n: neutral (cytosolic) invertase, Inv_p: plastidic invertase, SPS: sucrose phosphate synthase, Suc: sucrose, Triose-P: triose phosphates.

The high complexity of the carbohydrate metabolism has led to varying observations of metabolic heat response, especially when considering different timeframes of heat exposure. In a study by Kaplan et al. (2004), carbohydrates such as hexoses and sucrose, as well as organic and amino acid levels were found to increase during 40°C treatment of up to 4 hours. However, when heat exposure is prolonged to several days, mostly at more moderate temperatures, dif-

ferent studies document contradicting findings. Exposure to moderate heat between 32°C and 34°C for 3 to 7 days quite consistently lead to accumulation of sucrose in *Arabidopsis* (Prasch & Sonnewald, 2013; Atanasov et al., 2020; Hernandez et al., 2023), but hexoses were reported to decrease in one study during an exposure to 34°C for 7 days (Hernandez et al., 2023), whereas in several other studies, glucose was reported to increase during exposure to 32°C for 3 to 7 days (Prasch & Sonnewald, 2013; Atanasov et al., 2020; Garcia-Molina et al., 2020). When analysing a shared pool of sucrose, glucose and fructose after 3 days of 30°C treatment, a decrease was reported (Vasseur et al., 2011), and in cereals, a 14-day temperature treatment of 30°C/ 27°C day/ night temperature resulted in a decrease of both sucrose and hexoses (Janda et al., 2021). Independent of the exact duration and severity of the applied heat, a stark drop in starch content was reported consistently (Vasseur et al., 2011; Atanasov et al., 2020; Hernandez et al., 2023). This decrease is most likely caused by the inhibition of starch synthesis and the enzyme ADP-glucose pyrophosphorylase at temperatures above 30°C, as opposed to an increased rate of starch degradation (Geigenberger et al., 1998; Awasthi et al., 2014). Invertases, responsible for cleaving sucrose, are also exhibiting changes due to heat. Transcripts of cell wall invertase were downregulated, whereas transcripts of vacuolar and cytosolic invertase were upregulated after 3 days of 32°C in one study (Prasch & Sonnewald, 2013). On the other hand, the activity of cytosolic and cell wall invertase was increased after 7 days of 32°C or 34°C, whereas vacuolar invertase activity only increased in one natural accession of *Arabidopsis* from the Cape Verde Islands, Cvi-0 (Atanasov et al., 2020; Hernandez et al., 2023). However, the activity that is measured *in vitro* can not always be assumed *in vivo*, as there is feedback-inhibition by the cleavage products glucose and fructose (Sturm, 1999; Nägele et al., 2010). Other findings also hint towards an importance of sucrose levels in heat response. It was shown that sucrose is important for thermomemory at the shoot apical meristem of *Arabidopsis* (Olas et al., 2021) and supplementing growth media with sucrose led to increased survival of *Arabidopsis* seedlings subjected to 37°C for several days (Reichelt et al., 2023). Sucrose allocation played an important role in heat tolerance in tomato flowers and fruit, showing a contribution of invertases to heat tolerance by increasing sink strength and sugar signalling activity (Li et al., 2012). But also external glucose application led to increased thermotolerance in tomato (Wang et al., 2024), and soluble sugars are hypothesised to play a role in ROS scavenging (Morelli et al., 2003).

1.3. Mathematical modelling of metabolic networks

Describing dynamics of metabolism represents a challenging task. A rapid methodological development in experimental high-throughput analysis during the last two decades has enabled the simultaneous detection and quantification of hundreds to thousands of transcripts, proteins

and metabolites. As a consequence, it has become apparent that the analysis of such high-dimensional datasets needs to be supported by computational routines. In systems biology, a central tool to combine and analyse information about biological networks is mathematical description and computational simulation. It has been in use for many years and was applied in various fields of biological study, ranging from describing unicellular organisms in the field of microbiology (Arkin et al., 1998; Fang et al., 2017; Lopatkin & Collins, 2020) to complex multicellular lifeforms (Nägele et al., 2010; Sweetlove & Ratcliffe, 2011; Nägele, 2022; Adler et al., 2025).

A mathematical model can be utilised to simulate and predict the behaviour of the experimentally analysed system under dynamic environmental conditions. But when a complex and multifaceted biological system is represented that way, it can hardly be described in its entirety. The manifold interconnections of systems within an organism are of such a diverse nature that an accurate, holistic depiction is not possible with current experimental and computational methods. Thus, the complexity of those systems needs to be reduced in a way that still allows for a description of the biological circumstances without compromising too much of the accuracy. Sometimes, it can even be beneficial to reduce the complexity of the model and optimise it to gather meaningful insights (Lopatkin & Collins, 2020). This reduction is mainly achieved by restricting the model to parts of the network that are relevant to the research question and then iteratively modelling, simulating network behaviour, and collecting experimental evidence (Nägele & Weckwerth, 2012; Rohwer, 2012).

In a kinetic model, ordinary differential equations (ODEs) or partial differential equations (PDEs) are used to describe and predict time-dependent dynamics of metabolism. It is well suited to describe changes over time in complex systems, but requires a lot of detailed biochemical information that needs to be determined experimentally and in a statistically sound way, such as substrate and product concentrations, reaction velocity of involved enzymes at substrate saturation, substrate affinities, and inhibitory processes (Nägele & Weckwerth, 2012; Rohwer, 2012; Nägele et al., 2016). If determination of those parameters is not possible in a study, they need to be estimated based on published values from different organisms or conditions, introducing a source of uncertainty into the model (Schaber et al., 2009). However, despite such uncertainties, kinetic modelling was instrumental in elucidating details about plant metabolism, e.g. finding a connection between starch and flavonoid metabolism and the photorespiratory pathway (Hernandez & Nägele, 2022; Kitashova et al., 2023; Adler et al., 2025).

In contrast to kinetic modelling, structural modelling does not require exact enzyme kinetic parameters but rather describes a reaction network with its stochiometrics, assuming a steady state for all involved reactions (Rohwer, 2012; Töpfer, 2021). Some flux modes in the tricarboxylic acid (TCA) cycle were described with the help of metabolic flux analysis, a modelling approach

where radioactive isotopes are introduced into the system and the resulting compounds are then analysed for occurrence of this isotope. The flux of the carbon through the observed system can then be described by ODEs (Sweetlove & Ratcliffe, 2011; Rohwer, 2012; Basler et al., 2018; Rao & Liu, 2025). Flux balance analysis focuses on characterising a network based on the stochiometrics of a system and how the different pools of compounds can be balanced without quantifying enzyme kinetics. It has been used to model reaction fluxes in developing rice leaves on a genome scale (Poolman et al., 2013), or interactions between bundle sheath and mesophyll cells in maize (Simons et al., 2014). Additionally, it was instrumental in development of an extensive model of *Arabidopsis* that encompassed different tissues and a day-night cycle to analyse leaf and root growth during carbon or nitrogen-limited conditions (Cheung et al., 2014; Shaw & Cheung, 2018). Whichever approach is used for describing metabolic networks, the success of the final modelling depends not only on the choice of a fitting mathematical description of the dynamic processes in the network, but also on the modelling approach being suitable for the available experimental evidence, correct assumptions about network architecture and adequate experimental validation.

1.4. Subcellular compartmentation

The study of metabolism in eukaryotes is complicated by the high degree of cellular compartmentation. When researching processes within the plant cell, such as metabolic reactions, it is crucial to consider the spatial separation of those processes. This enables the simultaneous activity of metabolic pathways that use the same substrate, and the differential compartmentation avoids competition for those compounds. Such kind of optimisation, however, is also necessitating tight regulation of concentration gradients, maintaining stable pH milieus and establishing transport and shuttle processes of metabolites, proteins and signalling components over several lipid bilayers. Not only pH and osmolarity, but also the supply of substrate, the abundance of proteins and enzymes, and the export of the product are essential to sustain the complex reactions within the compartment, as well as the separation of toxic byproducts (Lunn, 2007; Linka & Weber, 2010). In plants, compartmentation is even more complex than in other eukaryotic cells. New components to cellular organisation are introduced, such as the cell wall and the vacuole, and an increased variety of metabolic pathways. Also, a second organelle of endosymbiotic origin, the plastid, is incorporated into the cell (Lunn, 2007).

The plastid still possesses bacterial components that are tightly incorporated into the eukaryotic cell due to coevolution of the nuclear and plastidial genomes. It can be considered a semi-autonomous organelle, having retained some properties from its cyanobacterial predecessor, but additionally having adapted and incorporated various elements of its host. The plastid possesses

remnants of the genome, as well as transcription and translation machinery of its ancestor, for example, the ribosomes, which share characteristics with bacterial ribosomes, or a bacterial-type RNA polymerase in the chloroplast transcription machinery (Barkan, 2011; Sun & Guo, 2016). But those components do not stand alone. They are rather tightly intertwined, as can be observed in the electron transport chain, which is built up of multimeric complexes that are composed of nuclear- and organelle-encoded polypeptides (Pogson et al., 2008). This integration of the plastid into the plant cell requires information transfer between nucleus and plastid and vice versa, anterograde and retrograde signalling (Bräutigam et al., 2007).

But not only the connection between chloroplast and nucleus needs to work properly. Other compartments are also involved in signalling to and from the chloroplast, and are an integral part in stress response (Kleine et al., 2021). Signalling between chloroplasts and mitochondria, for example, is critical, as they are the two organelles responsible for energy metabolism. Communication between them ensures a stable energy balance, even under stressful conditions (Sun & Guo, 2016). Also, the mitochondrial metabolism is crucial for the functioning of photosynthesis, and photosynthesis, in turn, supplies the basis for respiration in the mitochondria. This reciprocal dependency is illustrated by several cases where mutation-induced mitochondrial malfunction led to chlorosis and problems with chloroplast biogenesis (Rhoads, 2011). To understand those complex and interlinked processes, all the intricate details ensuring the smooth operation of the metabolism need to be elucidated and connected. In addition to the chemical reactions that need to be considered, the (sub-)cellular architecture is of importance, too. Changes in organisation can hint towards changes in chemical reaction balances, importance of certain compounds and processes, and can be tied to impairment of the changed structures. Thus, it can yield important insights to bring together form and function of the different compartments.

1.4.1. Effect of heat on plant architecture and cellular ultrastructure

Heat affects the plant's architecture on many levels. On the whole plant level, a thermomorphogenic response can be observed from the first hours of heat application. This response is initiated by the light sensor PHYB sensing increased temperature by conformational change and inducing Phytochrome Interacting Factor 4, which in turn is activating other transcriptional regulators responsible for early flowering or hypocotyl elongation (Kumar et al., 2012; Jung et al., 2016; Ma et al., 2016). One hour after the onset of heat, rosette leaves are lifted to a more upright position, either in order to optimise photosynthesis, prevent heat accumulation by removing the leaves from heated earth or to promote cooling by increased transpiration (Koini et al., 2009; van Zanten et al., 2009; Vile et al., 2012). It was observed that, after 20 days of 30°C, fewer leaves were produced, whereas inflorescences were induced earlier, although

the quality of the flowers and seed pods was adversely affected by the heat (Vile et al., 2012). Cell size was reported to decrease during high temperatures, and stomata as well as trichomes were reported to increase in abundance (Wahid et al., 2012). Several processes responsible for growth are impacted by heat, such as activity of meristematic regions, differentiation of cells and elongation of the cell wall (Wahid et al., 2012).

When observing subcellular ultrastructure, chloroplasts are gravely impacted by severe heat, which has been extensively studied due to their central role in photosynthesis and plant physiology. Quite consistently throughout several studies, chloroplast swelling was reported after heat exposure in various species, being attributed to a higher membrane fluidity (Zhang et al., 2010; Grigorova et al., 2012; Zhang et al., 2014; Zou et al., 2017). The change in chloroplast size might influence ion concentration gradients between compartments and light scattering, reducing the absobance of green light by the leaf (Zhang et al., 2010). Thylakoids are known to be flexible and react to environmental cues, as the balance between light absorption and energy requirements needs to be optimised. The thylakoid grana were shown to be involved in this balancing by shrinking, unstacking, swelling, or accumulating more membrane material in response to stress (Kirchhoff, 2013). In *Arabidopsis*, as well as wucai (*Brassica campestris* ssp. *chinensis*) and tomato, thylakoids were reported to unstack in response to heat treatment and form fewer grana whilst increasing the count of discs in a granum (Zhang et al., 2010, 2014; Zou et al., 2017; Paul et al., 2020). However, a study in wheat reported a lowered number of discs per stack, whilst still reporting unstacking of thylakoid membranes (Grigorova et al., 2012). Plastoglobules were also consistently reported to change in high temperature conditions. They were reported to increase in number (Zhang et al., 2010; Grigorova et al., 2012; Zhang et al., 2014; Paul et al., 2020), and, sometimes additionally, in size (Zou et al., 2017). An increase in plastoglobule size and number is understood to be an indicator for many types of stress, such as drought, senescence, pathogens and toxicity (Staehelin, 1986; Arzac et al., 2022). Further, an increase of plastoglobule size and number during heat treatment has also been connected to heat-induced chloroplast senescence (Zhang et al., 2014). Whether plastoglobules increase their number or their size might also be of importance for their function, as their core and coat compounds support different processes and an increase in size leads to a differing core to coat ratio compared to an increase in number (Arzac et al., 2022). But not only chloroplasts change in response to heat, it has been reported that in wheat, mitochondria increase in size and change their appearance when subjected to high temperature. This coincides with an increase in mitochondrial activity being observed in another study during heat stress (Rizhsky et al., 2004). Those results might be a sign of increased demand for ATP and mitochondrial stress proteins during heat (Rizhsky et al., 2004; Grigorova et al., 2012).

Generally, it can be hypothesised that a smaller size of cells and changed volumes of compart-

ments and thus reduced physical distance between compartments can facilitate vesicle transport or contact-based membrane lipid transfer during stressful conditions (Shomo et al., 2024). Even though there have been studies analysing the proportions of cell types (Wuyts et al., 2010), of subcellular compartments (Winter et al., 1993, 1994; Koffler et al., 2013) and of one or a few organelles (Armstrong et al., 2006; Bouchekhima et al., 2009; Crumpton-Taylor et al., 2012; Poulet et al., 2015), there is still a lack of comprehensive data regarding the three-dimensional architecture of plant tissue and cells, especially during stress conditions. With advances in volume (electron) microscopy, the generation of 3D datasets in different scales has become more feasible. Currently, data from different studies still needs to be combined to gather insights about ultrastructural proportions and relations, even though the data is not always from the same tissue, developmental stage or even species (Tolleter et al., 2024). Nonetheless, an estimate of ultrastructural proportions can be made, and from there, each new study provides another piece of this complex puzzle.

1.4.2. Compartmentation of metabolism

Sugars are important in the highly compartmented environment of the plant cell. They can act as substrate for synthesis of other primary or secondary metabolites, but also for polysaccharides such as (hemi-)cellulose, for modifications of proteins and lipids, and for the process of oxidative phosphorylation. Additionally, they can stabilise membranes and proteins in stressed cells. However, their function strongly depends on their type, concentration and localisation (Pommerrenig et al., 2018). For example, sucrose has a special role as transport sugar, because it is more stable than e.g. hexoses due to its non-reducing structure. The only other naturally occurring nonreducing disaccharide, trehalose, fulfils similar functions in insects and fungi (Huber & Huber, 1996).

Plant primary carbohydrate metabolism is distributed across different cellular compartments (see Figure 2). For example, CO_2 fixation takes place in the chloroplast within the CBBC, providing triose phosphates, which are a substrate for daily starch biosynthesis. During the night, starch is degraded to maltose, which is exported to the cytosol where it is hydrolysed to glucose, which then feeds into sucrose biosynthesis (Lunn, 2007; Stitt et al., 2010). Glucose is phosphorylated to form glucose-6-phosphate (G6P) by glucokinase, which in turn is converted to fructose-6-phosphate (F6P) by G6P isomerase. Sucrose-6-phosphate (S6P) is synthesised in photosynthetically active leaves from F6P and uridine diphosphate glucose (UDPG) by sucrose-phosphate synthase (SPS) (Leloir & Cardini, 1955; Ruan, 2014). This enzyme is crucial for regulation of sucrose synthesis, as it can be activated and deactivated by protein phosphorylation and its activity is positively impacted by G6P, and negatively by phosphate (Huber & Huber,

1996; Ruan, 2014). S6P is then further dephosphorylated by sucrose-phosphate phosphatase (SPP) to yield sucrose. The fast pace of the SPP reaction removes available S6P quickly from the cytosol, preventing the reversion of the SPS reaction (Huber & Huber, 1996).

As sucrose is important not only for energy metabolism, but also plays a crucial role in regulation of metabolism, export to sink tissues, and in signalling, its concentration in the various compartments is tightly regulated. This regulation can encompass activation and deactivation of SPS, but also shuttling between different compartments and degradation into hexoses (Ruan, 2014). Degradation of sucrose is catalysed by invertases, which are located in various compartments in different isoforms. They can be characterised according to their optimal pH. Neutral invertase (pH optimum 7.0-7.8) is located in the cytosol (Inv_n), acidic invertase (pH optimum 4.5-5.5) can be found in the vacuole (Inv_a) or bound to the cell wall in the apoplasm (Inv_{cw}) (Wan et al., 2018). The products of sucrose hydrolysis, glucose and fructose, are non-competitive and competitive inhibitors for invertases, respectively (Sturm, 1999). To enable balancing of sugar amounts between compartments, the sugars have to cross the membranes of compartments, such as the tonoplast, the chloroplast membranes, and the plasma membrane. Transport proteins are embedded in the membranes to ensure regulated transport of sugars (Hedrich et al., 2015; Patzke et al., 2019). Those transporters can shuttle sucrose into the vacuole, where it can be hydrolysed by invertase and the products, hexoses, can be transported back into the cytosol, where they act as a substrate for SPS after being phosphorylated by hexokinases. This results in a sucrose cycle, which consumes energy in the form of ATP. The seemingly futile cycle is instrumental in finely balancing the amount of sucrose within cytosol and vacuole, contributing to the regulation of this important metabolite (Geigenberger & Stitt, 1991).

The energy stored in the form of sugars needs to be accessed at some point, which is facilitated by glycolysis, a process that ultimately converts glucose to pyruvate, which in turn can be used for respiration in the mitochondria. During glycolysis, ATP is produced in the cytosol when 1,3-biphosphoglycerate is converted to 3-phosphoglycerate and when phosphoenolpyruvate is converted to pyruvate (Kadereit et al., 2021). After import into the mitochondria, pyruvate is decarboxylated oxidatively to acetyl-CoA, and then further funnelled through the TCA cycle in the mitochondrial matrix until complete oxidation of one molecule pyruvate to three molecules CO_2 is achieved (Møller et al., 2021). During this process, electrons are transferred to the respiration chain in the inner mitochondrial membrane where they are used to build up a proton gradient, which is utilised for ATP synthesis by oxidative phosphorylation (Møller et al., 2021). Intermediates of the TCA cycle are, in turn, substrates for other metabolic reactions. For example, citrate is exported and converted to glutamate, which in turn is used for synthesis of porphyrins and α-ketoglutarate is imported into the plastid for glutamate synthesis (Kadereit et al., 2021). This still only describes a minor part of the different metabolic pathways that are

spread throughout the cellular compartments. Photorespiration, for example, which reclaims a product from the Rubisco side reaction with O_2, 2-phosphoglycolate, is taking place in the cytosol, mitochondria and peroxisomes, before the product glycerate 3-phosphate is funnelled back to the CBBC in the plastid (Stitt et al., 2010; Szecowka et al., 2013; Hernandez & Nägele, 2022). The connectivity between those reactions is immense, and it has been the subject of research for the past decades and will probably remain so.

1.4.3. Experimental analysis of subcellular metabolism

Isolation of organelles and subsequent analysis is a prevalent form of elucidating the processes occurring in the different cellular compartments (Stitt et al., 2010). Also, predictions of protein localisation, based on signal peptides, coupled to microscopic localisation studies, are a common analytic method (Arrivault et al., 2014). However, some compounds, such as metabolites, are more challenging to analyse, as they possess high turnover rates that prove too fast for conventional organelle fractionation procedures. To reliably resolve subcellular metabolism, it is crucial to quench metabolism instantly by snap-freezing the plant tissue, followed by lyophilisation, inhibiting any further metabolic reactions. Subsequently, tissue material can be fractionated in an organic, non-aqueous solvent, which inhibits any metabolic reaction during the fractionation procedure. This makes the method suitable for resolving metabolism at a subcellular level (Gerhardt & Heldt, 1984; Stitt et al., 1989; Arrivault et al., 2014; Fürtauer et al., 2016). The solubilised material can be separated by subsequent centrifugation and resuspension in non-aqueous solvent mixtures of differing densities. Finally, correlation of specific marker enzyme activities with metabolite abundances indicates relative proportions of metabolites for each resolved compartment (Fürtauer et al., 2016; Hernandez et al., 2023). Currently, this workflow is successful for cytosolic, plastidic and vacuolar fractions, whereas mitochondria and peroxisomes seem to cluster with other compartments, mostly between the cytosolic and the plastidic fraction, making this four-compartment approach only feasible under reservation (Stitt et al., 1989; Arrivault et al., 2014; Fürtauer et al., 2019; Kitashova et al., 2024).

In summary, during the last decades, our understanding of photosynthesis and plant performance under elevated temperature has been significantly advanced by numerous studies. However, due to the high degree of compartmentation, the study of plant metabolism and its regulation remains challenging both in experiment and theory. In this thesis, both dynamics and subcellular distribution of the central plant carbohydrate metabolism was resolved experimentally to provide detailed insights into the response towards elevated temperatures. Finally, a theoretical framework was developed to simulate and predict regulation of sucrose metabolism in a changing environment.

2. Aims of the thesis

This work aims to describe the metabolic, photosynthetic and ultrastructural response of the model organism *Arabidopsis thaliana* to heat exposure, both transiently and prolonged. It explores methods to better analyse diurnal fluctuations of the carbohydrate metabolism, as well as gaining insight into the subcellular partitioning of carbohydrates, and highlights the importance of soluble sugar distribution for the plant heat response.

Transiently elevated temperature, such as in heat waves or during diurnal temperature fluctuations, is a common occurrence in a natural environment. The resulting dynamic changes in the metabolic network are of high importance for plant survival. To better understand those changes and their effect, and to deduce the carbon flux through the system, mathematical balance modelling with Fourier polynomials was employed.

Further, subcellular data is important to unravel the intricacies of primary carbohydrate metabolism during heat acclimation. Subcellular sugar distribution and information about cellular ultrastructure can be combined to provide a new layer of information about the observed system. The implications of subcellular sugar concentrations for enzymatic reactions, carbon flux, and metabolic stabilisation can shape our mechanistic understanding of the primary carbohydrate metabolism.

3. Results

The results of this dissertation consist of two studies and one review that are included in the following chapter. All three papers were published as open access articles in international peer reviewed journals. Detailed information about author contribution can be found in the chapter List of Publications.

3.1. Predicting plant growth response under fluctuating temperature by carbon balance modelling

Seydel, C., Biener, J., Brodsky, V., Eberlein, S., & Nägele, T. (2022a). Predicting plant growth response under fluctuating temperature by carbon balance modelling. Commun Biol, 5(1), 164

communications biology

ARTICLE

https://doi.org/10.1038/s42003-022-03100-w OPEN

Predicting plant growth response under fluctuating temperature by carbon balance modelling

Charlotte Seydel [1,2], Julia Biener[2,3], Vladimir Brodsky[2,3], Svenja Eberlein[2,3] & Thomas Nägele [2]✉

Quantification of system dynamics is a central aim of mathematical modelling in biology. Defining experimentally supported functional relationships between molecular entities by mathematical terms enables the application of computational routines to simulate and analyse the underlying molecular system. In many fields of natural sciences and engineering, trigonometric functions are applied to describe oscillatory processes. As biochemical oscillations occur in many aspects of biochemistry and biophysics, Fourier analysis of metabolic functions promises to quantify, describe and analyse metabolism and its reaction towards environmental fluctuations. Here, Fourier polynomials were developed from experimental time-series data and combined with block diagram simulation of plant metabolism to study heat shock response of photosynthetic CO_2 assimilation and carbohydrate metabolism in *Arabidopsis thaliana*. Simulations predicted a stabilising effect of reduced sucrose biosynthesis capacity and increased capacity of starch biosynthesis on carbon assimilation under transient heat stress. Model predictions were experimentally validated by quantifying plant growth under such stress conditions. In conclusion, this suggests that Fourier polynomials represent a predictive mathematical approach to study dynamic plant-environment interactions.

[1] Ludwig-Maximilians-Universität München, Faculty of Biology, Plant Development, 82152 Planegg-Martinsried, Germany. [2] Ludwig-Maximilians-Universität München, Faculty of Biology, Plant Evolutionary Cell Biology, 82152 Planegg-Martinsried, Germany. [3] These authors contributed equally: Julia Biener, Vladimir Brodsky, Svenja Eberlein. ✉email: thomas.naegele@lmu.de

Capturing dynamics in biological systems by mathematical terms is the general aim of biomathematical modeling. Differential equations represent an adequate strategy to describe dynamics over space and time. Ordinary differential equations (ODEs) and partial differential equations (PDEs) have been successfully applied to reveal biological system dynamics and to develop predictive models of growth rates, transcription, translation, or metabolic processes[1]. In a metabolic context, ODE models are frequently applied to simulate enzyme kinetic reactions and, by this, to explain dynamics of observed metabolite concentrations. Kinetic models, based on ODEs, have frequently been applied in a broad field of biological research, e.g., in the context of metabolic engineering of microbial systems and strain design[2], disease research[3], and plant metabolism[4–6]. In contrast to the high diversity of application fields, the principle of ODE kinetic modeling remains conserved: based on genome sequence information or biochemical evidence from literature a biochemical reaction network is established, substrate and product concentrations are quantified, and enzyme kinetics are applied to calculate reaction rates within a metabolic system. Enzyme kinetic parameters, e.g., velocity under substrate saturation (V_{max}) or substrate affinity (K_M) of Michaelis–Menten equations, are experimentally determined and used for computationally assisted parameter estimation. A well-defined and experimentally validated kinetic ODE model enables computational simulation and prediction of complex system behavior. A clear limitation of such an approach, however, is the requirement of kinetic parameters which are (frequently) difficult and/or expensive to quantify. Initiatives like KiMoSys, a public repository of published experimental data, summarize and concentrate data on metabolites, protein abundance, and fluxes providing a solid database for model construction and initial development[7]. Yet, under highly dynamic conditions, e.g., in a fluctuating environment, it still remains a challenge to resolve system dynamics on an enzyme kinetic level. This is due to the high dynamics of metabolites, transcripts, protein levels, and enzyme activities[8,9]. Although being laborious, the development and optimization of ODE kinetic models provide an important and informative mathematical method to study biochemical system behavior. Simultaneously, however, diverse problems might occur with solving and applying such models due to uncertainties about parameters, model structure, kinetic rate laws or parameter sensitivities[10,11]. Depending on the research question focused on by a study, an explicit knowledge about enzymatic activities and their dynamics might not be essential to derive a mathematical description of metabolite dynamics. For example, metabolic fluxes might be estimated by tracing labeled atoms or molecules in a metabolic pathway system[12]. While only very limited information about single enzyme activities or kinetics can be derived from flux estimations, they still provide comprehensive insights into metabolic states and pathway activities, also on a large scale[13]. Beyond, algorithms and user interfaces have been developed which enable the combination of flux data with relative metabolite levels[14].

For estimating metabolic functions, i.e., the sum of synthesizing and degrading/consuming reactions of metabolite pools, under dynamic environmental conditions we have previously suggested a method for implicit estimation of metabolic functions[15]. Similar to flux analysis, dynamics of metabolite concentrations in time-series experiments were used in this approach to derive a time-continuous mathematical function to identify regulatory cascades in metabolic pathways. This approach made use of spline interpolations which were composed of cubic polynomials which were fitted to adjacent pairs of data points in a time-series data set. While such an approach is suitable for accurate data fitting, underlying mathematical functions are frequently not related to biological function and, thus, are less predictive than enzyme kinetic models. In the present study, we developed a mathematical model based on Fourier polynomials to simulate and analyze dynamics of photosynthesis and carbohydrate metabolism under transient heat exposure by function superposition. Model simulations indicated a significant impact of sucrose and starch biosynthesis on the stabilization of carbon assimilation and growth under elevated temperatures.

Results

A block diagram model based on Fourier polynomials for carbon balancing of plant metabolism. A block diagram model of the central carbohydrate metabolism of plants was developed to integrate experimental data on net photosynthesis (NPS), starch, and sugar metabolism (Fig. 1). The net carbon input block, i.e., NPS block, represented a Fourier polynomial describing NPS dynamics depending on genotypes and environments (see Fig. 2, solid lines). This input flux was multiplied by the stoichiometric factor 1/6 to enable quantitative summation with starch and sugar fluxes (unit: µmol C6 h^{-1} gDW^{-1}). Carbon balance Eq. (1) (BE_1) comprised the summation of NPS rates and negative starch rates, balance Eq. (2) (BE_2) additionally comprised summation of negative sugar rates (Fig. 1). As a result, BE_1 revealed the net carbon flux (in C6 equivalents per hour and gram dry weight) which was left from photosynthetically assimilated CO_2 after starch synthesis, e.g., for sugar biosynthesis or biomass production. Further, BE_2 revealed residual net carbon flux after additional sugar biosynthesis.

Rates of net starch and sugar biosynthesis were determined by differentiating Fourier polynomials of starch and sugar dynamics with respect to time. Hence, the Fourier polynomial balance models comprised three input functions, FP_{input} (Eqs. (1–3)), and two balance equations, $BE_{1,2}$ (Eqs. (4) and (5)).

$$FP_{input,NPS} = a_{0,NPS} + \sum_{k=1}^{n}[a_{k,NPS}\ \cos(k\omega_{NPS}t) + b_{k,NPS}\ \sin(k\omega_{NPS}t)] \quad (1)$$

$$FP_{input,Starch} = a_{0,Starch} + \sum_{k=1}^{n}[a_{k,Starch}\ \cos(k\omega_{Starch}t) + b_{k,Starch}\ \sin(k\omega_{Starch}t)] \quad (2)$$

$$FP_{input,Sugars} = a_{0,Sugars} + \sum_{k=1}^{n}[a_{k,Sugars}\ \cos(k\omega_{Sugars}t) + b_{k,Sugars}\ \sin(k\omega_{Sugars}t)] \quad (3)$$

$$BE_1 = \left(\frac{1}{6}\right) \cdot FP_{input,NPS} - \frac{d(FP_{input,Starch})}{dt} \quad (4)$$

$$BE_2 = BE_1 - \frac{d(FP_{input,Sugars})}{dt} \quad (5)$$

Here, a_k and b_k represent the Fourier coefficients for NPS, starch, and sugar equations. ω is the fundamental frequency of the signal ($\omega = 2\pi/T$, where T is the period). This Fourier polynomial-based balance equation model was applied to simulate dynamics of carbohydrate metabolism in plants of *Arabidopsis thaliana*, accession Columbia-0, under transient heat exposure. In addition, NPS and carbohydrate dynamics were recorded and simulated in a starch-deficient mutant *pgm1* and a mutant with a deficiency in sucrose biosynthesis capacity, *spsa1*. Coefficients of Fourier polynomials are provided in the supplements (Supplementary Data 1).

Fourier polynomials reflect dynamics of net CO_2 assimilation rates. During the first 30–45 min of the light period, rates of net

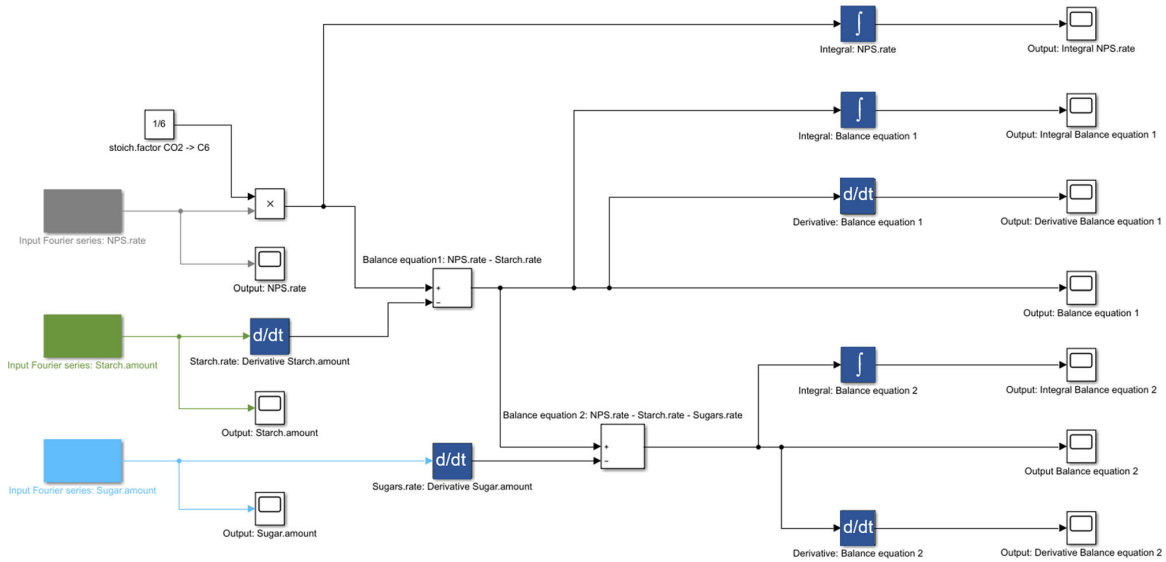

Fig. 1 Block diagram applied for Fourier polynomial balance modeling. Input functions are marked in gray (NPS), green (starch amount), and light blue (sugar amount) colored blocks (left side). Arrows indicate the direction of flux and connect input blocks via multiplication ("x") summation ("+/-"), differentiation ("d/dt"), and integration ("$\int$") with output blocks.

CO_2 assimilation increased steeply in all genotypes and reached a first plateau at ~1250 µmol CO_2 h^{-1} gDW^{-1} which was stable during the first half of the light period before it slightly increased until the end of the day at 22 °C (Fig. 2, gray-colored lines; data provided in Supplementary Data 2). No significant difference was observed between genotypes, yet *spsa1* had slightly higher assimilation rates compared to Col-0 while rates of *pgm1* were slightly lower (Fig. 2a, d, g). Temperature increase from 22 to 32 °C resulted in a drop in assimilation rates during the first hour of the treatment before the rates stabilized again and reached similar values than in the control (22 °C) experiment (Fig. 2a, d, g). At 32 °C, starch-deficient *pgm1* plants were most susceptible, and mean values differed most from 22 °C rates (Fig. 2d). During the last 2 hours of the light period in which temperature was decreased to 22 °C, all genotypes increased assimilation rates to control rates again. A similar scenario was observed within the 36 °C experiment for *pgm1* and *spsa1* while Col-0 had significantly decreased assimilation rates during the last 2 h of temperature treatment compared to the control experiment (Fig. 2b). In *pgm1*, assimilation rates dropped significantly during the first 30 min of the recovery phase, i.e., between 6 h and 6.5 h, when the temperature was decreased from 36 °C to 22 °C (Fig. 2e). Such a significant recovery drop was also observed for both *pgm1* and *spsa1* mutants in the 40 °C experiment, but not for Col-0 which showed again significantly decreased CO_2 assimilation rates between the last 2 h of the temperature treatment, i.e., between 4 and 6 h of the light period (Fig. 2c, f, i). Experimentally determined mean values of CO_2 assimilation rates and, by this, all described effects were covered by Fourier polynomials with $R^2 > 0.94$ (exception: *pgm1*, 32 °C, $R^2 = 0.8177$). In contrast to significant genotype-effects in net CO_2 assimilation under temperature fluctuation, transpiration rates were similar in Col-0, *spsa1* and *pgm1* under each tested condition and no significant genotype effect was detected (Supplementary Fig. S1). Transpiration rates increased during temperature treatment (2 h→6 h) and decreased again with temperature during the last 2 h of the light phase (6 h→8 h). Peak values of transpiration rates at 40 °C were about ~threefold higher than at 22 °C (Supplementary Fig. S1a, d).

To test whether differential efficiency of photosystems could reflect observed differences in CO_2 assimilation under transient heat, maximum quantum yield (Fv/Fm), electron transport rates (ETR), photochemical (qP), and non-photochemical quenching parameters (qN) were determined by pulse-amplitude modulation before and after transient exposure to 40 °C (Figs. 3 and 4; data provided in Supplementary Data 3). While Col-0 was affected significantly in Fv/Fm only during recovery from transient 40 °C treatment at 22 °C (Fig. 3a), Fv/Fm of *pgm1* dropped significantly during 40 °C treatment and showed a significant increase during recovery (Fig. 3b). In *spsa1*, no significant effect was observed for Fv/Fm (Fig. 3c). In contrast, *spsa1* was most significantly affected in electron transport rates (ETR), photochemical (qP), and non-photochemical quenching (qN) parameters recorded within rapid light curves (RLCs; Fig. 4g–i). At 40 °C, ETR and qP were significantly higher than at 22 °C, also under high PPFD, i.e., >1000 µmol photons m^{-2} s^{-1} (Fig. 4g, h). A similar trend was also observed in Col-0 where qP was also found to increase significantly under transient exposure to 40 °C (Fig. 4b). In *pgm1*, photosystems were found to be least significantly affected (Fig. 4d–f). Here, only qP showed a significant drop when plants were transferred from 40 to 22 °C (Fig. 4e).

Transient heat exposure significantly affects dynamics of starch and soluble carbohydrates. The exposure to transient heat lead to a significant change in starch dynamics in Col-0 and *spsa1* (Fig. 5; all metabolite data are provided in Supplementary Data 4). Starch amount in *pgm1* was below the detection limit of the applied photometric detection method (Fig. 5e–h). Starch concentration dropped significantly after transient heat exposure (6 h) in comparison to control conditions in Col-0 and *spsa1* (ANOVA, $P < 0.001$). This drop did not change significantly among the different temperatures. In the recovery phase after the heat shock (8 h), plants increased their starch content depending on the temperature they were subjected to. Plants of both genotypes treated with 32 °C increased their starch concentration by ~40% between 6 and 8 h (Fig. 5b, j), whereas plants treated with 36 °C increased it by over 90% (Fig. 5c, k). Col-0 subjected to the

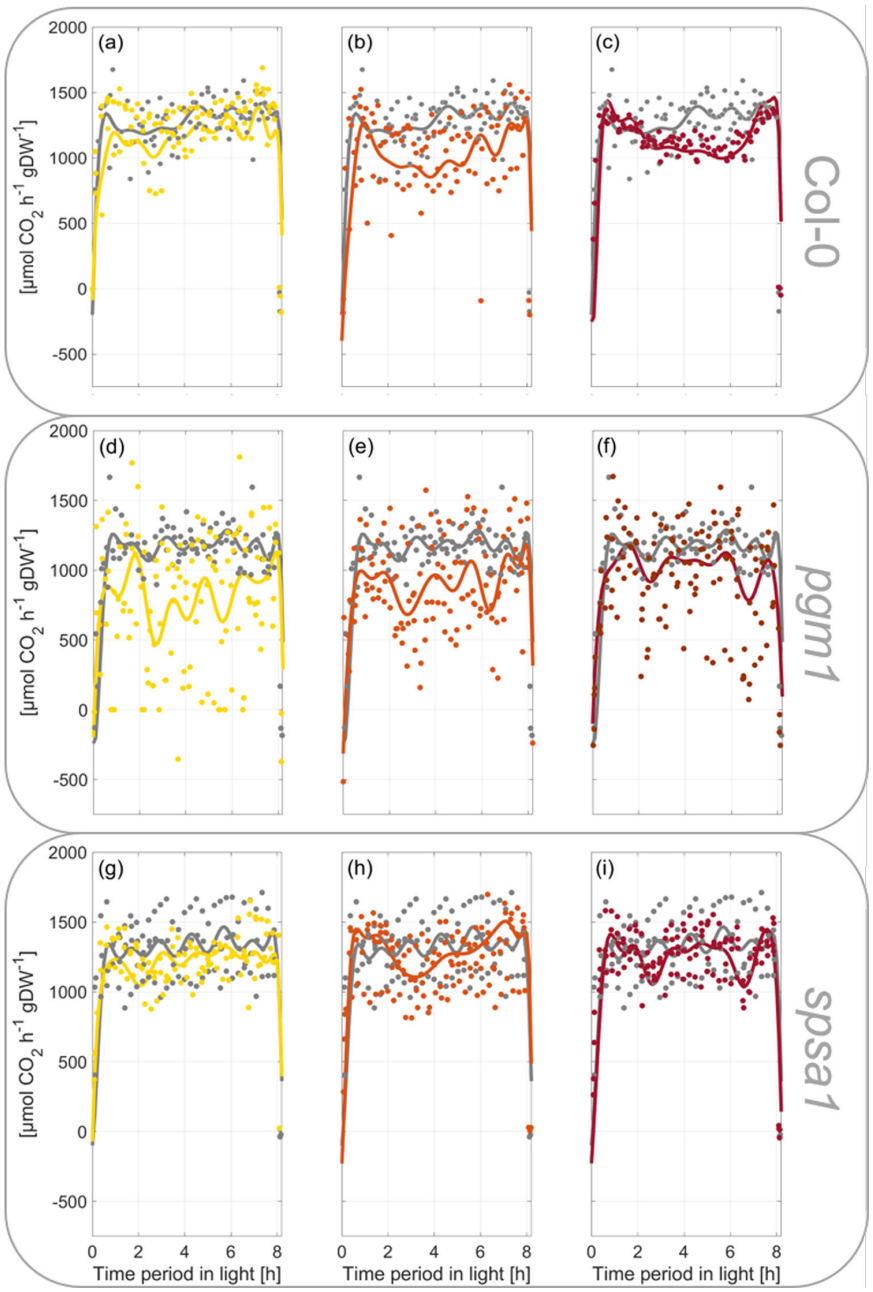

Fig. 2 Rates of net CO_2 uptake during short-day transient heat exposure. Scattered dots represent experimental data ($n = 3$), lines represent Fourier series fits. **a–c** Col-0, **d–f** *pgm1*, **g–i** *spsa1*. Gray lines: 22 °C experiment; yellow lines: 32 °C experiment; orange lines: 36 °C experiment; red lines: 40 °C experiment. The temperature was set to 22 °C between 0–2 h and 6–8 h. The temperature was transiently increased between 2 and 6 h. Temperature curves recorded during the experiments are illustrated in Supplementary Fig. S3a. A summary of Fourier polynomial coefficients is provided in the supplements together with NPS data (Supplementary Data 1 and Supplementary Data 2).

36 °C transient heat exposure was even able to reach the level of the control plants at the 8-h time point.

An effect of transient heat exposure on sucrose levels was only detectable for higher temperatures, i.e., within 36 °C and 40 °C experiments (Fig. 6). When subjected to 32 °C of transient heat, no significant change in sucrose levels was detected in all genotypes (Fig. 6b, f, j). In Col-0, only heat exposure of 40 °C resulted in a significant increase in sucrose concentration at the 6 h time point ($P < 0.001$), but no further change was observed after the recovery phase at 8 h (Fig. 6d). Under all conditions, *pgm1* accumulated more sucrose over the course of the light phase compared to Col-0 and *spsa1* (Fig. 6e–h). Nevertheless, heat treatment with 36 and 40 °C reduced the amount of sucrose in the *pgm1* plants almost significantly ($P = 0.05$). In the recovery phase, the sucrose concentration in the heat-treated *pgm1* plants returned to a level comparable to control conditions (Fig. 6e–h). Due to high variance

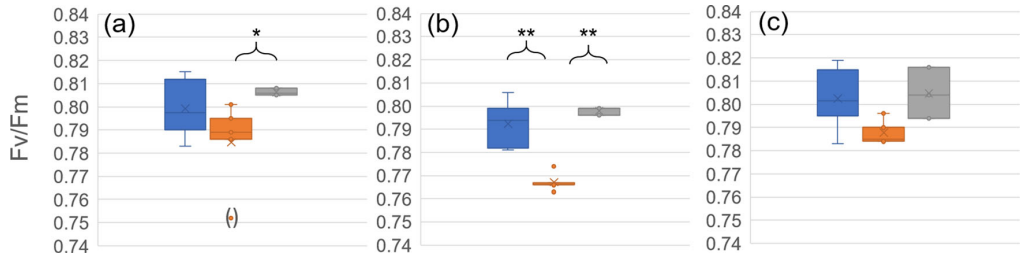

Fig. 3 Maximum photochemical quantum yield of PSII (Fv/Fm) under transient heat. Fv/Fm under 22 °C during the first 2 h of the light phase (blue), during transient exposure to 40 °C (orange) and after 2 h of recovery at 22 °C (gray). **a** Col-0, **b** *pgm1*, **c** *spsa1*. Box-and-whisker plots: center line, median; box limits, upper and lower quartiles; whiskers, 1.5× interquartile range; points, outliers. Asterisks indicate significant differences (ANOVA; $*P < 0.05$; $**P < 0.01$). $n = 3$–6. Experimental data are provided in Supplementary Data 3.

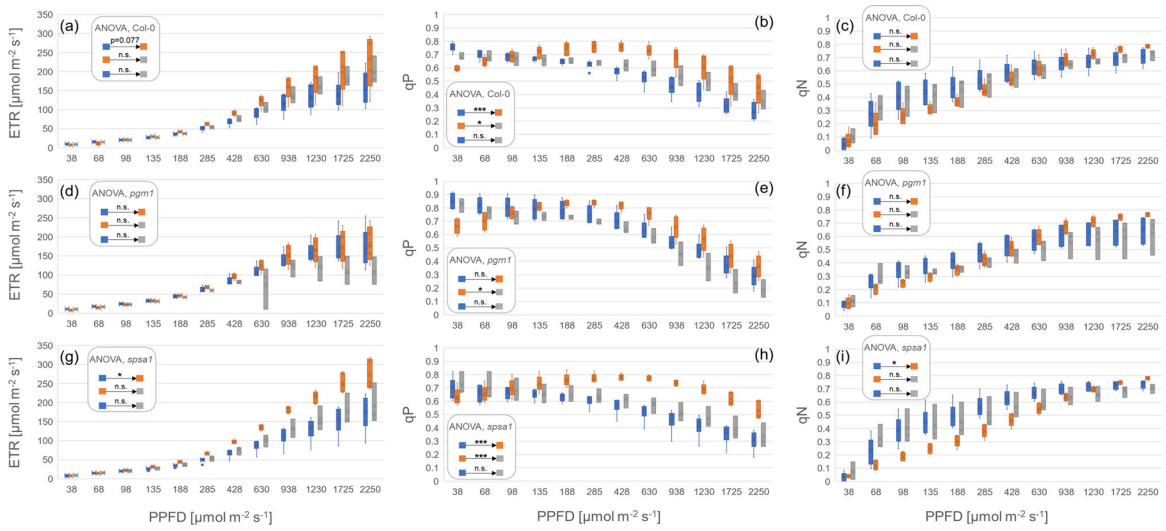

Fig. 4 Electron transport rates and quenching parameters under transient heat. Electron transport rates (ETR), photochemical (qP), and non-photochemical (qN) quenching were recorded within a rapid light curve (RLC) protocol. Blue: at 22 °C during the first 2 h of the light phase. Left panel: ETR; middle panel: qP; right panel: qN. Orange: during exposure to 40 °C. Gray: after 2 h recovery at 22 °C. **a**–**c** Col-0, (**d**–**f**) *pgm1*, (**g**–**i**) *spsa1*. Box-and-whisker plots: center line, median; box limits, upper and lower quartiles; whiskers, 1.5× interquartile range; points, outliers. $n = 3$–6. Significances, revealed by ANOVA, are summarized in boxes; n.s.: not significantly different ($P > 0.05$); $*P < 0.05$; $***P < 0.001$. Experimental data are provided in Supplementary Data 3.

in the sucrose measurements of *spsa1* plants, there was no significant difference between Col-0 and *spsa1* in the control plants and the plants exposed to 32 and 36 °C of transient heat (Fig. 6i–k). Only at 40 °C, *spsa1* showed significantly higher sucrose levels than Col-0 at 40 °C before and after the recovery phase (6 and 8 h, $P < 0.001$) or *spsa1* under control conditions (6 h: $P < 0.004$, 8 h: $P < 0.01$), while exhibiting very low variance (Fig. 6l).

In *pgm1*, glucose and fructose dynamics differed significantly from Col-0 (Fig. 7). Starting at similar hexose content at the start of the light period, the difference between *pgm1* and Col-0 and *spsa1* increased almost tenfold over the course of the day. Whilst in *pgm1* hexose amount increased steeply under control conditions, reaching a plateau after 6 h, hexose concentrations in Col-0 and *spsa1* peaked after 2 h and subsequently decreased again.

Col-0 and *spsa1* showed a significant drop in glucose levels after heat exposure to 32 and 36 °C ($P < 0.001$, Fig. 7). Within the 32 °C experiment, glucose levels at 8 h after recovery did not differ significantly from control conditions. Within the 36 and 40 °C experiments, however, the recovery phase after heat exposure resulted in a significant increase in glucose concentration compared to control conditions ($P < 0.001$). In addition, in Col-0 glucose levels were increasing above the level of control plants already during heat exposure to 40 °C at 6 h ($P < 0.001$). Fructose dynamics in Col-0 were similar to the glucose dynamics in Col-0 (Fig. 7). In *spsa1*, however, fructose dynamics did not change significantly in response to transient heat exposure. The only differences were observable after the recovery phase at 8 h in 36 and 40 °C. Here, a significantly higher fructose content could be measured compared to 22 °C ($P < 0.001$). In *pgm1*, hexose levels decreased significantly after temperature treatment (6 h, $P < 0.001$), with the lowest values being reached at 40 °C. After recovery (8 h), hexose levels did not change significantly from the 6 h time point in the 32 °C plants. After exposure to 36 and 40 °C, however, hexose levels increased significantly from 6 to 8 h ($P < 0.001$).

Numerical differentiation and integration of carbon balance equations reveals genotype-dependent system fluctuations due to transient heat exposure. To reveal how dynamics of carbon balance equations, which combine net photosynthesis, starch

(BE_1), and sugar metabolism (BE_2), are affected by transient heat exposure, derivatives were built with respect to time (Fig. 8). In Col-0, increasing temperature resulted in less fluctuating derivatives of BE_1 and BE_2 (Fig. 8a–f). Particularly under 40 °C, oscillations were significantly damped. Also, in *pgm1*, oscillations of derivatives decreased with increasing temperature (Fig. 8g–l). Yet, particularly during the recovery phase (6 h → 8 h) from 36 °C and 40 °C to ambient temperature, fluctuations had a higher amplitude than in Col-0 (Fig. 8h, I, k, l). In *spsa1*, oscillation amplitudes were damped most notably under 36 °C. Remarkably, in all genotypes, 32 °C had the smallest observed effect on derivative oscillations compared to 22 °C (yellow lines, Fig. 8a, d, g, j, m, p).

In addition to derivative functions which revealed the absolute changing rates of balance equations, fundamental frequencies of Fourier polynomials of BE_1 and BE_2 further suggested a differential effect of high temperature on genotypes' carbon balances (Supplementary Fig. S2). In Col-0, frequencies of BE_1 and BE_2 under 32 and 36 °C were almost doubled compared to the 22 °C experiment before they dropped in the 40 °C experiment (Supplementary Fig. S2a, b). This decrease was more emphasized in BE_2 than in BE_1 indicating a contribution of sugar dynamics. In *pgm1*, frequencies of BE_1 constantly increased with temperature in experiments (Supplementary Fig. S2a). Frequencies of BE_2 peaked under 32 °C and, finally, were lower under 40 °C than under 22 °C (Supplementary Fig. S2b). In *spsa1*, dynamics of BE_1 and BE_2 frequencies across experiments were similar, yet more pronounced in BE_2. In contrast to Col-0 and *pgm1*, lowest frequency of both balance equations was observed for the 36 °C experiment.

Numerical integration of NPS rates over time period in light revealed a decreased amount of assimilated carbon due to heat exposure in Col-0 (Fig. 9a) and *pgm1* (Fig. 9d). A detailed summary of numerical values of integrals is provided in the supplements (Supplementary Data 5). In Col-0, transient heat effects on NPS rates became strongest after 2 h of temperature treatment, i.e., after 4 h in the light period. Between 4 and 6 h, particularly the amount of carbon assimilated at 36 and 40 °C deviated clearly from the 22 °C experiment (Fig. 9a). In *pgm1*, this effect was observed 2 h earlier, i.e., during the first 2 h of heat treatment between 2 h and 4 h in the light period (Fig. 9d). Surprisingly, however, the 40 °C effect on carbon assimilation was not as strong as observed for 32 and 36 °C. In *spsa1*, carbon assimilation under heat was most robust and similar to control conditions, i.e., 22 °C (Fig. 9g).

Integrals of BE_1, which in addition to NPS rates also accounted for starch dynamics, revealed that starch dynamics in Col-0 were adjusted proportionally to affected NPS rates during transient heat exposure (Fig. 9b). In particular, integrals of 32 and 40 °C experiments became similar to the control experiment (22 °C). Due to starch deficiency, this effect was not observed in *pgm1* (Fig. 9e) while heat exposure resulted in larger integrals of BE_1 in *spsa1* (Fig. 9h). These heat-induced effects became more pronounced in BE_2 integrals which further accounted for net carbon flux into soluble sugar biosynthesis. In Col-0, the discrepancy of integrals between heat and control experiments was minimized during the first half of the light period, i.e., within the first 2 h of heat exposure (Fig. 9c). During the second half of the light period, discrepancy increased for 36 and 40 °C

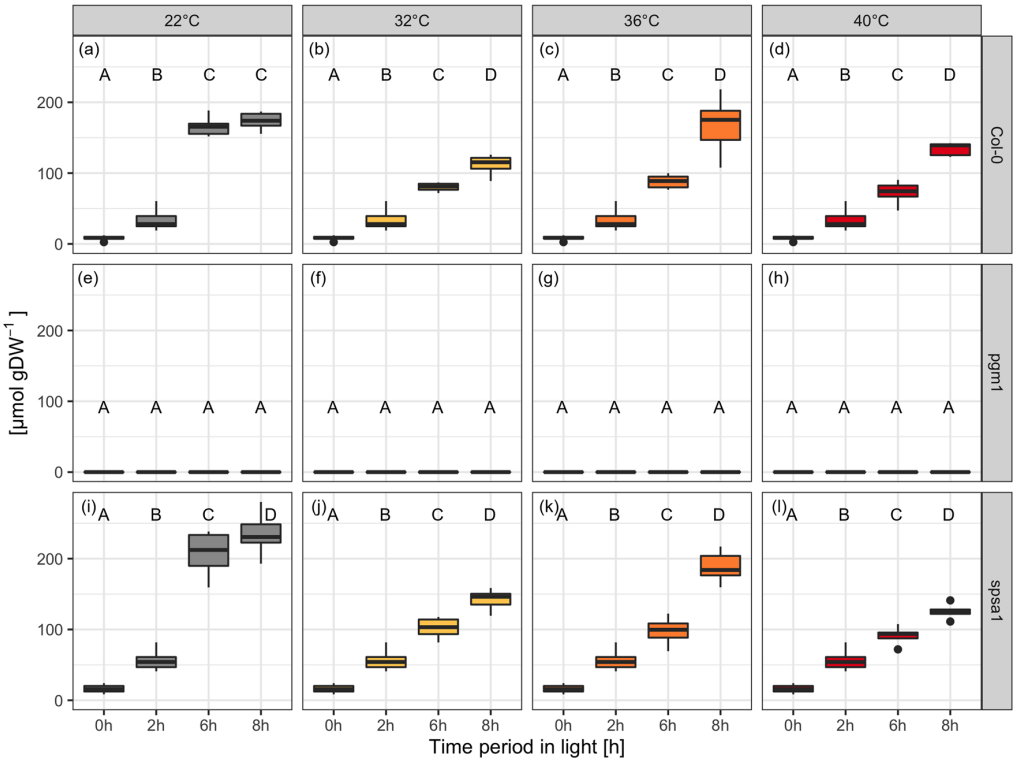

Fig. 5 Starch amounts during short-day transient heat exposure in glucose equivalents. a–d Col-0 ($n \geq 5$); **e–h** *pgm1* ($n \geq 3$); **i–l** *spsa1* ($n \geq 5$). Gray: 22 °C experiment; yellow: 32 °C experiment; orange: 36 °C experiment; red: 40 °C experiment. The temperature was set to 22 °C between 0–2 h and 6–8 h. The temperature was transiently increased between 2 and 6 h. Box-and-whisker plots: center line, median; box limits, upper and lower quartiles; whiskers, 1.5× interquartile range; points, outliers. Capital letters indicate groups of significance within genotype and condition (ANOVA, $P < 0.05$). Experimental data are provided in Supplementary Data 4.

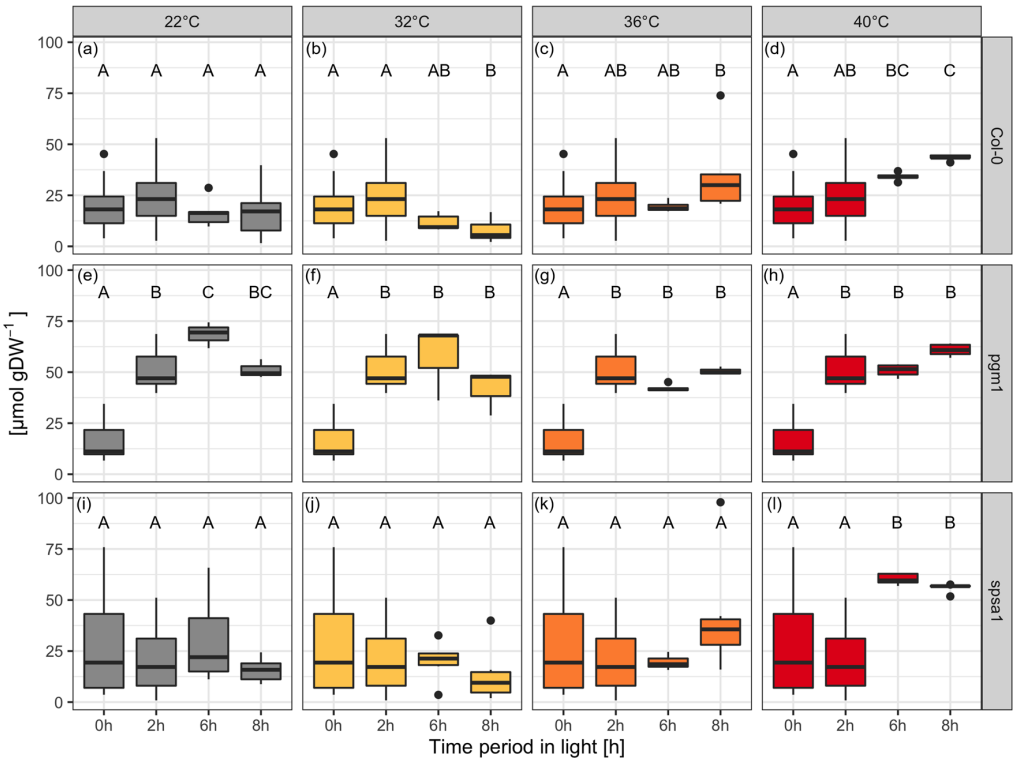

Fig. 6 Sucrose concentrations during short-day transient heat exposure. a–d Col-0 ($n \geq 5$); **e–h** *pgm1* ($n \geq 3$); **i–l** *spsa1* ($n \geq 5$). Gray: 22 °C experiment; yellow: 32 °C experiment; orange: 36 °C experiment; red: 40 °C experiment. The temperature was set to 22 °C between 0–2 h and 6–8 h. The temperature was transiently increased between 2 and 6 h. Box-and-whisker plots: center line, median; box limits, upper and lower quartiles; whiskers, 1.5× interquartile range; points, outliers. Capital letters indicate groups of significance within genotype and condition (ANOVA, $P < 0.05$). Experimental data are provided in Supplementary Data 4.

experiments. In *pgm1*, net carbon flux into sugar biosynthesis was reduced in a temperature-dependent manner which resulted in an (over-)compensation of reduced CO_2 assimilation rates under 36 and 40 °C (Fig. 9f). Also, in *spsa1* integrals of BE_2 increased under transient heat but this effect was less pronounced than in *pgm1* and Col-0 (Fig. 9i).

During the recovery phase, in which the temperature was set to 22 °C again (6 h → 8 h of light period), changes in starch and sugar dynamics became obvious in integrals of BE_1 and BE_2 for all genotypes. In Col-0, this effect was most pronounced within 36 and 40 °C experiments (Fig. 9b, c). In this phase, curves of integrals showed an inflection point directing the curve of integrals towards the control samples. In summary, this indicated reversibility of temperature-induced metabolic effects and a most robust carbon metabolism under heat in *spsa1*.

To test if integrals of BE_1 and BE_2 can predict whole-plant performance under heat, the surface of leaf rosettes were quantified before and after heat exposure (Fig. 10; data provided in Supplementary Data 6). For this experiment, plants were grown for 5 weeks under short-day standard growth conditions (see "Methods"). Then, changes of the leaf surface of the full shoot were determined within a growth experiment in which heat exposure was prolonged to 3 days to reinforce the transient heat effect on carbon assimilation (details about the experimental design are provided in Supplementary Fig. S3). Relative increase of leaf surface of Col-0 was found to be significantly reduced by transient heat exposure (Fig. 10). Similarly, and slightly stronger, also *pgm1* was negatively affected in growth. In contrast, for plants of *spsa1* no significant heat effect on leaf surface dynamics was observed which corresponded to the observation that integrals of NPS, BE_1, and BE_2 were least affected by heat in *spsa1* (see Fig. 9).

Discussion

In temperate regions, plants are frequently exposed to a changing temperature regime, and these changes might occur both over short- and long-time scales. For example, the temperature typically changes between day and night, and beyond, the temperature might also change transiently within the diurnal light and dark period. While temperature acclimation of plants typically can be observed after days of exposure to non-lethal cold or heat[16,17], transient temperature changes and plant stress response occur within minutes or hours. Interestingly, *Arabidopsis thaliana* was found to memorize already 5 minutes of heat stress which indicates a tightly regulated molecular network involved in heat stress response[18]. High temperature, e.g., between 35 and 40 °C, is well known to result in a reduced rate of photosynthesis[19] which has also been observed in the present study. While in Col-0 and *spsa1*, 32 °C resulted in only slightly decreased NPS rates, higher temperatures of 36 and 40 °C resulted in a significantly decreased NPS rate during the second half of the heat exposure period only in Col-0 (see Fig. 2). As previously summarized, a decreased NPS rate is not due to photosystem damage, but rather due to rubisco deactivation[19]. Consistent with this, Fv/Fm of neither genotype analyzed in the present study dropped irreversibly due to transient heat exposure (see Fig. 3). Further, consistent with previous findings which show a decreased rubisco activation at leaf

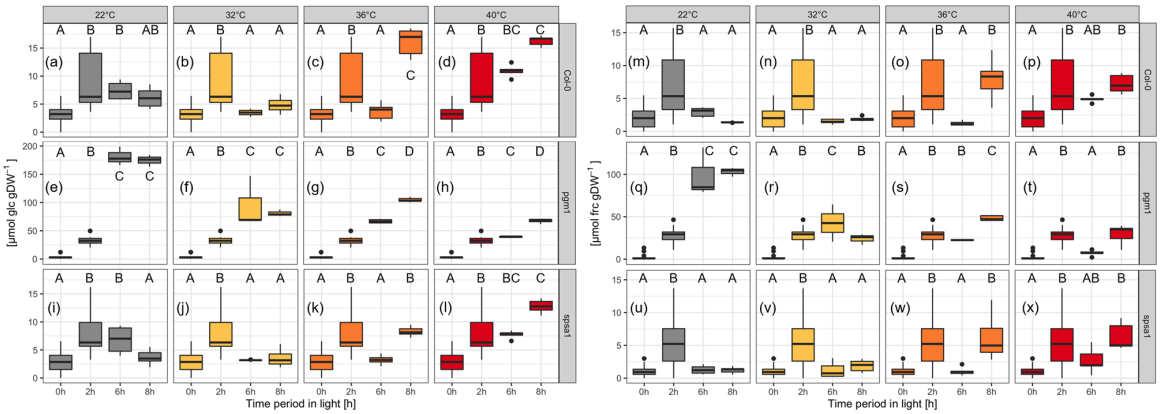

Fig. 7 Hexose concentrations during short-day transient heat exposure. Range of the *y* axes differs for *pgm1* due to the high difference in concentration. **a**–**l** Glucose concentrations; **a**–**d** Col-0 ($n \geq 5$); **e**–**h** *pgm1* ($n \geq 3$); **i**–**l** *spsa1* ($n \geq 5$). **m**–**x** Fructose concentrations. **m**–**p** Col-0 ($n \geq 5$); **q**–**t** *pgm1* ($n \geq 3$); **u**–**x** *spsa1* ($n \geq 5$). Gray: 22 °C experiment; yellow: 32 °C experiment; orange: 36 °C experiment; red: 40 °C experiment. The temperature was set to 22 °C between 0–2 h and 6–8 h. The temperature was transiently increased between 2 and 6 h. Box-and-whisker plots: center line, median; box limits, upper and lower quartiles; whiskers, 1.5× interquartile range; points, outliers. Capital letters indicate groups of significance within genotype and condition (ANOVA, $P < 0.05$). Experimental data are provided in Supplementary Data 4.

temperature >35 °C[20], the effect of 32 °C on NPS rates was much less significant than at 36 and 40 °C. In *spsa1*, however, NPS rates were less affected by heat than in Col-0 which might have several reasons. First, PSII maximum quantum yield was least affected by heat in *spsa1* (see Fig. 3). Only in *spsa1*, rates of linear electron transport (ETR), detected within a rapid light curve protocol, showed a significant increase during heat exposure suggesting a differential photosystem and/or thylakoid organization compared to Col-0 and *pgm1*. Further, compared to Col-0, *spsa1* might have had a reduced rate of photorespiration and/or mitochondrial respiration during heat exposure. While it remains speculation from our study, a higher starch accumulation rate in *spsa1* might result in a lowered respiration rate under heat because carbon equivalents may be fixed more efficiently. The observation of a destabilized NPS rate in starchless *pgm1* plants would support the stabilizing role of starch biosynthesis under transient heat exposure. Comparison of transpiration revealed similar rates across all genotypes, which suggests that observed NPS effects are unlikely due to differential stomata closure and/or secondary effects like leaf cooling[21,22]. However, previous reports under ambient conditions have shown that SPS knockout mutants have rather enhanced than lowered dark respiration rates which do not directly support the hypothesis of NPS stabilization by starch biosynthesis[23]. Another explanation might be a secondary effect of the *spsa1* mutation on rubisco and/or rubisco activase which, to our knowledge, has not been shown in current literature but which needs to be proven in future studies.

While sucrose and glucose metabolism showed a dynamic and differential accumulation profile between 32, 36, and 40 °C experiments, dynamics of fructose concentrations were most conserved across all temperature treatments and, remarkably, also across genotypes (see Fig. 7). An initial accumulation within the first 2 h of the light period was followed by a significant decrease until the end of heat exposure and an accumulation during the recovery phase between 6 and 8 h of the light period. Only *pgm1* showed a differential pattern at 22 and 32 °C but became similar in its fructose profile to Col-0 and *spsa1* under 36 and 40 °C. In mature *Arabidopsis* leaves, fructose levels are significantly affected by invertases that catalyze the hydrolysis of sucrose and release free hexoses[24], and by fructokinase catalyzing ATP-dependent phosphorylation which yields fructose-6-phosphate[25]. As fructose and glucose profiles differed in the present study, this cannot (solely) be explained by invertase reactions which release equimolar concentrations of both hexoses. However, differential regulation of hexokinase and fructokinase could explain the different hexose profiles. Fructokinase yields the direct substrate for glycolysis, TCA cycle, and mitochondrial respiration. In a previous study that analyzed transcript levels in *Arabidopsis thaliana* under combined drought and heat stress found increased transcripts for both hexokinase and fructokinase[26]. Although the experimental design differed significantly from this study, together with other findings this suggests a central role of hexose phosphorylation in heat stress response and acclimation[17]. As leaf respiration rates typically increase under elevated temperature[27], observed consistent fructose dynamics might be due to a relatively high rate of glycolytic consumption under transient heat exposure.

Integrating net CO_2 assimilation rates with starch and sugar turnover allows for balancing of the central carbohydrate metabolism. In this context, Fourier polynomials support the functional and time-continuous estimation of dynamics of metabolism. Integration and differentiation of Fourier polynomials is straightforward, and, at the same time, provides a comprehensive mathematical framework that is applied in diverse fields of natural sciences and engineering[28–30]. As described in the block diagram model (see Fig. 1), metabolic dynamics were simulated by the addition of Fourier polynomials comprising input functions (NPS rates) and consuming functions (starch and sugar dynamics). With such a design, dynamics of plant carbon balancing become traceable without the need for the application of composed spline functions. Further, the properties of Fourier polynomials can reveal further insight into metabolic regulation and consequences of environmental changes. For example, in the present study both amplitude and frequency of derivatives of balancing equations differed with regard to genotype and environment. A different pattern was observed in Col-0 and *spsa1* than in *pgm1*, indicating that the starchless mutant has a less buffered metabolic response towards heat stress than both other genotypes. This was supported by the comparison of fundamental frequencies of BE_1 and BE_2 Fourier polynomials. Here, a genotype-specific pattern was observed which reflected the impact of starch deficiency in *pgm1* and comparatively high metabolic dynamics in *spsa1* within the 40 °C experiment (see Fig. 8 and Supplementary Fig. S1). Thus, summarizing the effects of

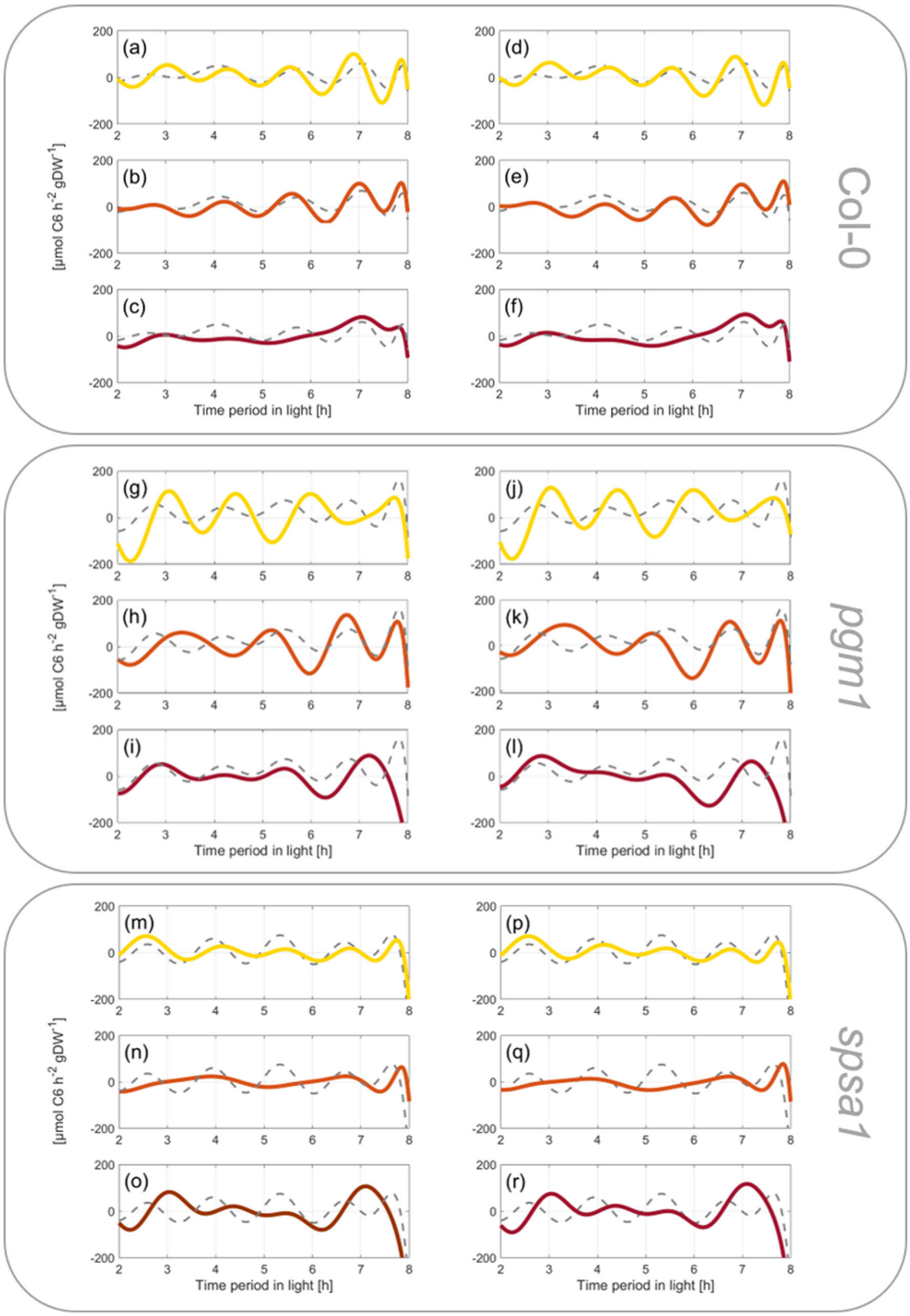

Fig. 8 Derivatives of carbon balance equations with respect to time. Derivatives of balance equations were built for the experiments "22 °C" (control; gray dashed lines), "32 °C" (yellow lines), "36 °C" (orange lines), and "40 °C" (red lines). Upper panel: Col-0, **a**–**c** derivatives of Col-0 balance Eq. (1) (BE_1), **d**–**f** derivatives of Col-0 balance Eq. (2) (BE_2). In the middle: *pgm1*, **g**–**i** derivatives of *pgm1* BE_1, **j**–**l** derivatives of *pgm1* BE_2. Lower panel: *spsa1*, **m**–**o** derivatives of *spsa1* BE_1, **p**–**r** derivatives of *spsa1* BE_2.

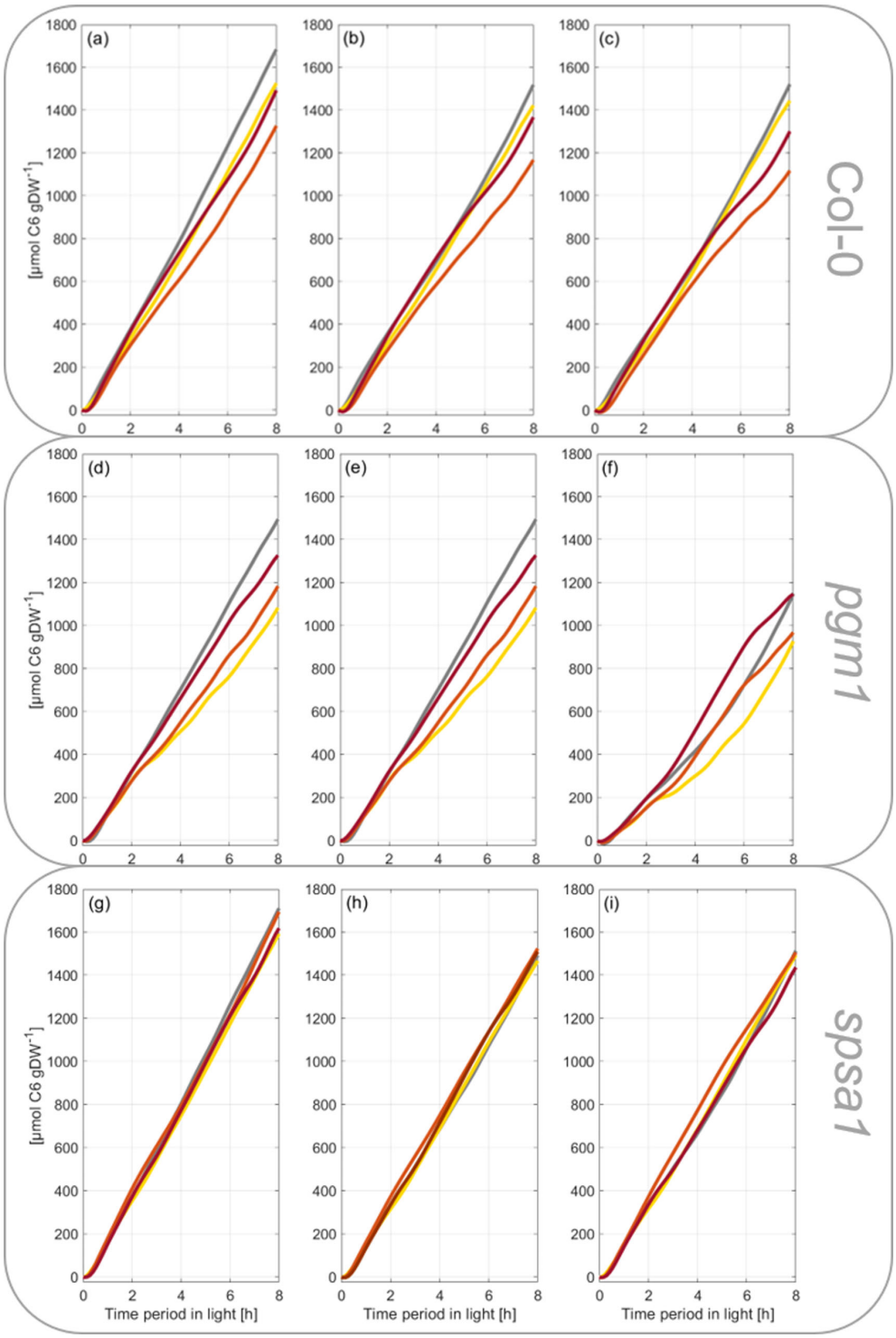

Fig. 9 Integrals of carbon balance rates during transient heat exposure. NPS rates and rates derived from BE_1 and BE_2 were integrated over time to reveal the total sum of net carbon gain during the light period. **a**–**c** Col-0 integrals of NPS rates (**a**), BE_1 (**b**), and BE_2 (**c**). **d**–**f** *pgm1* integrals of NPS rates (**d**), BE_1 (**e**), and BE_2 (**f**). **g**–**i** *spsa1* integrals of NPS rates (**g**), BE_1 (**h**), and BE_2 (**i**). Numerical values of integrals are provided in the supplements (Supplementary Data 5).

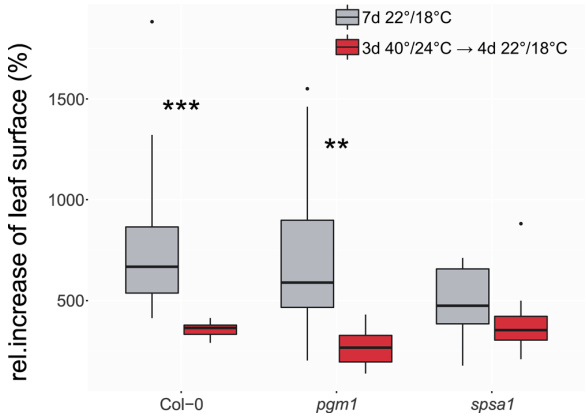

Fig. 10 Relative increase of leaf surface during a 7-day growth period. Leaf surface was determined before and after a growth period of 7 days at 22 °C/18 °C day/night temperature (gray boxes), or after 3 days at 40 °C/24 °C followed by 4 days at 22 °C/18 °C (red boxes). Left: Col-0; middle: *pgm1*; right: *spsa1*. Box-and-whisker plots: center line, median; box limits, upper and lower quartiles; whiskers, 1.5× interquartile range; points, outliers. $n \geq 10$. Asterisks indicate level of significance (Student's *t* test, $^{***}P < 0.001$; $^{**}P < 0.01$). Experimentally determined ratios of leaf surface are provided in the supplements (Supplementary Data 6).

transient heat on NPS rates and carbohydrate metabolism resulted in characteristic Fourier polynomials which enabled the discrimination of genotypes by their derivatives and fundamental frequencies. Genotypes could further be discriminated by integrals of Fourier polynomials derived from very short (4 h), transient temperature profiles. A prolonged heat exposure over 8 h and 3 days (with decreased night temperature) finally resulted in measurable and significant differences in leaf size as a proxy for plant growth. Hence, although the experimental design of heat treatment was changed in the growth experiments (compare Supplementary Figs. S3 and S5), this emphasizes the suitability of such a modeling approach to detect and quantify (relatively) small differences in balance equations over short time periods (see Fig. 9), and to predict significant effects of dynamic plant-environment interactions on (long-term) plant performance and physiology (see Fig. 10).

Fourier analysis and spectra of frequencies have been applied before in a different context, e.g., to analyze gene-expression time-series data[31]. These authors coupled Fourier analysis to supervised learning algorithms to discriminate between housekeeping genes and non-housekeeping genes in HeLa cells. This example provides evidence for the suitability of Fourier analysis to be combined with machine learning algorithms which is of particular interest for large-scale data sets. However, also data sets with only a relatively low number of variables may need mathematical functions for quantitative analysis and integration, e.g., as shown in the present study. This is due to the need for combining dynamics of variables rather than steady-state values under one condition. Here, Col-0, *pgm1*, and *spsa1* could successfully be discriminated by the dynamics of fundamental frequencies of Fourier polynomials across different experiments rather than by one absolute value of a frequency. This observation further emphasizes the need for a functional mathematical description of experimentally observed system dynamics because underlying attributes, e.g., monotonicity or curvature, can be derived from such a description. These attributes provide valuable information about system properties like stability or predictability which need to be essentially addressed for predictive modeling[32,33]. Conclusively, Fourier polynomial-based balance modeling provides a mathematical approach that can essentially support nonlinear modeling of metabolism, and which might, in future studies, even serve as a mathematical framework to connect oscillations in metabolism with quantum theory[34,35].

Methods

Plant cultivation and stress treatment. Plants of *Arabidopsis thaliana*, accession Columbia-0 (Col-0), *spsa1*(AT5G20280, SALK line 148643C) and *pgm1* (AT5G51820; TAIR stock CS3092) were grown on a 1:1 mixture of GS90 soil and vermiculite in a climate chamber under short-day conditions (8 h/16 h light/dark; 100 µmol m^{-2} s^{-1}; 22 °C/18 °C; 60% relative humidity). The *spsa1* line was confirmed via PCR to be homozygous and activity was found to be decreased to 30-50% of the wildtype Col-0 (Supplementary Fig. S4). The *pgm1* mutant had a dwarf phenotype and starch content was below the detection limit. After 4 weeks, plants were transferred to a growth cabinet (Conviron®, www.conviron.com) and grown for 2 further weeks under short-day conditions with the same settings as in the climate chamber. After 6 weeks, on the day of sampling, the temperature in the growth cabinet was kept at 22 °C during the first 2 h in the light (0 h → 2 h, 22 °C). Then, in three independent experiments, the temperature was increased to (i) 32 °C, (ii) 36 °C, or (iii) 40 °C for a total of 4 h (2 h → 6 h, temperature increase). In the control experiment, the temperature was set constantly to 22 °C. Between 6 and 8 h, i.e., until the end of the light period, the temperature was set to 22 °C in all experiments. A graphical representation of the experimental setup is provided in Supplementary Fig. S5. Plants were sampled at each time point (0 h, 2 h, 6 h, 8 h) by cutting the full leaf rosette at the hypocotyl. Samples were immediately frozen in liquid nitrogen and stored at −80 °C until further use.

Pulse-amplitude modulation and quantification of net CO_2 uptake. Maximum quantum yield of photosystem II (Fv/Fm) and electron transport rates (ETR) were quantified by pulse-amplitude modulation (PAM) using a WALZ® Junior-PAM (Heinz Walz GmbH, Effeltrich, Germany, https://www.walz.com/). Plants were dark incubated at 22 °C for 15 min prior to measurements. After dark incubation, Fv/Fm was determined by applying a saturating light pulse (photosynthetic photon flux density (PPFD) = 4000 µmol m^{-2} s^{-1}). A rapid light curve protocol was applied to quantify ETR, qP and qN under increasing PPFD[36]. Sequentially, every 20 s, actinic irradiance was increased from 0 up to 2250 µmol photons m^{-2} s^{-1} (0, 38, 68, 98, 135, 188, 285, 428, 630, 938, 1230, 1725, 2250 µmol photons m^{-2} s^{-1}).

Rates of net photosynthesis were recorded within the Conviron® growth cabinet using a WALZ® GFS-3000FL system equipped with measurement head 3010-S (Heinz Walz GmbH, Effeltrich, Germany, https://www.walz.com/). Temperature, light, and humidity control of the measurement head were set to follow ambient conditions, i.e., to follow surrounding growth cabinet conditions. A summary of recorded temperature, light, and humidity curves is provided in the supplement (Supplementary Fig. S6). Rates of transpiration were recorded together with net CO_2 uptake and are summarized in the supplement (Supplementary Fig. S1). For each genotype and growth condition, i.e., temperature setup, three independent samples were measured.

Extraction and quantification of carbohydrates. Plant material was ground to a fine powder under constant freezing with liquid nitrogen. The powder was lyophilized for three days and subsequently used for carbohydrate analytics. Starch and soluble carbohydrates were extracted and photometrically determined as described before[37]. Plant powder was incubated with 80% ethanol at 80 °C for 30 min. After centrifugation, the supernatant was transferred to a new tube, and extraction was repeated with the pellet. Supernatants were unified and dried in a desiccator. The starch-containing pellet was hydrolyzed with 0.5 M NaOH for 45 min at 95 °C. After acclimation to room temperature, 1 M CH_3COOH was added and the suspension was digested with amyloglucosidase solution, finally releasing glucose moieties from starch granules. Glucose was photometrically determined by applying a coupled glucose oxidase/peroxidase/o-dianisidine assay.

Soluble sugars sucrose, glucose, and fructose were determined from dried ethanol extracts after dissolving in water. After incubation with 30% KOH at 95 °C, sucrose was quantified using an anthrone assay. Anthrone was dissolved in 14.6 M H_2SO_4 (0.14% w/v), incubated with the prepared sample for 30 min at 40 °C and absorbance was determined photometrically at 620 nm. Glucose amount was determined photometrically by a coupled hexokinase/glucose 6-phosphate dehydrogenase assay resulting in NADPH + H^+ at 340 nm. For fructose quantification, phosphoglucoisomerase was added to the reaction mixture after glucose determination.

Quantification of SPS activity. The activity of sucrose phosphate synthase (SPS) was determined using the anthrone assay[37]. In brief, freeze-dried leaf tissue was suspended in extraction buffer containing 50 mM HEPES–KOH (pH 7.5), 10 mM $MgCl_2$, 1 mM EDTA, 2.5 mM DTT, 10% (v/v) glycerol and 0.1% (v/v) Triton-X-100. Following incubation on ice, extracts were incubated for 30 min at 25 °C with a reaction buffer containing 50 mM HEPES–KOH (pH 7.5), 15 mM $MgCl_2$, 2.5 mM DTT, 35 mM UDP-glucose, 35 mM F6P, and 140 mM G6P. Reactions were

stopped by adding 30% KOH and heating to 95 °C. Sucrose was determined photometrically after incubation with anthrone in H_2SO_4.

Statistics and reproducibility. Statistical analysis was performed in R and R Studio (www.r-project.org)[38]. Fourier series fitting was done within MATLAB® (www.themathworks.com), and block diagram models were created in Simulink® (www.themathworks.com). Plant total leaf surface was quantified using the Fiji software)[39] with the SIOX plugin (https://imagej.net/plugins/siox). The sample size was chosen according to (maximal) measurement and growth capacities (most limiting: growth cabinet, gas analyzer). Replicates represent biological replicates which were treated independently from each other to test and validate reproducibility. Plants were grown in pots with randomized order within the climate chamber to minimize or exclude any position or sampling effect. Samples were randomly chosen for molecular analysis. Investigators were blinded to group allocation during data collection.

Reporting summary. Further information on research design is available in the Nature Research Reporting Summary linked to this article.

Data availability

Data presented in this study are provided within Supplementary Data files 1–6.

Received: 23 June 2021; Accepted: 2 February 2022;
Published online: 24 February 2022

References

1. Lopatkin, A. J. & Collins, J. J. Predictive biology: modelling, understanding and harnessing microbial complexity. *Nat. Rev. Microbiol.* **18**, 507–520 (2020).
2. Costa, R. S., Hartmann, A. & Vinga, S. Kinetic modeling of cell metabolism for microbial production. *J. Biotechnol.* **219**, 126–141 (2016).
3. Ramos, M. P. M., Ribeiro, C. & Soares, A. J. A kinetic model of T cell autoreactivity in autoimmune diseases. *J. Math. Biol.* **79**, 2005–2031 (2019).
4. Feldman-Salit, A., Veith, N., Wirtz, M., Hell, R. & Kummer, U. Distribution of control in the sulfur assimilation in *Arabidopsis thaliana* depends on environmental conditions. *N. Phytol.* **222**, 1392–1404 (2019).
5. Weiszmann, J., Fürtauer, L., Weckwerth, W. & Nägele, T. Vacuolar sucrose cleavage prevents limitation of cytosolic carbohydrate metabolism and stabilizes photosynthesis under abiotic stress. *FEBS J.* **285**, 4082–4098 (2018).
6. Rohwer, J. M. Kinetic modelling of plant metabolic pathways. *J. Exp. Bot.* **63**, 2275–2292 (2012).
7. Mochao, H., Barahona, P. & Costa, R. S. KiMoSys 2.0: an upgraded database for submitting, storing and accessing experimental data for kinetic modeling. *Database* **2020**, baaa093 (2020).
8. Nägele, T. & Heyer, A. G. Approximating subcellular organisation of carbohydrate metabolism during cold acclimation in different natural accessions of *Arabidopsis thaliana*. *N. Phytol.* **198**, 777–787 (2013).
9. Espinoza, C. et al. Interaction with diurnal and circadian regulation results in dynamic metabolic and transcriptional changes during cold acclimation in Arabidopsis. *PLoS ONE* **5**, e14101 (2010).
10. Schaber, J., Liebermeister, W. & Klipp, E. Nested uncertainties in biochemical models. *IET Syst. Biol.* **3**, 1–9 (2009).
11. Gutenkunst, R. N. et al. Universally sloppy parameter sensitivities in systems biology models. *PLoS Comput Biol.* **3**, 1871–1878 (2007).
12. Crown, S. B., Long, C. P. & Antoniewicz, M. R. Optimal tracers for parallel labeling experiments and (13)C metabolic flux analysis: a new precision and synergy scoring system. *Metab. Eng.* **38**, 10–18 (2016).
13. Basler, G., Fernie, A. R. & Nikoloski, Z. Advances in metabolic flux analysis toward genome-scale profiling of higher organisms. *Biosci. Rep.* **38**, 6 (2018).
14. Sajitz-Hermstein, M., Topfer, N., Kleessen, S., Fernie, A. R. & Nikoloski, Z. iReMet-flux: constraint-based approach for integrating relative metabolite levels into a stoichiometric metabolic models. *Bioinformatics* **32**, i755–i762 (2016).
15. Nägele, T., Fürtauer, L., Nagler, M., Weiszmann, J. & Weckwerth, W. A strategy for functional interpretation of metabolomic time series data in context of metabolic network information. *Front. Mol. Biosci.* **3**, 6 (2016).
16. Garcia-Molina, A. et al. Translational components contribute to acclimation responses to high light, heat, and cold in Arabidopsis. *iScience* **23**, 101331 (2020).
17. Atanasov, V., Fürtauer, L. & Nägele, T. Indications for a central role of hexokinase activity in natural variation of heat acclimation in *Arabidopsis thaliana*. *Plants* **9**, 819 (2020).
18. Oyoshi, K., Katano, K., Yunose, M. & Suzuki, N. Memory of 5-min heat stress in *Arabidopsis thaliana*. *Plant Signal Behav.* **15**, 1778919 (2020).
19. Sharkey, T. D. Effects of moderate heat stress on photosynthesis: importance of thylakoid reactions, rubisco deactivation, reactive oxygen species, and thermotolerance provided by isoprene. *Plant Cell Environ.* **28**, 269–277 (2005).
20. Crafts-Brandner, S. J. & Salvucci, M. E. Rubisco activase constrains the photosynthetic potential of leaves at high temperature and CO2. *Proc. Natl Acad. Sci. USA* **97**, 13430–13435 (2000).
21. Jagadish, S. V. K., Way, D. A. & Sharkey, T. D. Plant heat stress: concepts directing future research. *Plant Cell Environ.* **44**, 1992–2005 (2021).
22. Santelia, D. & Lawson, T. Rethinking guard cell metabolism. *Plant Physiol.* **172**, 1371–1392 (2016).
23. Bahaji, A. et al. Characterization of multiple SPS knockout mutants reveals redundant functions of the four Arabidopsis sucrose phosphate synthase isoforms in plant viability, and strongly indicates that enhanced respiration and accelerated starch turnover can alleviate the blockage of sucrose biosynthesis. *Plant Sci.* **238**, 135–147 (2015).
24. Wan, H., Wu, L., Yang, Y., Zhou, G. & Ruan, Y. L. Evolution of sucrose metabolism: the dichotomy of invertases and beyond. *Trends Plant Sci.* **23**, 163–177 (2018).
25. Claeyssen, E. & Rivoal, J. Isozymes of plant hexokinase: occurrence, properties and functions. *Phytochemistry* **68**, 709–731 (2007).
26. Rizhsky, L. et al. When defense pathways collide. The response of Arabidopsis to a combination of drought and heat stress. *Plant Physiol.* **134**, 1683–1696 (2004).
27. Dusenge, M. E., Duarte, A. G. & Way, D. A. Plant carbon metabolism and climate change: elevated CO_2 and temperature impacts on photosynthesis, photorespiration and respiration. *N. Phytol.* **221**, 32–49 (2019).
28. Li, J., Liu, P., Yu, W. & Cheng, X. The morphing of geographical features by Fourier transformation. *PLoS ONE* **13**, e0191136 (2018).
29. Wang, L., Bert, J. L., Okazawa, M., Pare, P. D. & Pinder, K. L. Fast Fourier transform analysis of dynamic data: sine wave stress-strain analysis of biological tissue. *Phys. Med. Biol.* **42**, 537–547 (1997).
30. Plonka, G., Potts, D., Steidl, G. & Tasche, M. *Numerical Fourier Analysis* (Springer, 2018).
31. Dong, B. et al. Predicting housekeeping genes based on Fourier analysis. *PLoS ONE* **6**, e21012 (2011).
32. Angeli, D. Monotone systems in biology. in *Encyclopedia of Systems and Control* (eds Baillieul, J. & Samad, T.) https://doi.org/10.1007/978-1-4471-5102-9_90-1 (Springer, London, 2014).
33. Sontag, E. D. Monotone and near-monotone biochemical networks. *Syst. Synth. Biol.* **1**, 59–87 (2007).
34. Iotti, S., Borsari, M. & Bendahan, D. Oscillations in energy metabolism. *Biochim Biophys. Acta* **1797**, 1353–1361 (2010).
35. Jaffe, A., Jiang, C., Liu, Z., Ren, Y. & Wu, J. Quantum Fourier analysis. *Proc. Natl Acad. Sci. USA* **117**, 10715–10720 (2020).
36. White, A. J. & Critchley, C. Rapid light curves: a new fluorescence method to assess the state of the photosynthetic apparatus. *Photosynth Res.* **59**, 63–72 (1999).
37. Kitashova, A. et al. Impaired chloroplast positioning affects photosynthetic capacity and regulation of the central carbohydrate metabolism during cold acclimation. *Photosynth Res.* **147**, 49–60 (2021).
38. R Core Team. *R: A Language and Environment for Statistical Computing*. (R Foundation for Statistical Computing, Vienna, Austria, 2021).
39. Schindelin, J. et al. Fiji: an open-source platform for biological-image analysis. *Nat. Methods* **9**, 676–682 (2012).

Acknowledgements

We thank the members of Plant Evolutionary Cell Biology and Plant Development at LMU for fruitful discussions. Especially, we would like to thank Prof. Andreas Klingl, Plant Development at LMU, for support of C.S. Further, we thank Laura Schröder, Anastasia Kitashova, and Lisa Fürtauer for lab support. This work was supported by Deutsche Forschungsgemeinschaft (DFG), TRR175/D03.

Author contributions

C.S., J.B., V.B., S.E., and T.N. performed experiments. C.S. and T.N. performed statistics and modeling and wrote the paper. All authors approved the paper.

Funding

Open Access funding enabled and organized by Projekt DEAL.

Competing interests

The authors declare no competing interests.

Additional information

Supplementary information The online version contains supplementary material available at https://doi.org/10.1038/s42003-022-03100-w.

Correspondence and requests for materials should be addressed to Thomas Nägele.

Peer review information *Communications Biology* thanks Matthias Thalmann and the other, anonymous, reviewers for their contribution to the peer review of this work. Primary Handling Editors: Luke R. Grinham.

3.2. Subcellular plant carbohydrate metabolism under elevated temperature

Seydel, C., Heß, M., Schröder, L., Klingl, A., & Nägele, T. (2025). Subcellular plant carbohydrate metabolism under elevated temperature. Plant Physiol

The article and supplementary information can be found at https://doi.org/10.1093/plphys/kiaf117.

Plant Physiology®

Plant Physiology, 2025, **198**, kiaf117
https://doi.org/10.1093/plphys/kiaf117
Advance access publication 16 April 2025
Research Article

Subcellular plant carbohydrate metabolism under elevated temperature

Charlotte Seydel,[1,2] Martin Heß,[3] Laura Schröder,[2] Andreas Klingl,[1,*] Thomas Nägele[2,*]

[1]LMU München, Faculty of Biology, Plant Development, Großhaderner Str. 2-4, Planegg 82152, Germany
[2]LMU München, Faculty of Biology, Plant Evolutionary Cell Biology, Großhaderner Str. 2-4, Planegg 82152, Germany
[3]LMU München, Faculty of Biology, Zoology, Großhaderner Str. 2-4, Planegg 82152, Germany
*Author for correspondence: a.klingl@lmu.de (A.K.); thomas.naegele@lmu.de (T.N.)
The author responsible for distribution of materials integral to the findings presented in this article in accordance with the policy described in the Instructions for Authors (https://academic.oup.com/plphys/pages/General-Instructions) is Thomas Nägele (thomas.naegele@lmu.de).

Abstract

In many plant species, exposure to a changing environmental temperature regime induces an acclimation response that ultimately increases thermotolerance. Under elevated temperatures, membrane systems undergo remodeling to counteract destabilizing thermodynamic effects. Elevated temperature also affects photosynthesis and carbohydrate metabolism due to altered protein functions, enzyme activities, and transport across membrane systems. Here, a combination of electrolyte leakage assays and chlorophyll fluorescence measurements was applied to quantify heat tolerance before and after heat acclimation in *Arabidopsis thaliana* under different temperature regimes. Subcellular carbohydrate concentrations were determined through nonaqueous fractionation and 3D reconstruction of mesophyll cells and subcellular compartments using serial block-face scanning electron microscopy. Across temperature regimes between 32 and 38 °C, 7 d of heat acclimation at 34 °C most efficiently increased tissue heat tolerance. Under such conditions, cytosolic sucrose concentrations were stabilized by a shift in sucrose cleavage rates into the vacuolar compartment, while invertase-driven cytosolic sucrose cleavage was efficiently quenched by fructose and glucose acting as competitive and noncompetitive inhibitors, respectively. Finally, this study provides strong evidence for a sucrose concentration gradient from the cytosol to the vacuole, which might directly affect the physiological role and direction of sugar transport across cellular membrane systems.

Introduction

Changing temperature regimes have diverse effects on plant growth, development, and metabolism. While a sudden and strong temperature drop or increase typically results in irreversible tissue damage and yield loss, a constant and moderate change of temperature induces an acclimation response which increases temperature tolerance. This acclimation response represents a multigenic process and comprises, among others, signaling cascades, reprogramming of photosynthesis, and the primary and secondary metabolism (Herrmann et al. 2019; Garcia-Molina et al. 2020; Seydel et al. 2022). Increasing temperatures due to global warming have been shown to negatively impact the fitness of plants in their natural habitat and, especially in combination with drought, the yield of crop species (Lippmann et al. 2019; Gampe et al. 2021). Thus, understanding and predicting plant heat response and acclimation capacity is a vital component to understanding and dealing with the impact of globally increasing temperatures on plants.

Heat is perceived by a changing membrane permeability which, for example, influences transmembrane calcium flux (Ranty et al. 2016; Sajid et al. 2018). Also, reactive oxygen species, kinase and phosphatase activation, phytohormone cascades, activation of transcription factors, and heat shock proteins (HSPs) are involved in the perception of heat (Iba 2002; Qu et al. 2013). The immediate recognition of a changing temperature regime is central to stabilizing photosynthesis and metabolism. Photosynthesis is known to be a highly temperature-sensitive process, being inhibited both at low and high temperatures (Berry and Björkman 1980). The photosynthetic performance can already be impacted negatively at moderate heat by Rubisco inactivation (Law and Crafts-Brandner 1999; Crafts-Brandner and Salvucci 2000; Salvucci and Crafts-Brandner 2004; Yamori et al. 2014). The thylakoids are influenced by heat-induced changes in membrane properties and the regulatory connection between ATP synthesis and electron transport can be disrupted (Havaux 1996; Pastenes and Horton 1996; Bukhov et al. 1999, 2000). However, actual damage to photosystem II, quantified by measuring the critical temperature at which the minimal chlorophyll fluorescence is rapidly increasing, is mostly occurring between 40 and 55 °C, depending on the plant species and growth environment (Terzaghi et al. 1989; Zhu et al. 2018).

Carbohydrates are direct products of photosynthesis and represent energy sources and substrates for diverse anabolic pathways. Recent work has shown that carbohydrates are also an important factor in the thermomemory of the shoot apical meristem (Olas et al. 2021). Further, it has been shown that RGS1, a plasma membrane located glucose sensor, is connected to the regulation of thermotolerance in tomatoes, and externally applying glucose to the plants actually increased their thermotolerance (Wang et al. 2024). The enormous plasticity of heat responses in carbohydrate metabolism can also be seen when comparing heat treatments of different durations and severity. Comparing

Received January 23, 2025. Accepted February 19, 2025.

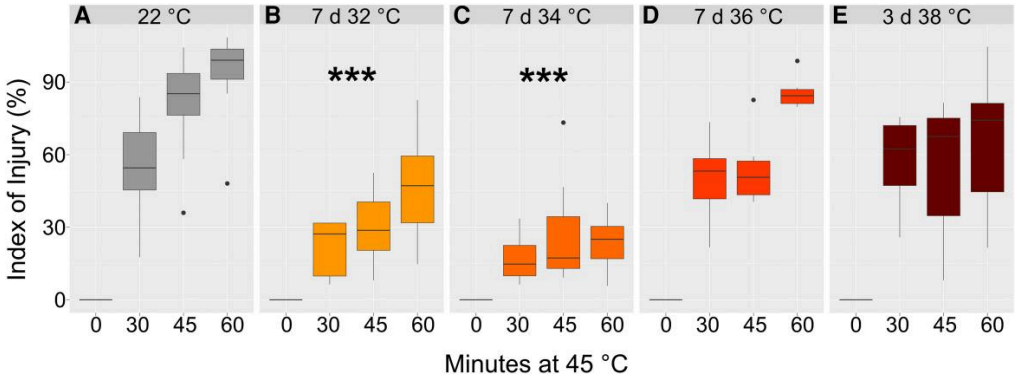

Figure 1. Heat tolerance of leaf tissue before and after acclimation. The index of injury (%) was based on the quantified electrolyte leakage of leaf tissue of plants grown at 22 °C **(A)** and heat acclimated **(B)** 7 d at 32 °C, **(C)** 7 d at 34 °C, **(D)** 7 d at 36 °C, and **(E)** 3 d at 38 °C. Asterisks indicate significant differences from the control, i.e. values at 22 °C (ANOVA and Tukey HSD post-hoc test, *** $P < 0.001$), $n = 6$. Center line, median; box limits, upper and lower quartiles; whiskers, 1.5× interquartile range; points, outliers.

moderate with severe transient heat exposure revealed that sucrose phosphate synthase (SPS) activity is negatively associated with the stability of CO_2 assimilation rates under elevated temperature (Seydel et al. 2022). Another study showed that, in *Arabidopsis*, the amount of primary carbohydrates, e.g. sucrose, raffinose, and maltose, increases after treatment at 40 °C for up to 240 min which represents a shared feature with cold stress (Ahsan et al. 2010). Additionally, within the first 24 h of heat exposure, 15% of upregulated proteins in soybean were found to be related to carbohydrate metabolism, but proteins that were associated with carbon assimilation and photosynthesis were found to be downregulated in the same plants (Ahsan et al. 2010).

Pathways of cellular plant carbohydrate metabolism are located in different subcellular compartments. For example, the Calvin–Benson–Bassham cycle (CBBC) takes place in the chloroplasts, while sucrose biosynthesis is catalyzed in the cytosol. The high degree of compartmentalization of plant cells impacts the analysis and understanding of their metabolic pathways profoundly (Lunn 2007). The method of nonaqueous fractionation (NAF) has been applied to resolve compartment-specific metabolic regulation (Gerhardt and Heldt 1984; Fürtauer et al. 2016; Hernandez et al. 2023). This method allows for continuous quenching of metabolism and prevents enzymatic interconversion of metabolites after sampling and during fractionation. The correlation of metabolite abundance with marker enzyme activity, or marker protein abundance, provides information about relative metabolite distributions over analyzed compartments (Fürtauer et al. 2019). If available, absolute amounts of metabolites can then be multiplied with relative distributions to provide an estimate of compartment-specific absolute metabolite amounts. A current limitation is the estimation of effective subcellular metabolite concentrations which also needs to consider compartment-specific volumes.

In the present study, we have combined leakage assays and chlorophyll fluorescence measurements with the NAF methodology and serial block-face scanning electron microscopy (SBF-SEM) to quantify thermotolerance and photosynthetic efficiency together with carbohydrate concentrations in the plastids, cytosol, and vacuole of leaf mesophyll cells of *Arabidopsis thaliana*. Effective compartment-specific concentrations were determined before and after acclimation to 34 °C to unravel heat-induced regulation of subcellular carbohydrate metabolism.

Results

Electrolyte leakage indicates efficient Arabidopsis heat acclimation between 32 and 34 °C

Susceptibility to heat stress was determined by quantifying the electrolyte leakage of leaf tissue to estimate membrane damage, described by the index of injury I_d. Leaf tissue acclimated to 22 °C was damaged to ~80% after 45 to 60 min of incubation in 45 °C water (Fig. 1A). Heat acclimation of leaf tissue after 7 d was most efficient for acclimation temperatures 32 and 34 °C which resulted in a significant reduction of I_d values (ANOVA, Fig. 1, B and C). Acclimation at 36 (7 d) and 38 °C (3 d) resulted in a slight decrease of I_d when compared to 22 °C plants, but the condition effect was not significant (Fig. 1, D and E). This was also in accordance with the growth phenotype of the plants after the heat treatment which indicated severe tissue damage at 36 and 38 °C, whereas for 32 and 34 °C, only an early induction of the inflorescence and slight yellowing of the leaves was observed (Supplementary Fig. S1).

To reveal how elevated temperature affected photosynthetic efficiency and CO_2 assimilation, the maximum quantum yield of photosystem II (F_v/F_m) was quantified together with rates of net photosynthesis (NPS) (Fig. 2). Under control conditions (22 °C), F_v/F_m values were >0.8 while they dropped significantly after 7 d at 32, 34, and 36 °C to values between 0.76 and 0.78. After 3 d at 38 °C, F_v/F_m showed the strongest decrease to a median of ~0.64, and the data variance distinctly increased (Fig. 2A, dark red box). Due to the observation that leaf tissue acclimated most efficiently during 7 d at 34 °C, we also quantified CO_2 assimilation under these conditions (Fig. 2B). Similar to F_v/F_m, NPS rates were slightly affected, but the decrease of the median under 34 °C was not significant.

Heat response of the central carbohydrate metabolism

Starch amounts decreased significantly under elevated temperatures (Fig. 3A). Plants acclimated for 7 d at 32 °C had approximately 20% of starch found in the tissue of nonacclimated plants while amounts dropped even more for higher temperature regimes.

While, compared to nonacclimated plants, sucrose amounts also dropped in plants acclimated at 34 °C, they significantly increased approximately 1.5-fold after 3 d at 38 °C (Fig. 3B). Both

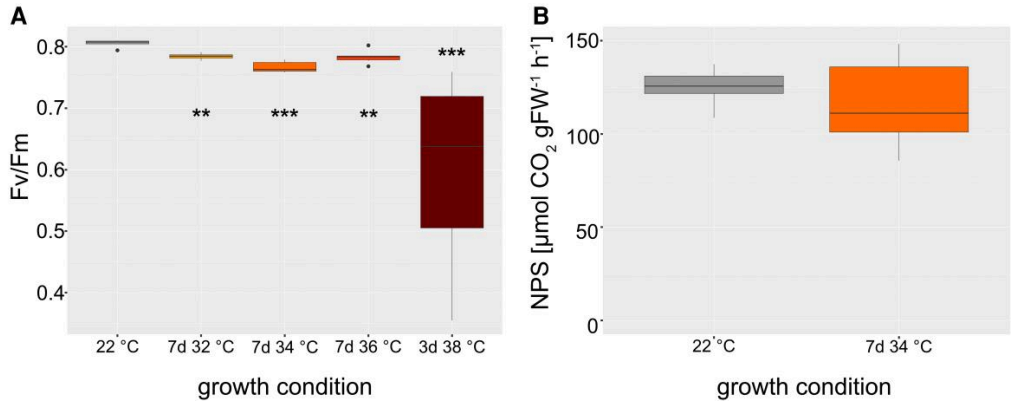

Figure 2. Photosynthesis under elevated temperature. **A)** Maximum quantum yield of photosystem II (F_v/F_m) as a function of acclimation duration and temperature. **B)** Rates of NPS. Asterisks indicate significant differences from the control (ANOVA and Tukey HSD post-hoc test, ** $P < 0.01$, *** $P < 0.001$), $n = 6$. Center line, median; box limits, upper and lower quartiles; whiskers, 1.5 × interquartile range; points, outliers. FW: fresh weight.

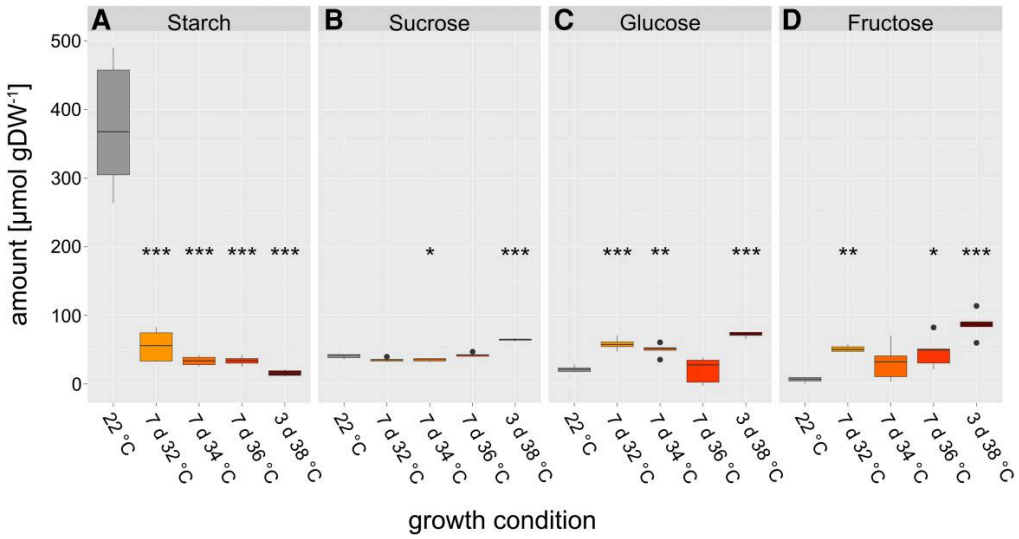

Figure 3. Metabolite amount per gram dry weight in control and acclimated plants. **A)** Starch amount in C6 equivalents. **B)** Sucrose amount. **C)** Glucose amount. **D)** Fructose amount. Asterisks indicate significant differences from the control (ANOVA and Tukey HSD post-hoc test, * $P < 0.05$, ** $P < 0.01$, *** $P < 0.001$), $n \geq 5$. Center line, median; box limits, upper and lower quartiles; whiskers, 1.5 × interquartile range; points, outliers. DW: dry weight.

glucose and fructose amounts were found to significantly increase during heat exposure with an exception at 36 °C for glucose and 34 °C for fructose (Fig. 3, C and D).

Dynamics of subcellular sugar compartmentation under heat

Based on the finding that heat acclimation resulted in the highest tolerance after 7 d at 34 °C (Fig. 1, A and C), this condition was chosen for further detailed analysis of subcellular compartmentation of carbohydrates. The compartment-specific relative distribution of soluble sugars sucrose, glucose, and fructose was quantified before (22 °C) and after heat acclimation (7 d at 34 °C).

For subcellular sucrose distribution, it was observed that heat induced a significant shift from chloroplasts to the vacuole (Fig. 4A). Due to heat exposure, the plastidial sucrose proportion decreased to less than 10%, while it increased to ~80% in the vacuole. This shift was neither observed for glucose nor for fructose (Fig. 4, B and C). Under heat, glucose was slightly shifted from the vacuole to the cytosol, and fructose proportions remained relatively constant.

The observed shifts in the relative proportion of sugars indicated a heat-induced regulation of subcellular compartmentation of carbohydrate metabolism. To reveal the effect of these relative shifts on compartment-specific metabolite concentrations, volumes of chloroplasts, cytosol, and vacuole were experimentally resolved by 3D SBF-SEM for mesophyll tissue at 22 and 34 °C (Fig. 5; Supplementary Fig. S2).

The evaluation of compartmental proportions revealed ~14% chloroplasts, 3.5% cytosol, and ~83% vacuole at 22 and 34 °C (Table 1). Together with the measured dry weight-to-fresh weight ratio and the average thickness of a leaf, fractions of compartment volumes in fresh leaves were determined. At 22 °C, the

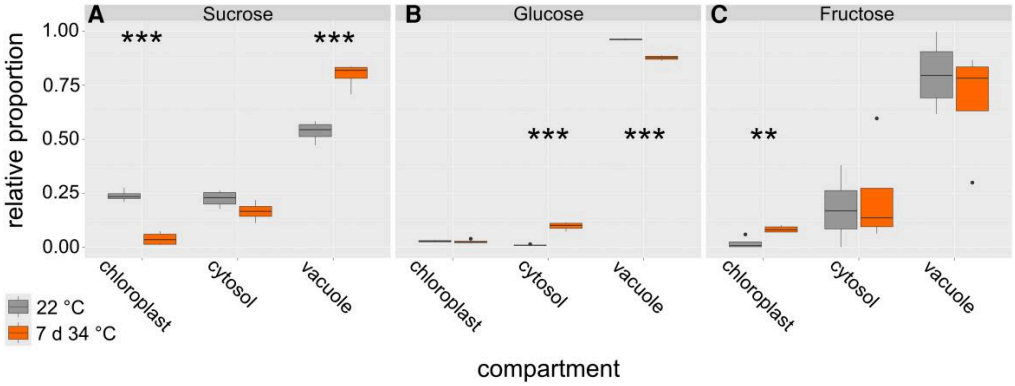

Figure 4. Effects of heat acclimation on subcellular distribution of soluble carbohydrates. Relative proportions for **(A)** sucrose, **(B)** glucose, and **(C)** fructose were resolved for chloroplasts, cytosol, and vacuole before (22 °C; gray boxes) and after heat acclimation at 7 d 34 °C (orange boxes). Asterisks indicate significance between both conditions (ANOVA and Tukey HSD post-hoc test; ** $P < 0.01$, *** $P < 0.001$), $n = 4$. Center line, median; box limits, upper and lower quartiles; whiskers, 1.5× interquartile range; points, outliers.

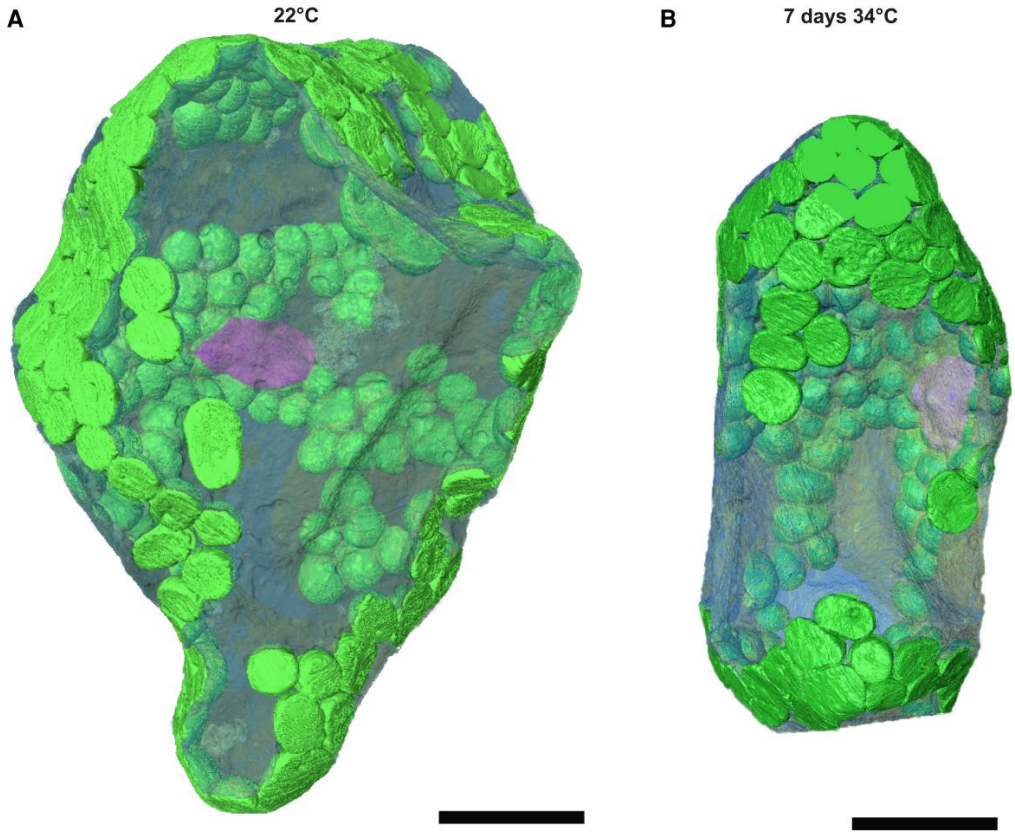

Figure 5. 3D models of mesophyll cells. **A)** Control (22 °C) mesophyll cell. **B)** Heat-treated (7 d at 34 °C) mesophyll cell. Chloroplasts are shown in green, the nucleus in pink, and the vacuole in translucent blue. The cytosol encompassing other organelles such as mitochondria, Golgi apparatus, or endoplasmic reticulum, surrounding the vacuole and the chloroplasts is omitted in this view. Scale bars: 20 μm.

tissue volume per gram dry weight was about 1.5-fold higher than in heat-treated plants. Considering the estimated porosity from SBF-SEM analysis, this finally allowed for estimating the volume of cell material which was 10,932 mm^3 gDW^{-1} at 22 °C and 8,267 mm^3 gDW^{-1} at 34 °C. This information was combined with the compartmental proportions to estimate volumes of chloroplasts, cytosol, and vacuole with the dimension of mL gDW^{-1} (Table 1).

This revealed that, although relative proportions of analyzed compartments remained stable under heat, absolute compartment volumes decreased by about 25% after 7 d at 34 °C due to a reduced volume of leaf tissue per gDW.

Table 1. Compartment volumes and leaf measures

Measurement	22 °C	34 °C
Proportion chloroplasts	13.89%	13.65%
Proportion cytosol	3.51%	3.63%
Proportion vacuole	82.6%	82.72%
Leaf height (mm) (*)	0.187 ± 0.005	0.138 ± 0.003
Leaf disc volume (mm^3) (*)	9.415 ± 0.240	6.916 ± 0.130
Dry weight per leaf disc (mg) (NS)	0.622 ± 0.017	0.645 ± 0.074
Volume per gDW ($mm^3\ g^{-1}$) (*)	15,131 ± 813	10,732 ± 1,616
Porosity (SBF-SEM)	27.8%	22.9%
Volume of gas space ($mm^3\ gDW^{-1}$)	4,199.5 ± 225.6	2,465.5 ± 371.3
Volume cell material ($mm^3\ gDW^{-1}$)	10,931.8 ± 587	8,266.5 ± 1,245
Estimated volume chloroplasts ($mL\ gDW^{-1}$)	1.52 ± 0.08	1.13 ± 0.17
Estimated volume cytosol ($mL\ gDW^{-1}$)	0.38 ± 0.02	0.30 ± 0.05
Estimated volume vacuole ($mL\ gDW^{-1}$)	9.03 ± 0.49	6.84 ± 1.03

Proportions in percent were determined from SBF-SEM data. For leaf material at 22 °C, 13 cells were evaluated in the resin block. For leaf material at 7 d 34 °C, 28 cells were evaluated in the resin block. Leaf height was derived from light micrographs. Leaf disc volume was calculated from leaf height and punchout size (4 mm radius, i.e. 50.26 mm^2 area). Dry weight (DW) per leaf disc was determined by drying and weighing leaf discs. Volume per gram DW was calculated from leaf disc volume and dry weight. The porosity was acquired from SBF-SEM data and used to determine the volume of cell material per gram DW. This volume and the compartment proportions were used to estimate the volume of the different cell compartments per gram DW. Detailed calculations are collected in the supplements (Supplementary Table S2). NS: nonsignificant difference between both conditions. (*) significant difference between both conditions (ANOVA, $P < 0.05$). Means ± SE.

Table 2. Percentage of cell types in a leaf section

Cell type	22 °C	34 °C
Palisade mesophyll (NS)	22.81 ± 2.68%	24.23 ± 1.24%
Spongy mesophyll (NS)	33.83 ± 2.68%	33.47 ± 1.11%
Epidermis (NS)	15.11 ± 1.18%	16.08 ± 1.89%
Vascular bundle (NS)	2.23 ± 0.95%	2.38 ± 1.44%
Porosity (NS)	26.01 ± 1.26%	23.84 ± 3.22%

The area of cell types was measured in light micrographs of semi-thin sections of embedded leaf material. Means ± SE, $n = 4$. NS: nonsignificant difference between both conditions (ANOVA, $P > 0.05$).

The percentage of different cell types in a sampled leaf was then determined by light microscopy (Table 2). This analysis revealed approximately 57% mesophyll cells, 15% epidermal cells, 2% vascular bundle cells, and 26% porosity at 22 °C. During heat, mesophyll and epidermal cell proportions slightly increased to 58% and 16%, respectively. Vascular bundles did not change, whereas the porosity decreased to 24%.

Combining the absolute sugar amounts with NAF-derived subcellular proportions revealed absolute sugar amounts of chloroplasts, cytosol, and vacuole at 22 °C and after 7 d at 34 °C (Fig. 6, A to C). Absolute sucrose amount differed significantly between both conditions across all compartments (Fig. 6A). The trend observed for relative proportions (see Fig. 4) was augmented, and cytosolic amounts now also differed significantly. Absolute amounts of glucose were significantly elevated due to heat acclimation across all compartments (Fig. 6B). In the vacuole, this contrasted the relative proportions which significantly decreased at 34 °C (compare Fig. 4B). However, due to a higher total amount of glucose under heat, this relative decrease still resulted in an absolute increase in the vacuolar compartment. Fructose was found to significantly accumulate in the vacuole which was not observed for relative proportions (compare Figs. 4C and 6C). As described for glucose, this was due to an increase in total fructose amounts. Yet, fructose dynamics were less significant than for glucose and sucrose.

Next, absolute compartment-specific sugar concentrations were derived from amounts normalized to estimated volumes of a mesophyll cell (Fig. 6, D to F). Interestingly, this emphasized accumulation effects in the cytosol which now also became significant for fructose (Fig. 6F). In general, while subcellular sugar amounts (in $\mu mol\ gDW^{-1}$) were highest in the vacuole, subcellular sugar concentrations (in mM) peaked in the cytosol which was due to the strong discrepancy of vacuolar and cytosolic volumes (see Table 1).

Heat-induced dynamics of enzyme activities in sucrose metabolism

Based on the observation that heat significantly affected the compartmentation of sucrose and its hydrolytic cleavage products glucose and fructose, activities of central enzymes of sucrose biosynthesis (SPS) and cleavage (neutral, acidic, and cell wall-associated invertases; nInv, aInv, cwInv) were quantified before and after 7 d at 34 °C (Fig. 7). Activities were normalized to the volume of leaf cells, i.e. 10.93 $mL\ gDW^{-1}$ at 22 °C and 8.26 $mL\ gDW^{-1}$ at 34 °C. The activities of SPS and nInv decreased significantly under heat (Fig. 7, A and B), while cwInv and aInv activities increased nonsignificantly (Fig. 7, C and D).

Enzyme activities were quantified under substrate saturation at temperature optimum, which was 25 °C for SPS and 30 °C for invertases, respectively. To adjust those activities to the growth temperature of the plants, activation enthalpies were applied and used to solve the Arrhenius equation (Arrhenius 1889; Equation (1)).

$$V_{max,\,adj} = C \cdot e^{-E_a/RT} \quad (1)$$

Here, C represents the Arrhenius factor, E_a is the activation energy, R is the gas constant, and T the temperature. The Arrhenius factor was estimated from experimentally determined enzyme activities at their temperature optimum as described earlier (Weiszmann et al. 2018; Supplementary Table S1). The adjustment to physiologically more relevant temperature regimes resulted in similar activities of SPS and nInv at 22 and 34 °C, respectively (Fig. 7, E and F). In contrast, adjustment resulted in significantly different activities of cwInv and aInv at 22 and 34 °C (Fig. 7, G and H). In summary, thermodynamic adjustment of enzyme activities revealed that both reactions located in the cytosol, SPS, and nInv, were efficiently stabilized under heat to maintain similar maximum enzyme activities as under 22 °C. In contrast, both enzymes located in acidic environments, i.e. apoplast (cwInv) and vacuole (aInv), significantly increased their maximum activities.

Using the subcellular concentrations of sucrose, glucose, and fructose together with adjusted activities of enzymes, in vivo rates of

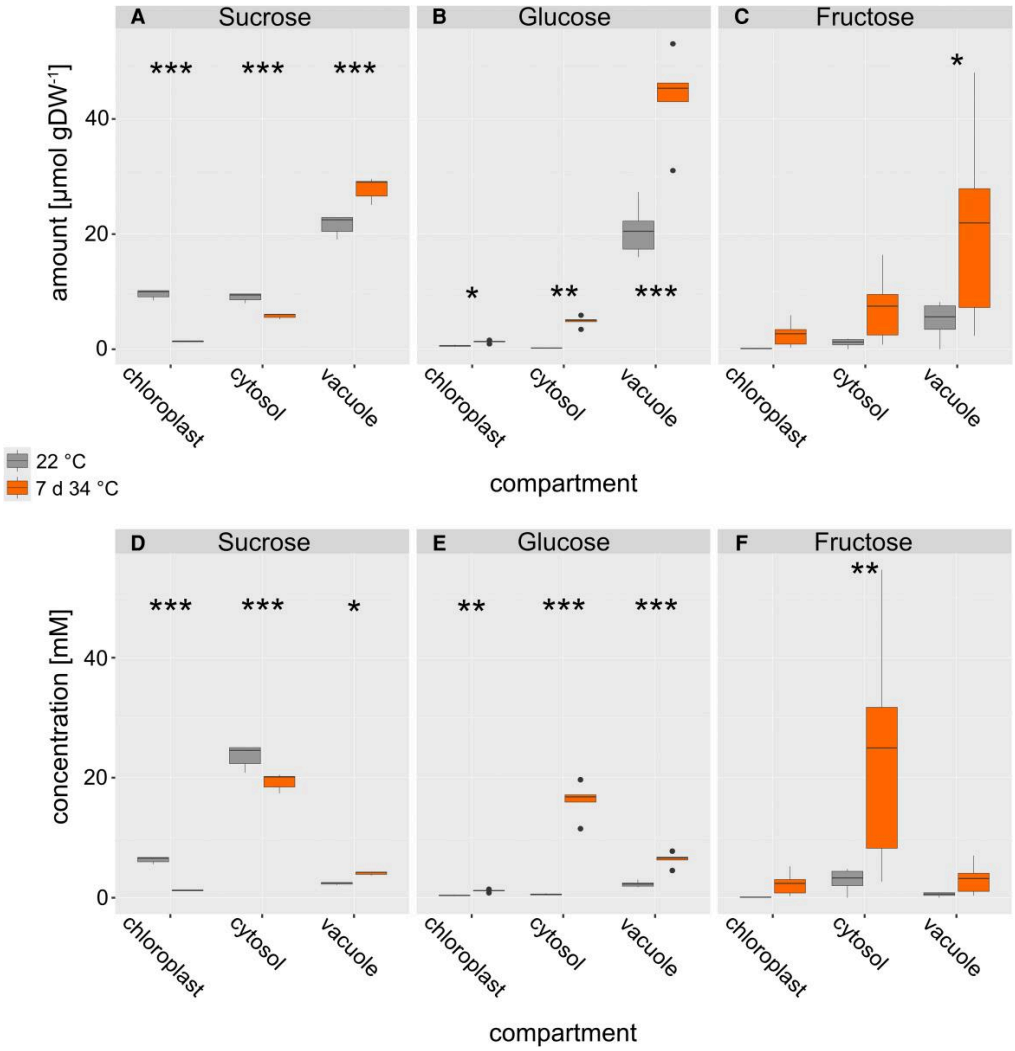

Figure 6. Compartment-specific sugar amounts and concentrations. Absolute amounts of sugars (µmol gDW^{-1}) in chloroplasts, cytosol, and vacuole are shown in the upper panels **(A** to **C)**, and concentrations (mM) are shown in the lower panels **(D** to **F)**. Gray boxes: 22 °C, orange boxes: 7 d at 34 °C. Asterisks indicate significance (ANOVA and Tukey HSD post-hoc test, * $P < 0.05$, ** $P < 0.01$, *** $P < 0.001$), $n = 5$. Center line, median; box limits, upper and lower quartiles; whiskers, 1.5× interquartile range; points, outliers. DW: dry weight.

cytosolic (nInv) and vacuolar (aInv) sucrose cleavage were estimated assuming Michaelis–Menten kinetics with competitive (Frc) and non-competitive (Glc) inhibition (Sturm 1999, Fig. 8). Simulations showed that, under heat, cytosolic rates of sucrose cleavage were dramatically reduced due to the increased cytosolic hexose feedback inhibition of nInv (Fig. 8B). For aInv, which represents soluble acidic invertases with vacuolar localization, V_{max} was significantly increased at 34 °C which resulted in a maintenance of sucrose cleavage rates (Fig. 8, C and D) although also vacuolar concentrations of Frc and Glc increased under these conditions (see Fig. 6).

Discussion

A changing temperature regime needs to be efficiently perceived and sensed by plants in order to initiate stress and acclimation response. Particularly, if temperature decreases or rises below or above critical values, molecular and physiological adjustments become essential to prevent irreversible cell and tissue damage. Adjustment and stabilization of photosynthesis and carbohydrate metabolism are central to temperature acclimation because a deflection of involved processes and pathways directly affects plant performance (Anderson et al. 1995; Qu et al. 2023). To quantify the heat tolerance of *A. thaliana* on levels of tissue structure and photosynthetic efficiency, electrolyte leakage assays were combined with measurements of F_v/F_m in the present study. While a 7-d acclimation period at 32 and 34 °C resulted in a significant reduction of leakage of leaf tissue when compared to nonacclimated plants, exposure to higher temperatures did not significantly improve tissue heat tolerance. Also, although F_v/F_m significantly dropped under all tested regimes of elevated temperature, it stabilized at ~0.75 (except for the 38 °C treatment) which still indicated a relatively high efficiency of photosystem II. The functionality of photosynthesis was further proved by NPS rates which were stabilized after acclimation at 34 °C. However, pulse amplitude modulation (PAM) measurements were conducted on green chlorophyll-containing tissue while growth phenotypes at 36 °C already showed pale areas (see

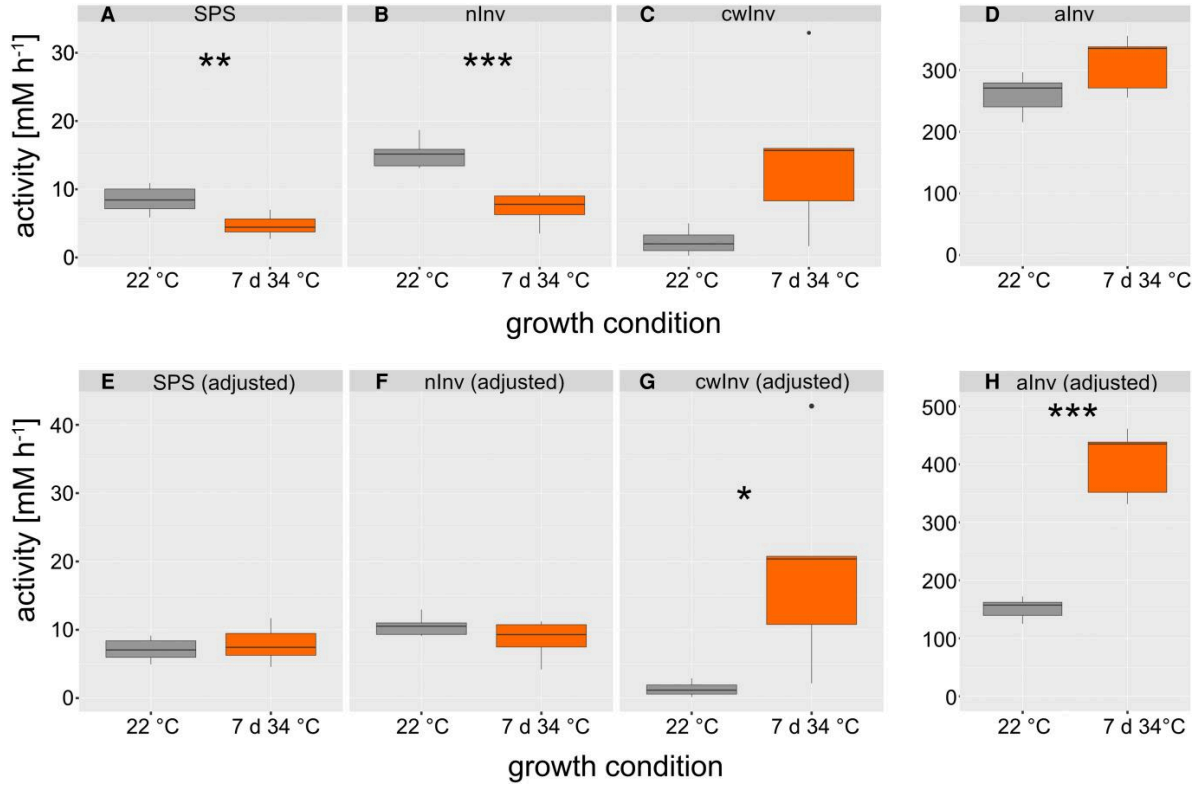

Figure 7. Activities of enzymes in sucrose metabolism. Invertase and SPS activity of plants grown at 22 °C (gray) and 34 °C acclimated plants (orange) were determined under substrate saturation (i.e. V_{max}). The upper panel **(A** to **D)** represents experimentally quantified activities at temperature optimum (SPS: 25 °C; invertases: 30 °C). The lower panel **(E** to **H)** shows activities which were adjusted to the growth temperatures using the Arrhenius equation (see main text). Asterisks indicate significance in Student's *t*-test (* $P < 0.05$, ** $P < 0.01$, *** $P < 0.001$), $n = 5$. Center line, median; box limits, upper and lower quartiles; whiskers, 1.5× interquartile range; points, outliers. nInv: neutral invertase; cwInv: cell wall-associated invertase; aInv: acidic invertase.

Supplementary Fig. S1), which are not reflected by these F_v/F_m values, and which were most probably a consequence of heat-induced senescence (Li et al. 2021). In summary, these findings suggest that heat exposure to temperatures between 32 and 34 °C significantly increases the heat tolerance of the plasma membrane of *A. thaliana*, which was not observed for higher temperatures. Heat-induced effects on F_v/F_m are robust across a wide range of acclimation temperatures which limits its applicability as a heat stress indicator. A limitation, which might affect the interpretation of heat-induced effects on photosynthesis and metabolism, was, however, the different developmental stages of 22 °C and 7 d heat-exposed plants. While plants at 22 °C were sampled and analyzed before bolting, heat-treated plants showed an inflorescence (see Supplementary Fig. S1). Such developmental differences might affect photosynthesis and metabolism (Rolland et al. 2006). However, as plant development directly depends on growth temperature (Ibañez et al. 2017), this could not be resolved in the chosen experimental setup, as a control experiment at 22 °C cannot be expected to result in the same developmental trajectory as under 32, 34, or 36 °C.

Relative proportions of subcellular compartments and leaf tissues remain constant during heat acclimation

Heat can influence the architecture of plant cells and the different organelles within, varying depending on the duration and severity of the heat exposure. In chloroplasts, grana thylakoids were found to disorganize and unstack during heat exposure, especially at temperatures higher than 34 °C, and plastoglobuli numbers and sizes were found to increase with acclimation temperature (Supplementary Fig. S3). This has also been reported before, together with swelling of chloroplasts and mitochondria due to heat exposure (Gounaris et al. 1984; Vani et al. 2001; Zhang et al. 2010; Grigorova et al. 2012; Zhang et al. 2014; Zou et al. 2017; Jampoh et al. 2023). The reconstruction of leaf cells based on SBF-SEM in the present study revealed constant relative proportions of chloroplasts (13% to 14%), cytosol (3% to 4%), and vacuole (82% to 83%) before and after heat acclimation at 34 °C. Previously, similar proportions were reported and summarized for *Arabidopsis* epidermal pavement cells and mesophyll cells under ambient temperature (Tolleter et al. 2024). In this study, the authors derived a relative chloroplast volume of 9.4%, a cytosol volume of 3.8%, and a vacuole volume of 84.3%. Thus, while cytosol and vacuole directly correspond to the percentage determined in the present study, estimations of chloroplast volumes differed by 4% to 5% between both studies. Main reasons for this discrepancy might be that Tolleter and colleagues assembled data from various studies. This might imply (slightly) different growth conditions which might directly affect compartment-specific volumes in the observed range of discrepancy. Further, in the present study, leaf tissue was sampled at the end of the night which differs from studies compiled in the cell atlas (Tolleter et al. 2024).

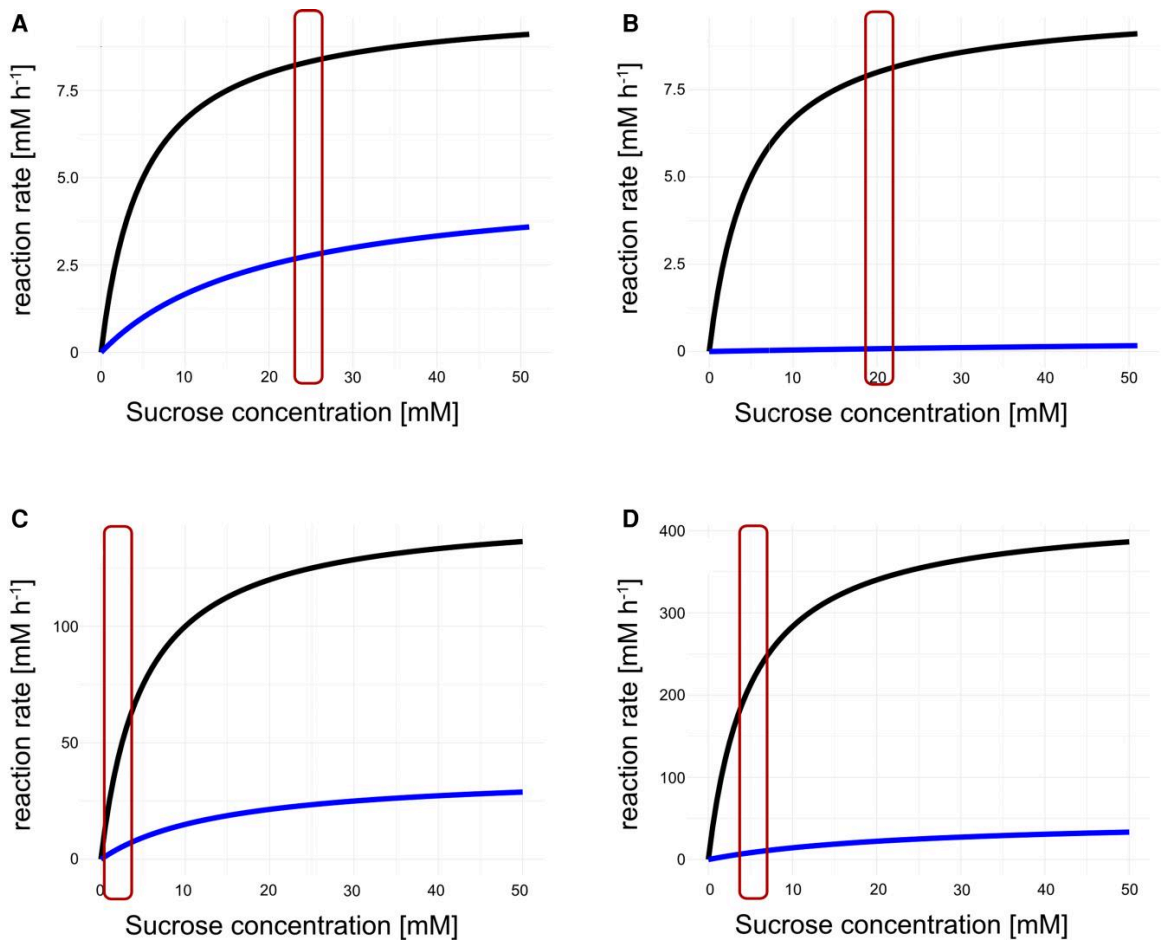

Figure 8. Simulation of Michaelis–Menten kinetics using subcellular metabolite concentrations and temperature-adjusted enzyme activities. **A)** Simulation of nInv catalyzed reaction at 22 °C, **B)** Simulation of nInv catalyzed reaction at 34 °C, **C)** Simulation of aInv catalyzed reaction at 22 °C, and **D)** Simulation of aInv catalyzed reaction at 34 °C. Black lines: no inhibition; Blue lines: combined competitive and noncompetitive inhibition by Frc and Glc, respectively. Red boxes indicate the relevant ranges of sucrose concentrations in vivo. Parameter settings are provided in the supplement (Supplementary Table S2). For simulations, the code for an R Shiny app is provided on GitHub: https://github.com/cellbiomaths/Shiny_MM_simulation).

Nevertheless, although this indicates that chloroplast volumes might be over- or underestimated by up to 5%, the consistency across cytosolic and vacuolar volume estimations provides evidence for the applicability and robustness of the presented cellular volume information. In contrast, leaf disc volumes decreased by ~30% in heat-acclimated plants while dry weight of the discs was not affected. This indicates a reduced (leaf) water content of heat-acclimated plants which might be due to higher transpiration rates under such conditions (Romero-Montepaone et al. 2021). Thus, while relative proportions of compartments remained constant, their absolute volumes decreased because of reduced total leaf tissue volume which suggests control of rather relative subcellular proportions than absolute compartment sizes. Similarly, also proportions of tissue types remained constant during heat acclimation (see Table 2). The proportions of palisade mesophyll, spongy mesophyll, epidermal tissue, and vascular bundles were similar before and after heat acclimation. We estimated porosity by 2D and 3D analysis to show the robustness of our results depending on the method. Both methods consistently showed a (nonsignificant) decrease in porosity during heat acclimation, ranging between 26% and 28% for leaf material at 22 °C and 23% and 24% after 7 d at 34 °C (see Tables 1 and 2). These estimates for plants grown at ambient temperature are in a similar range to those previously reported using microCT measurements of *A. thaliana* leaf discs (Dorca-Fornell et al. 2013; Lehmeier et al. 2017; Mathers et al. 2018).

In the present study, leaf cell structure was not analyzed for plants which were less efficiently heat acclimated, e.g. after 7 d at 36 °C. This leaves room for speculation if the observed proportional reduction of (sub)cellular structures and leaf tissue composition is a prerequisite for or a consequence of heat tolerance. Yet, as membrane remodeling was proven earlier to be essential for efficient heat acclimation (Kunst et al. 1989; Murakami et al. 2000; Shiva et al. 2020), the proportional reduction of compartment size might be accompanied by, or even facilitate, remodeling processes, e.g. changes in saturation degrees of membrane lipids and classes, due to reduced physical distances between membrane systems. Particularly, for vesicle trafficking and membrane contact-based lipid transfer (Shomo et al. 2024), such a reduction of physical distance might be beneficial. Finally, however,

follow-up studies need to validate if the observed changes significantly affect remodeling and/or transport processes, or if the proportional reduction results in a maintenance of the homeostasis before heat exposure.

Heat acclimation induces subcellular sugar allocation to stabilize sucrose metabolism during heat acclimation

A characteristic feature of eukaryotic cells is their compartmentation of metabolism which enables the separation and specification of pathways and their regulation (Hurry 2017). Carbohydrates are direct products of chloroplast-located photosynthetic CO_2 assimilation which, following the fixation and reduction reactions of the CBBC, are allocated to different subcellular compartments. This results in metabolite dynamics which are difficult to trace because transport processes across membrane systems and enzymatic interconversions are versatile (Sweetlove et al. 2017; Pommerrenig et al. 2018). The method of NAF enables the immediate and persistent quenching of enzymatic reactions which conserves the metabolic status at the sampling timepoint (Gerhardt and Heldt 1984). In the present study, NAF revealed that, under heat, relative sucrose proportions are significantly decreased in the chloroplast and significantly increased in the vacuole. Together with the absolutely quantified metabolite amounts, this resulted in a significant increase of sucrose and glucose amounts in the vacuole. While such a vacuolar shift has also been reported before for cold acclimation (Knaupp et al. 2011; Fürtauer et al. 2016), the observed plastidial depletion of sucrose during heat acclimation contrasted findings made for low temperature (Nägele and Heyer 2013). Together with members of the raffinose family oligosaccharides (RFOs), sucrose was shown to protect liposomes in vitro against damage by fusion which suggested also a protective function in vivo, e.g. under drought or freezing temperatures (Hincha et al. 2003; Knaupp et al. 2011). In contrast to cold or freezing, membrane fluidity is increased under heat which may not need the accumulation of sucrose or raffinose in the chloroplast to prevent fusion of thylakoid membranes. Instead, when subcellular sugar concentrations were calculated from total sugar amounts and estimated compartment volumes, cytosolic sucrose concentrations became highest under both 22 and 34 °C due to the comparatively low cytosolic volume. For glucose and fructose, a significant heat-induced cytosolic increase was observed which immediately raised the hypothesis of hexose accumulation due to affected invertase activity. Quantifying cytosolic neutral invertase activity revealed a stabilized activity between 22 and 34 °C, which became evident after normalization to leaf tissue volumes and correction for thermodynamic effects by applying the Arrhenius equation. Hence, although previous studies have shown that several proteins involved in carbon assimilation and metabolism are downregulated under heat stress, this might not necessarily result in a downregulation of the in vivo reaction rates due to additional thermodynamic effects (Ahsan et al. 2010). Vacuolar invertase activity was significantly elevated by heat exposure. This led to the hypothesis that sucrose is transported along its concentration gradient from the cytosol to the vacuole where it is cleaved hydrolytically to release glucose and fructose. Such metabolite transport across the tonoplast might be facilitated by monosaccharide transporters as explained and outlined before (see e.g. Pommerrenig et al. 2018). Data from the present study suggests a concentration gradient of sucrose from the cytosol to the vacuole of mesophyll cells. While this gradient remained similar under 22 °C and after 7 d at 34 °C, cytosolic glucose and fructose concentrations rose significantly under heat. Further, sucrose concentrations in the chloroplast dropped significantly under heat (see Fig. 6, D to F). It remains speculation in the present study, but such dynamics of plastidial and cytosolic sugar concentrations might result in, or be a consequence of, dynamics of membrane transport. Previous studies have shown and summarized potential candidates of sugar transporters across intracellular membrane systems, which strongly affect plant stress response, acclimation, and development (Klemens et al. 2013; Guo et al. 2023; Valifard et al. 2023). A decreasing sucrose concentration in the chloroplast might suggest a changing expression or activity of transport proteins located in the chloroplast envelope. Interestingly, the chloroplast sucrose exporter pSUT has previously been found to critically affect flowering and cold response (Patzke et al. 2019). Further, flowering has earlier been shown to be potently induced by elevated growth temperature (Balasubramanian et al. 2006). While, in the present study, we did not statistically uncouple plant development from heat exposure, it became obvious from the phenotypes that heat exposure at least temporally fell together with flowering (see Supplementary Fig. S1). As it was shown that suppressed pSUT expression results in impaired inflorescence development (Patzke et al. 2019), this further supports the hypothesis that pSUT expression and activity might critically affect development and acclimation under heat by modifying the sucrose concentration gradient across the chloroplast envelope.

Dynamics of both subcellular metabolite concentrations and enzyme activities result in dynamics of enzymatic reaction rates if metabolites act as substrates, products, or regulatory effectors of enzymes. The simulation of reaction rates catalyzed by neutral and acidic invertases showed that, under heat, neutral invertase flux became very low which was caused by the accumulation of hexoses in the cytosol which act as inhibitors (Sturm 1999). While also acidic invertase flux was affected by the heat-induced accumulation of hexoses in the vacuole, a strong and significant increase of V_{max} counteracted this inhibition resulting in similar reaction rates at 22 and 34 °C (see Fig. 8). Similarly, for plant cold acclimation, it was discussed earlier that temperature-induced shift of sucrose cleavage into the vacuolar compartment might stabilize metabolism and photosynthesis (Weiszmann et al. 2018). Together with the observed heat-induced depletion of plastidial sucrose concentration, these findings suggest that sucrose transport across the chloroplast envelope and tonoplast is coordinated with subcellular invertase activities during heat exposure to stabilize cytosolic sucrose concentration which plays a central role in regulation of photosynthesis, energy metabolism, and sink–source interactions (Ruan 2014).

Materials and methods

Plant material

Plants of *A. thaliana*, Columbia-0 (Col-0), were grown at 22 °C in the greenhouse (~100 to 125 μmol m^{-2} s^{-1}, ~12 h/12 h light/dark, 60% to 70% rel. humidity). After 4 weeks of growth, at the initial bolting stage, the control plants were harvested. For heat acclimation, plants were transferred to the respective temperature at a light intensity of 100 μmol m^{-2} s^{-1}, 12 h/12 h light/dark, 60% to 70% rel. humidity, and watered regularly to prevent drought stress. Temperature treatment included 32, 34, 36, and 38 °C. After 7 d of heat treatment, the plants were harvested. For 38 °C, harvesting took place after 3 d of heat treatment due to the high mortality of the plants beyond that timepoint. Harvesting for analysis of metabolism took place at mid-day, i.e. after 6 h in light, by cutting

the plants at the hypocotyl and plunge-freezing them in liquid nitrogen. The inflorescences, if established, were excluded from analysis. The frozen plant material was stored at −80 °C until it was ground to a fine powder and freeze-dried. Samples for electron microscopy were collected at the end of the night to prevent starch accumulation in the chloroplasts.

Electrolyte leakage

An electrolyte leakage assay was performed on intact leaves from control plants and acclimated plants. Two leaves per sample and 6 samples per temperature step ($n = 6$) were cut from 1 plant and fully submerged in 7 mL of distilled H_2O. The samples were heated to 46 °C for 0, 30, 45, and 60 min. They were cooled down and shaken overnight at room temperature. Then, 1 mL of water was taken from the samples, diluted 1:4 in H_2O and initial electrical conductivity $EC_{initial}$ ($\mu S\ cm^{-1}$) was determined. Then, the samples were heated to 95 °C for 1 h, and total electrical conductivity EC_{total} ($\mu S\ cm^{-1}$) was determined again. The index of injury I_d was calculated individually for the different timepoints with the fractional release of electrolytes from nonheated and heated samples, R_0 and R_t (Equations (2) and (3); Flint et al. 1967).

The index of injury I_d from exposure to temperature

$$I_d = 100\frac{R_t - R_0}{1 - R_0} \quad (2)$$

Fractional release of electrolytes from nonheated R_0 and heated sample R_t

$$R_0,\ R_t = \frac{EC_{initial}}{EC_{total}} \quad (3)$$

Chlorophyll fluorescence and gas exchange measurements

To evaluate the effect of prolonged heat exposure on photosystem II, maximum quantum yield (F_v/F_m) was recorded by supplying a saturating light pulse after 15 min of dark adaptation at 22 °C (WALZ JUNIOR-PAM; Heinz Walz GmbH, Germany). Gas exchange was quantified at 22 and 34 °C using the GFS-3000 with measuring head 3010-S (Heinz Walz GmbH, Germany).

Metabolite quantification

The amounts of carbohydrates were determined as described before (Kitashova et al. 2023). Soluble carbohydrates were extracted twice with 400 µL 80% ethanol at 80 °C for 30 min. The supernatants were combined and dried for sugar analysis. The pellet was used for starch quantification by amyloglucosidase digestion and photometric detection of glucose equivalents by a coupled glucose oxidase/peroxidase/o-dianisidine reaction. Sucrose content was determined by an anthrone assay, whereas glucose concentration was determined by a coupled hexokinase/glucose-6-phosphate dehydrogenase assay, utilizing absorption measurement of produced $NADPH + H^+$. Fructose quantification followed glucose quantification by the addition of phosphoglucose isomerase (PGI) to the reaction buffer.

Invertase and SPS activity measurements

The activities of vacuolar (acidic), cytosolic (neutral), and cell wall-bound invertases, as well as of SPS, were quantified as described earlier with slight modifications (Nägele et al. 2012; Kitashova et al. 2023). Invertases were extracted on ice in extraction buffer (50 mM HEPES-KOH, pH 7.5, 5 mM $MgCl_2$, 2 mM ethylenediaminetetraacetic acid (EDTA), 1 mM phenylmethylsulfonylfluoride, 1 mM dithiothreitol (DTT), 0.1% (v/v) Triton-X-100, 10% (v/v) glycerol). After centrifugation, the supernatant was analyzed for vacuolar and cytosolic invertases, whereas the pellet was resuspended in an extraction buffer to analyze the cell wall-bound invertase activity. After the incubation of the supernatant at 30 °C in an acidic reaction buffer (20 mM sodium acetate, pH 4.7, 100 mM sucrose) for vacuolar and cell wall invertase measurements, or a neutral reaction buffer (20 mM HEPES-KOH, pH 7.5, 100 mM sucrose) for cytosolic invertase, the solution was neutralized with 1 M NaH_2PO_4, heated to 95 °C to stop the enzymatic reaction, and centrifuged. The glucose content in the supernatant was quantified photometrically by a coupled glucose oxidase/peroxidase/o-dianisidine reaction.

SPS was extracted in the extraction buffer (50 mM HEPES-KOH, pH 7.5, 20 mM $MgCl_2$, 1 mM EDTA, 2.7 mM DTT, 10% (v/v) glycerol, and 0.1% (v/v) Triton-X-100) on ice and centrifuged. The supernatant was incubated with a reaction buffer (50 mM HEPES-KOH, pH 7.5, 15 mM $MgCl_2$, 3 mM DTT, 35 mM uridine diphosphate [UDP]-glucose, 35 mM fructose-6-phosphate, and 140 mM glucose-6-phosphate) at 25 °C and the reaction was stopped by adding 30% KOH and heating the solution to 95 °C. Sucrose was quantified photometrically with an anthrone assay.

Nonaqueous fractionation

NAF was performed as described previously (Fürtauer et al. 2016; Hernandez et al. 2023). Briefly, 10 to 15 mg of lyophilized plant material was suspended in 1 mL of heptane (C_7H_{16}; "7H") -tetrachlorethylene (C_2Cl_4; "TCE") mixture with a density of $\rho = 1.35\ g\ cm^{-3}$ and sonicated on ice in 30 s pulses with pauses of 1 min for a total of 20 min (Hielscher UP200St Ultrasonic Homogenizer, 170 W, 100% power setting; Hielscher Ultrasonics GmbH, Teltow, Germany). The sonicated material was centrifuged for 20 min at 4 °C and 20,000×*g*. The supernatant was stored on ice and the pellet was suspended in a 7H-TCE mixture of higher density and sonicated for 10 s to facilitate the dissolving of the pellet. Subsequently, the material was centrifuged, and the new pellet was suspended in a higher density 7H-TCE mixture. This process was repeated with mixtures of increasing density, ranging from $\rho = 1.35$ to $1.6\ g\ cm^{-3}$. The fractions were split equally and dried in a vacuum desiccator. Pellets were stored at −20 °C until subsequent analysis. One aliquot per sample was used for photometric marker enzyme measurements for vacuole, cytosol, and chloroplast and the other for photometric evaluation of sugar content.

Marker enzyme activities

For photometric measurement of marker enzyme activities, the dried pellets of fractions were suspended in 750 µL extraction buffer (50 mM Tris-HCl, pH 7.3, 5 mM $MgCl_2$, 1 mM DTT), incubated on ice for 10 min and centrifuged at 4 °C and 20,000×*g* for 10 min. The supernatant was used for enzyme activity quantification. Plastidial pyrophosphatase was used as a marker enzyme for the chloroplast, cytosolic UDP glucose pyrophosphorylase (UGPase) for the cytosol, and vacuolar acidic phosphatase for the vacuole (Fürtauer et al. 2019). Plastidial pyrophosphatase was assayed as described earlier (Jelitto et al. 1992) and inorganic phosphate was detected by molybdenum blue reaction (Murphy and Riley 1962). UGPase was quantified photometrically as described before (Zrenner et al. 1993). Acidic phosphatase from the vacuole was measured according to Boller and Kende (1979), with some modifications. The assay buffer consisted of 125 mM sodium acetate and 0.125% Triton-X 100 and was

adjusted to pH 4.8 with acetic acid, whereas the substrate for the detection was composed of 1 mg mL^{-1} 4-nitrophenylphosphate in the assay buffer.

Sample fixation for microscopy

Several leaves per plant were fixed for microscopy. The plants were harvested at the end of the dark period to minimize starch content in the plastids, which improves the visibility of thylakoid membranes. The leaves were cut into 1 mm^2 pieces in fixation buffer (75 mM cacodylate, 2 mM $MgCl_2$, pH 7.0) supplemented with 2.5% glutaraldehyde and stored at 4 °C for several days until further processing.

Light and transmission electron microscopy

For light and transmission electron microscopy (TEM), fixation was carried out as described before (Garcia-Molina et al. 2021). After postfixation with 1% (w/v) OsO_4, the samples were contrasted en bloc with 1% (w/v) uranyl acetate in 20% acetone, dehydrated with a graded acetone series and embedded in Spurr's resin of medium rigidity (Spurr 1969). For TEM, ultrathin sections of approximately 60 nm were contrasted with lead citrate (Reynolds 1963) and examined with a Zeiss EM 912 transmission electron microscope with an integrated OMEGA energy filter, operated at 80 kV in the zero-loss mode (Carl Zeiss AG, Oberkochen, Germany). Images were acquired with a 2k × 2k slow-scan CCD camera (TRS Tröndle Restlichtverstärkersysteme, Moorenweis, Germany). For light microscopy, semi-thin sections of 1 μm were examined with a Zeiss Axiophot microscope and a SPOT Insight camera.

Serial block-face scanning electron microscopy

For SBF-SEM, 1 mm^2 pieces of *A. thaliana* leaves were fixed and stained following a protocol based on Hua et al. (2015). In brief, with intermittent washing steps, the samples were fixed as described above, treated with 2% OsO_4 + 1.5% potassium ferrocyanide on ice, with thiocarbohydracid solution at RT, again 2% OsO_4, 1% uranyl acetate, then lead aspartate at 60 °C. Following an ascending ethanol and acetone series, the samples were embedded in epon resin hard 812, mounted on aluminum stubs with conductive glue, trimmed to 500 μm cubes, and sputtered with 20 nm gold.

Serial sectioning and imaging took place on a ThermoFisher Apreo VS block-face scanning electron microscope (Thermo Fisher Scientific Inc., Waltham, USA) in low vacuum at 2.1 kV, 100 to 200 pA and a pixel dwell time of 3 μs. Digital image stacks (grayscale, 8 bit) of 8,192 × 8,192 pixels at 20 nm pixel size and 40 nm cutting thickness were generated and postaligned with Fiji, with stack 1 amounting to 1,872 planes and stack 2 amounting to 1,450 planes.

Segmentation of cellular compartments

The SBF-SEM image stacks were processed with the Amira Pro software (Versions 2019-2024.1, Thermo Fisher Scientific). In a fraction of the 2 datasets, chloroplasts, vacuole, cytoplasm, and nucleus were segmented manually with a graphic tablet. Smaller organelles such as mitochondria, peroxisomes, Golgi apparatus, and endoplasmic reticulum were not segmented but were included in the cytoplasm material. The Python Deep Learning environment of Amira was utilized for automated segmentation of the datasets with the manually segmented data serving as ground truth. Learning settings were adjusted between training steps and are summarized in Supplementary Table S3. The resulting labels were checked for mislabeling and corrected manually.

Data analysis and calculation of subcellular volumes

Subcellular sugar content was correlated to the marker enzyme measurements with the "NAFalyzer" app to estimate subcellular sugar concentrations relative to sample dry weight (Hernandez et al. 2023). The relative distribution of marker enzyme activities was correlated with metabolite abundances. For both conditions, i.e. 22 °C and 7 d 34 °C, plastidial marker enzymes showed a peak at the lowest density, $\rho = 1.35$ g cm^{-3}. In contrast, vacuolar marker enzyme activities peaked at the highest density, i.e. $\rho = 1.60$ g cm^{-3}. The distribution of the cytosolic marker was similar across all fractions but rather peaked at $\rho = 1.40$ to 1.45 g cm^{-3} (Supplementary Fig. S4). Hence, although each fraction contained a mixture of marker enzyme activities, these different distributions of marker enzymes across all fractions allowed for a reliable estimation of compartment-specific metabolite concentrations (Gerhardt and Heldt 1984).

Leaf discs of 4 mm radius were punched out and subsequently dried to quantify fresh and dry weight ($n = 45$). Average leaf height ($n \geq 22$) from light micrographs was multiplied with disc size to determine the leaf disc volume. The volume-to-dry weight ratio was calculated and corrected for gas space, i.e. porosity and percentage of the segmented SBF-SEM dataset. The volume per dry weight ratio of plastids, cytosol, and vacuole was calculated from the percentages of the compartments from the SBF-SEM dataset and further combined with the subcellular sugar amount to calculate the absolute subcellular sugar concentrations in mM (Supplementary Tables S4 and S5). The percentage of cell types in the leaf was measured in light microscopic images of semi-thin sections of embedded leaf material ($n = 4$). The area of different cell types was measured in Fiji with the help of the standard measurement tool and a graphic tablet. Image analysis of electron and light micrographs was carried out with Fiji. Data analysis and statistics were carried out with R (The R Project for Statistical Computing; https://www.r-project.org) and Microsoft Excel (https://www.microsoft.com). The development of the R shiny app for the simulation of Michaelis–Menten kinetics was supported by ChatGPT (October 2024). The code is provided via GitHub: https://github.com/cellbiomaths/Shiny_MM_simulation.

Acknowledgments

We thank all members of Plant Evolutionary Cell Biology and Plant Development at LMU München for constructive discussions and advice. We also thank Kareem Farghaly, Keshav Goyal, Niklas Kroll, Marius Kröll, and Suet Ying Wong for help with the annotation of the microscopy datasets.

Author contributions

C.S. performed leakage and PAM assay, NAF analysis, microscopy, data analysis, and wrote the paper. M.H. performed SBF-SEM microscopy. L.S. quantified enzyme activities. A.K. supervised and supported microscopy. T.N. conceived the study, analyzed data, developed the R Shiny app, and wrote the paper.

Supplementary data

The following materials are available in the online version of this article.

Supplementary Table S1. Temperature correction of enzyme activities.

Supplementary Table S2. Enzyme parameters for invertase simulations.

Supplementary Table S3. Settings for the "DL Training Segmentation 2D" module in Amira Pro for AI-based segmentation.

Supplementary Table S4. Data and calculation of subcellular volumes.

Supplementary Table S5. Total and subcellular metabolite amounts, relative distributions, and concentrations.

Supplementary Figure S1. Plant phenotypes after heat treatment.

Supplementary Figure S2. SBF-SEM imaging of plant tissue.

Supplementary Figure S3. Light and electron micrographs of control and heat-treated leaves of *Arabidopsis thaliana*.

Supplementary Figure S4. Relative distribution of marker enzyme activities across nonaqueous density fractions.

Funding

This work was supported by Deutsche Forschungsgemeinschaft (DFG, German Research Foundation)—INST86/1940-1 FUGG and TRR175/D03.

Conflict of interest statement. None declared.

Data availability

Data is provided in the supplements and, on request, by the corresponding authors. The code of the R Shiny app for kinetic simulations is provided on GitHub, https://github.com/cellbiomaths/Shiny_MM_simulation.

References

Ahsan N, Donnart T, Nouri MZ, Komatsu S. Tissue-specific defense and thermo-adaptive mechanisms of soybean seedlings under heat stress revealed by proteomic approach. *J Proteome Res*. 2010:9(8):4189–4204. https://doi.org/10.1021/pr100504j

Anderson JM, Chow WS, Park Y-I. The grand design of photosynthesis: acclimation of the photosynthetic apparatus to environmental cues. *Photosynth Res*. 1995:46(1–2):129–139. https://doi.org/10.1007/BF00020423

Arrhenius S. Über die Reaktionsgeschwindigkeit bei der Inversion von Rohrzucker durch Säuren. *Z Phys Chem*. 1889:4(1):226–248. https://doi.org/10.1515/zpch-1889-0416

Balasubramanian S, Sureshkumar S, Lempe J, Weigel D. Potent induction of *Arabidopsis thaliana* flowering by elevated growth temperature. *PLoS Genet*. 2006:2(7):e106. https://doi.org/10.1371/journal.pgen.0020106

Berry J, Björkman O. Photosynthetic response and adaptation to temperature in higher plants. *Ann Rev Plant Physiol*. 1980:31(1):491–543. https://doi.org/10.1146/annurev.pp.31.060180.002423

Boller T, Kende H. Hydrolytic enzymes in the central vacuole of plant cells. *Plant Physiol*. 1979:63(6):1123–1132. https://doi.org/10.1104/pp.63.6.1123

Bukhov NG, Samson G, Carpentier R. Nonphotosynthetic reduction of the intersystem electron transport chain of chloroplasts following heat stress. Steady-state rate. *Photochem Photobiol*. 2000:72(3):351–357. https://doi.org/10.1562/0031-8655(2000)0720351NROTIE2.0.CO2

Bukhov NG, Wiese C, Neimanis S, Heber U. Heat sensitivity of chloroplasts and leaves: leakage of protons from thylakoids and reversible activation of cyclic electron transport. *Photosynth Res*. 1999:59(1):81–93. https://doi.org/10.1023/A:1006149317411

Crafts-Brandner SJ, Salvucci ME. Rubisco activase constrains the photosynthetic potential of leaves at high temperature and CO_2. *Proc Natl Acad Sci U S A*. 2000:97(24):13430–13435. https://doi.org/10.1073/pnas.230451497

Dorca-Fornell C, Pajor R, Lehmeier C, Pérez-Bueno M, Bauch M, Sloan J, Osborne C, Rolfe S, Sturrock C, Mooney S, *et al.* Increased leaf mesophyll porosity following transient retinoblastoma-related protein silencing is revealed by microcomputed tomography imaging and leads to a system-level physiological response to the altered cell division pattern. *Plant J*. 2013:76(6):914–929. https://doi.org/10.1111/tpj.12342

Flint HL, Boyce BR, Beattie DJ. Index of injury—a useful expression of freezing injury to plant tissues as determined by the electrolytic method. *Can J Plant Sci*. 1967:47(2):229–230. https://doi.org/10.4141/cjps67-043

Fürtauer L, Küstner L, Weckwerth W, Heyer AG, Nägele T. Resolving subcellular plant metabolism. *Plant J*. 2019:100(3):438–455. https://doi.org/10.1111/tpj.14472

Fürtauer L, Weckwerth W, Nägele T. A benchtop fractionation procedure for subcellular analysis of the plant metabolome. *Front Plant Sci*. 2016:7:1912. https://doi.org/10.3389/fpls.2016.01912

Gampe D, Zscheischler J, Reichstein M, O'Sullivan M, Smith WK, Sitch S, Buermann W. Increasing impact of warm droughts on northern ecosystem productivity over recent decades. *Nat Clim Change*. 2021:11(9):772–779. https://doi.org/10.1038/s41558-021-01112-8

Garcia-Molina A, Kleine T, Schneider K, Mühlhaus T, Lehmann M, Leister D. Translational components contribute to acclimation responses to high light, heat, and cold in *Arabidopsis*. *iScience*. 2020:23(7):101331. https://doi.org/10.1016/j.isci.2020.101331

Garcia-Molina A, Lehmann M, Schneider K, Klingl A, Leister D. Inactivation of cytosolic FUMARASE2 enhances growth and photosynthesis under simultaneous copper and iron deprivation in *Arabidopsis*. *Plant J*. 2021:106(3):766–784. https://doi.org/10.1111/tpj.15199

Gerhardt R, Heldt HW. Measurement of subcellular metabolite levels in leaves by fractionation of freeze-stopped material in nonaqueous media. *Plant Physiol*. 1984:75(3):542–547. https://doi.org/10.1104/pp.75.3.542

Gounaris K, Brain APR, Quinn PJ, Williams WP. Structural reorganisation of chloroplast thylakoid membranes in response to heat-stress. *Biochim Biophys Acta*. 1984:766(1):198–208. https://doi.org/10.1016/0005-2728(84)90232-9

Grigorova B, Vassileva V, Klimchuk D, Vaseva I, Demirevska K, Feller U. Drought, high temperature, and their combination affect ultrastructure of chloroplasts and mitochondria in wheat (*Triticum aestivum* L.) leaves. *J Plant Interact*. 2012:7(3):204–213. https://doi.org/10.1080/17429145.2011.654134

Guo W-J, Pommerrenig B, Neuhaus HE, Keller I. Interaction between sugar transport and plant development. *J Plant Physiol*. 2023:288:154073. https://doi.org/10.1016/j.jplph.2023.154073

Havaux M. Short-term responses of photosystem I to heat stress. *Photosynth Res*. 1996:47(1):85–97. https://doi.org/10.1007/BF00017756

Hernandez JS, Dziubek D, Schröder L, Seydel C, Kitashova A, Brodsky V, Nägele T. Natural variation of temperature acclimation of *Arabidopsis thaliana*. *Physiol Plant*. 2023:175(6):e14106. https://doi.org/10.1111/ppl.14106

Herrmann HA, Schwartz JM, Johnson GN. Metabolic acclimation – a key to enhancing photosynthesis in changing environments? *J Exp Bot*. 2019:70(12):3043–3056. https://doi.org/10.1093/jxb/erz157

Hincha DK, Zuther E, Heyer AG. The preservation of liposomes by raffinose family oligosaccharides during drying is mediated by effects on fusion and lipid phase transitions. *Biochim Biophys*

Acta. 2003:1612(2):172–177. https://doi.org/10.1016/S0005-2736(03)00116-0

Hua Y, Laserstein P, Helmstaedter M. Large-volume en-bloc staining for electron microscopy-based connectomics. *Nat Commun*. 2015:6(1):7923. https://doi.org/10.1038/ncomms8923

Hurry V. Metabolic reprogramming in response to cold stress is like real estate, it's all about location. *Plant Cell Environ*. 2017:40(5):599–601. https://doi.org/10.1111/pce.12923

Iba K. Acclimative response to temperature stress in higher plants: approaches of gene engineering for temperature tolerance. *Annu Rev Plant Biol*. 2002:53(1):225–245. https://doi.org/10.1146/annurev.arplant.53.100201.160729

Ibañez C, Poeschl Y, Peterson T, Bellstädt J, Denk K, Gogol-Döring A, Quint M, Delker C. Ambient temperature and genotype differentially affect developmental and phenotypic plasticity in *Arabidopsis thaliana*. *BMC Plant Biol*. 2017:17(1):114. https://doi.org/10.1186/s12870-017-1068-5

Jampoh EA, Safran E, Babinyec-Czifra D, Kristof Z, Krarne Pentek B, Fabian A, Barnabas B, Jager K. Morpho-anatomical, physiological and biochemical adjustments in response to heat and drought co-stress in winter barley. *Plants (Basel)*. 2023:12(22):3907. https://doi.org/10.3390/plants12223907

Jelitto T, Sonnewald U, Willmitzer L, Hajirezeai M, Stitt M. Inorganic pyrophosphate content and metabolites in potato and tobacco plants expressing *E. coli* pyrophosphatase in their cytosol. *Planta*. 1992:188(2):238–244. https://doi.org/10.1007/BF00216819

Kitashova A, Adler SO, Richter AS, Eberlein S, Dziubek D, Klipp E, Nägele T. Limitation of sucrose biosynthesis shapes carbon partitioning during plant cold acclimation. *Plant Cell Environ*. 2023:46(2):464–478. https://doi.org/10.1111/pce.14483

Klemens PAW, Patzke K, Deitmer J, Spinner L, Le Hir R, Bellini C, Bedu M, Chardon F, Krapp A, Neuhaus HE. Overexpression of the vacuolar sugar carrier AtSWEET16 modifies germination, growth, and stress tolerance in *Arabidopsis*. *Plant Physiol*. 2013:163(3):1338–1352. https://doi.org/10.1104/pp.113.224972

Knaupp M, Mishra KB, Nedbal L, Heyer AG. Evidence for a role of raffinose in stabilizing photosystem II during freeze-thaw cycles. *Planta*. 2011:234(3):477–486. https://doi.org/10.1007/s00425-011-1413-0

Kunst L, Browse J, Somerville C. Enhanced thermal tolerance in a mutant of *Arabidopsis* deficient in palmitic acid unsaturation. *Plant Physiol*. 1989:91(1):401–408. https://doi.org/10.1104/pp.91.1.401

Law DR, Crafts-Brandner SJ. Inhibition and acclimation of photosynthesis to heat stress is closely correlated with activation of ribulose-1,5-bisphosphate carboxylase/oxygenase. *Plant Physiol*. 1999:120(1):173–181. https://doi.org/10.1104/pp.120.1.173

Lehmeier C, Pajor R, Lundgren MR, Mathers A, Sloan J, Bauch M, Mitchell A, Bellasio C, Green A, Bouyer D, *et al.* Cell density and airspace patterning in the leaf can be manipulated to increase leaf photosynthetic capacity. *Plant J*. 2017:92(6):981–994. https://doi.org/10.1111/tpj.13727

Li N, Bo C, Zhang Y, Wang L. PHYTOCHROME INTERACTING FACTORS PIF4 and PIF5 promote heat stress induced leaf senescence in *Arabidopsis*. *J Exp Bot*. 2021:72(12):4577–4589. https://doi.org/10.1093/jxb/erab158

Lippmann R, Babben S, Menger A, Delker C, Quint M. Development of wild and cultivated plants under global warming conditions. *Curr Biol*. 2019:29(24):R1326–R1338. https://doi.org/10.1016/j.cub.2019.10.016

Lunn JE. Compartmentation in plant metabolism. *J Exp Bot*. 2007:58(1):35–47. https://doi.org/10.1093/jxb/erl134

Mathers AW, Hepworth C, Baillie AL, Sloan J, Jones H, Lundgren M, Fleming AJ, Mooney SJ, Sturrock CJ. Investigating the microstructure of plant leaves in 3D with lab-based X-ray computed tomography. *Plant Methods*. 2018:14(1):99. https://doi.org/10.1186/s13007-018-0367-7

Murakami Y, Tsuyama M, Kobayashi Y, Kodama H, Iba K. Trienoic fatty acids and plant tolerance of high temperature. *Science*. 2000:287(5452):476–479. https://doi.org/10.1126/science.287.5452.476

Murphy J, Riley JP. A modified single solution method for the determination of phosphate in natural waters. *Anal Chim Acta*. 1962:27:31–36. https://doi.org/10.1016/S0003-2670(00)88444-5

Nägele T, Heyer AG. Approximating subcellular organisation of carbohydrate metabolism during cold acclimation in different natural accessions of *Arabidopsis thaliana*. *New Phytol*. 2013:198(3):777–787. https://doi.org/10.1111/nph.12201

Nägele T, Stutz S, Hörmiller II, Heyer AG. Identification of a metabolic bottleneck for cold acclimation in *Arabidopsis thaliana*. *Plant J*. 2012:72(1):102–114. https://doi.org/10.1111/j.1365-313X.2012.05064.x

Olas JJ, Apelt F, Annunziata MG, John S, Richard SI, Gupta S, Kragler F, Balazadeh S, Mueller-Roeber B. Primary carbohydrate metabolism genes participate in heat-stress memory at the shoot apical meristem of *Arabidopsis thaliana*. *Mol Plant*. 2021:14(9):1508–1524. https://doi.org/10.1016/j.molp.2021.05.024

Pastenes C, Horton P. Effect of high temperature on photosynthesis in beans—II. CO_2 assimilation and metabolite contents. *Plant Physiol*. 1996:112:1253–1260. https://doi.org/10.1104/pp.112.3.1253

Patzke K, Prananingrum P, Klemens PAW, Trentmann O, Rodrigues CM, Keller I, Fernie AR, Geigenberger P, Bölter B, Lehmann M, *et al.* The plastidic sugar transporter pSuT influences flowering and affects cold responses. *Plant Physiol*. 2019:179(2):569–587. https://doi.org/10.1104/pp.18.01036

Pommerrenig B, Ludewig F, Cvetkovic J, Trentmann O, Klemens PAW, Neuhaus HE. In concert: orchestrated changes in carbohydrate homeostasis are critical for plant abiotic stress tolerance. *Plant Cell Physiol*. 2018:59(7):1290–1299. https://doi.org/10.1093/pcp/pcy037

Qu AL, Ding YF, Jiang Q, Zhu C. Molecular mechanisms of the plant heat stress response. *Biochem Biophys Res Commun*. 2013:432(2):203–207. https://doi.org/10.1016/j.bbrc.2013.01.104

Qu Y, Mueller-Cajar O, Yamori W. Improving plant heat tolerance through modification of Rubisco activase in C3 plants to secure crop yield and food security in a future warming world. *J Exp Bot*. 2023:74(2):591–599. https://doi.org/10.1093/jxb/erac340

Ranty B, Aldon D, Cotelle V, Galaud JP, Thuleau P, Mazars C. Calcium sensors as key hubs in plant responses to biotic and abiotic stresses. *Front Plant Sci*. 2016:7:327. https://doi.org/10.3389/fpls.2016.00327

Reynolds ES. The use of lead citrate at high pH as an electron-opaque stain in electron microscopy. *J Cell Biol*. 1963:17(1):208–212. https://doi.org/10.1083/jcb.17.1.208

Rolland F, Baena-Gonzalez E, Sheen J. Sugar sensing and signaling in plants: conserved and novel mechanisms. *Annu Rev Plant Biol*. 2006:57:675–709. https://doi.org/10.1146/annurev.arplant.57.032905.105441

Romero-Montepaone S, Sellaro R, Esteban Hernando C, Costigliolo-Rojas C, Bianchimano L, Ploschuk EL, Yanovsky MJ, Casal JJ. Functional convergence of growth responses to shade and warmth in *Arabidopsis*. *New Phytol*. 2021:231(5):1890–1905. https://doi.org/10.1111/nph.17430

Ruan YL. Sucrose metabolism: gateway to diverse carbon use and sugar signaling. *Annu Rev Plant Biol*. 2014:65(1):33–67. https://doi.org/10.1146/annurev-arplant-050213-040251

Sajid M, Rashid B, Ali Q, Husnain T. Mechanisms of heat sensing and responses in plants. It is not all about Ca^{2+} ions. *Biol Plant*. 2018:62(3):409–420. https://doi.org/10.1007/s10535-018-0795-2

Salvucci ME, Crafts-Brandner SJ. Inhibition of photosynthesis by heat stress: the activation state of Rubisco as a limiting factor in photosynthesis. *Physiol Plant*. 2004:120(2):179–186. https://doi.org/10.1111/j.0031-9317.2004.0173.x

Seydel C, Kitashova A, Fürtauer L, Nägele T. Temperature-induced dynamics of plant carbohydrate metabolism. *Physiol Plant*. 2022:174(1):e13602. https://doi.org/10.1111/ppl.13602

Shiva S, Samarakoon T, Lowe KA, Roach C, Vu HS, Colter M, Porras H, Hwang C, Roth MR, Tamura P, *et al*. Leaf lipid alterations in response to heat stress of *Arabidopsis thaliana*. *Plants*. 2020:9(7):845. 10.3390/plants9070845

Shomo ZD, Li F, Smith CN, Edmonds SR, Roston RL. From sensing to acclimation: the role of membrane lipid remodeling in plant responses to low temperatures. *Plant Physiol*. 2024:196(3):1737–1757. https://doi.org/10.1093/plphys/kiae382

Spurr A. A low-viscosity epoxy resin embedding medium for electron microscopy. *J Ultrastruc Res*. 1969:26(1–2):31–43. https://doi.org/10.1016/S0022-5320(69)90033-1

Sturm A. Invertases. Primary structures, functions, and roles in plant development and sucrose partitioning. *Plant Physiol*. 1999:121(1):1–8. https://doi.org/10.1104/pp.121.1.1

Sweetlove LJ, Nielsen J, Fernie AR. Engineering central metabolism—a grand challenge for plant biologists. *Plant J*. 2017:90(4):749–763. https://doi.org/10.1111/tpj.13464

Terzaghi WB, Fork DC, Berry JA, Field CB. Low and high temperature limits on PSII: a survey using trans-panaric acid, delayed light emission, and F_o chlorophyll fluorescence. *Plant Physiol*. 1989:91(4):1494–1500. https://doi.org/10.1104/pp.91.4.1494

Tolleter D, Smith EN, Dupont-Thibert C, Uwizeye C, Vile D, Gloaguen P, Falconet D, Finazzi G, Vandenbrouck Y, Curien G. The *Arabidopsis* leaf quantitative atlas: a cellular and subcellular mapping through unified data integration. *Quant Plant Biol*. 2024:5:e2. https://doi.org/10.1017/qpb.2024.1

Valifard M, Fernie AR, Kitashova A, Nägele T, Schröder R, Meinert M, Pommerrenig B, Mehner-Breitfeld D, Witte CP, Bruser T, *et al*. The novel chloroplast glucose transporter pGlcT2 affects adaptation to extended light periods. *J Biol Chem*. 2023:299(6):104741. https://doi.org/10.1016/j.jbc.2023.104741

Vani B, Pardha Saradhi P, Mohanty P. Alteration in chloroplast structure and thylakoid membrane composition due to in vivo heat treatment of rice seedlings: correlation with the functional changes. *J Plant Physiol*. 2001:158(5):583–592. https://doi.org/10.1078/0176-1617-00260

Wang J, Luo Q, Liang X, Liu H, Wu C, Fang H, Zhang X, Ding S, Yu J, Shi K. Glucose-G protein signaling plays a crucial role in tomato resilience to high temperature and elevated CO_2. *Plant Physiol*. 2024:195(2):1025–1037. https://doi.org/10.1093/plphys/kiae136

Weiszmann J, Fürtauer L, Weckwerth W, Nägele T. Vacuolar sucrose cleavage prevents limitation of cytosolic carbohydrate metabolism and stabilizes photosynthesis under abiotic stress. *FEBS J*. 2018:285(21):4082–4098. https://doi.org/10.1111/febs.14656

Yamori W, Hikosaka K, Way DA. Temperature response of photosynthesis in C3, C4, and CAM plants: temperature acclimation and temperature adaptation. *Photosynth Res*. 2014:119(1–2):101–117. https://doi.org/10.1007/s11120-013-9874-6

Zhang J, Jiang XD, Li TL, Cao XJ. Photosynthesis and ultrastructure of photosynthetic apparatus in tomato leaves under elevated temperature. *Photosynthetica*. 2014:52(3):430–436. https://doi.org/10.1007/s11099-014-0051-8

Zhang R, Wise RR, Struck KR, Sharkey TD. Moderate heat stress of *Arabidopsis thaliana* leaves causes chloroplast swelling and plastoglobule formation. *Photosynth Res*. 2010:105(2):123–134. https://doi.org/10.1007/s11120-010-9572-6

Zhu L, Bloomfield KJ, Hocart CH, Egerton JJG, O'Sullivan OS, Penillard A, Weerasinghe LK, Atkin OK. Plasticity of photosynthetic heat tolerance in plants adapted to thermally contrasting biomes. *Plant Cell Environ*. 2018:41(6):1251–1262. https://doi.org/10.1111/pce.13133

Zou M, Yuan L, Zhu S, Liu S, Ge J, Wang C. Effects of heat stress on photosynthetic characteristics and chloroplast ultrastructure of a heat-sensitive and heat-tolerant cultivar of wucai (*Brassica campestris* L.). *Acta Physiol Plant*. 2017:39:30. 10.1007/s11738-016-2319-z

Zrenner R, Willmitzer L, Sonnewald U. Analysis of the expression of potato uridinediphpsphate-glucose pyrophosphorylade amd its inhibition by antisense RNA. *Planta*. 1993:190(2):247–252. https://doi.org/10.1007/BF00196618

3.3. Temperature-induced dynamics of plant carbohydrate metabolism

Seydel, C., Kitashova, A., Fürtauer, L., & Nägele, T. (2022b). Temperature-induced dynamics of plant carbohydrate metabolism. Physiol Plant, 174(1), e13602

The article can be found at https://onlinelibrary.wiley.com/doi/10.1111/ppl.13602.

Received: 22 October 2021 | Accepted: 16 November 2021
DOI: 10.1111/ppl.13602

SPECIAL ISSUE ARTICLE

Physiologia Plantarum

Temperature-induced dynamics of plant carbohydrate metabolism

Charlotte Seydel[1,2] | Anastasia Kitashova[2] | Lisa Fürtauer[3] | Thomas Nägele[2]

[1]Faculty of Biology, Plant Development, Ludwig-Maximilians-Universität München, Planegg-Martinsried, Germany

[2]Faculty of Biology, Plant Evolutionary Cell Biology, Ludwig-Maximilians-Universität München, Planegg-Martinsried, Germany

[3]Institute for Biology III, Unit of Plant Molecular Systems Biology, RWTH Aachen University, Aachen, Germany

Correspondence
Thomas Nägele, Ludwig-Maximilians-Universität München, Faculty of Biology, Plant Evolutionary Cell Biology, 82152 Planegg-Martinsried, München, Germany.
Email: thomas.naegele@lmu.de

Funding information
Deutsche Forschungsgemeinschaft, Grant/Award Numbers: NA 1545/4-1, TR175/D03

Edited by: V. Hurry

Abstract

Carbohydrates are direct products of photosynthetic CO_2 assimilation. Within a changing temperature regime, both photosynthesis and carbohydrate metabolism need tight regulation to prevent irreversible damage of plant tissue and to sustain energy metabolism, growth and development. Due to climate change, plants are and will be exposed to both long-term and short-term temperature changes with increasing amplitude. Particularly sudden fluctuations, which might comprise a large temperature amplitude from low to high temperature, pose a challenge for plants from the cellular to the ecosystem level. A detailed understanding of fundamental regulatory processes, which link photosynthesis and carbohydrate metabolism under such fluctuating environmental conditions, is essential for an estimate of climate change consequences. Further, understanding these processes is important for biotechnological application, breeding and engineering. Environmental light and temperature regimes are sensed by a molecular network that comprises photoreceptors and molecular components of the circadian clock. Photosynthetic efficiency and plant productivity then critically depend on enzymatic regulation and regulatory circuits connecting plant cells with their environment and re-stabilising photosynthetic efficiency and carbohydrate metabolism after temperature-induced deflection. This review summarises and integrates current knowledge about re-stabilisation of photosynthesis and carbohydrate metabolism after perturbation by changing temperature (heat and cold).

1 | INTRODUCTION

Unravelling the effects of a changing temperature regime on plant performance is challenging due to diverse molecular effectors, complex regulatory networks and a broad physiological response and plasticity. Drafting a mechanistic model of how cold, heat and fluctuating temperature affect plant growth and development is not only of specific relevance for basic research in plant physiology and biotechnology but also for a detailed understanding of how global warming acts upon (terrestrial) ecosystems. Long-term effects of global warming on plant species have been generalised before with a decreased fitness effect of many wild plant species in their current natural habitats (Lippmann et al. 2019). Particularly, warm droughts were observed to have a significant negative impact on the gross primary production of northern ecosystems (Gampe et al. 2021). Because of outpacing of adaption and natural selection by global

Charlotte Seydel and Anastasia Kitashova contributed equally to this study.

warming, species and populations may decline or go extinct (Thuiller et al. 2005; Wilczek et al. 2014). In addition to a steady increase of ambient temperature, temperature fluctuations and weather extremes are associated with global warming (Pachauri et al. 2014). Molecular and biochemical studies on plant metabolism under heat, cold or fluctuating temperature have revealed regulatory networks playing a central role in temperature stress response and acclimation. A prominent example for such a network is represented by the C-repeat binding factors (CBFs), which are transcription factors stimulating the transcription of target genes by binding to the C-repeat (CRT)/dehydration-responsive element (DRE) regulatory element of their promoters; also known as the CBF regulon (Fowler & Thomashow 2002; Gilmour et al. 1998). In *Arabidopsis thaliana*, three cold-inducible *CBF* genes (*CBF1-3*) are induced within 15 min of plant transfer to cold, followed by the induction of target genes within 2–3 h, finally leading to an increased freezing tolerance (more details are summarised in Thomashow (2010)). Comparing natural accessions of *Arabidopsis thaliana* with a wide range of geographical origin revealed central functions of CBFs during cold acclimation (Gehan et al. 2015; Hannah et al. 2006; Nagler et al. 2015), and their functional evolution has been hypothesised to be involved in adaptation to warmer climates (Monroe et al. 2016). This example indicates the necessity to combine analysis and interpretation of plant cold and heat responses to promote our understanding of the involved pathways and regulatory networks (Demmig-Adams et al. 2018). While drawing a complete map of CBF-induced or CBF-affected pathways, which are in turn connected to other signalling and redox networks (Ding et al. 2020), remains challenging and comprehensive, photosynthetic performance and carbohydrate metabolism are core components of underlying networks (Demmig-Adams et al. 2018; Kurepin et al. 2013). This is not surprising given that photosynthetic ATP and NADPH generation, CO_2 assimilation and carbohydrate biosynthesis are fundamental to plant growth and development. Previously, CBF overexpression in *Brassica napus* was found to significantly alter gene expression and enzyme activity of Rubisco (Ribulose 1,5-bisphosphate carboxylase/oxygenase), sucrose phosphate synthase (SPS) and cytosolic fructose-1,6-bisphosphatase (cFBPase), which resulted in enhanced photosynthetic capacity and freezing tolerance (Savitch et al. 2005). This finding immediately suggests a tight linkage between temperature sensing, induced signalling and adjustment of carbohydrate metabolism. Plant carbohydrates are direct products of photosynthetic CO_2 fixation and represent substrates for plant energy metabolism, secondary metabolism, growth, development and stress response. As a consequence, plant growth, development and stress response essentially depend on the tight regulation of photosynthesis and carbohydrate metabolism within a changing environment (Herrmann et al. 2019a). Transferring plants from ambient temperature (e.g. 22°C) to cold or heat has an immediate effect on translational processes and, maybe as a direct consequence, on enzyme activities, which determine reaction rates and metabolic fluxes (Garcia-Molina et al. 2020). Thus, the regulation of enzyme activities by modification of enzyme amount, post-translational modifications (PTMs) and by metabolites (as effectors) is a conserved element of temperature acclimation, decreasing rate-limiting steps to keep the metabolism going. For example, sucrose biosynthesis has been shown to limit photosynthetic acclimation at low temperatures

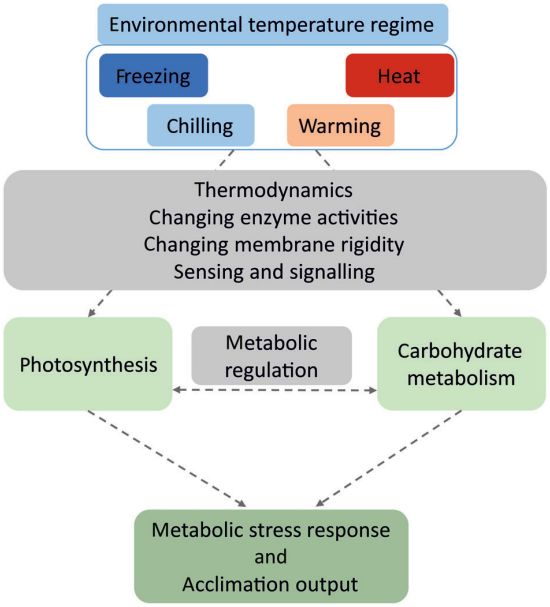

FIGURE 1 Effects of a changing environmental temperature regime on plant photosynthesis and carbohydrate metabolism. Thermodynamics, changes in membrane rigidity and cellular signalling induce plant stress response and acclimation. Metabolic regulation tightly links acclimation of photosynthesis and carbohydrate metabolism and strongly affects the acclimation output and plant performance within a changing temperature regime

(Nägele et al. 2012; Strand et al. 2003). Evidence has also been provided for the stabilisation of photosynthesis by vacuolar compartmentation and invertase-driven hydrolysis of sucrose (Nägele & Heyer 2013; Weiszmann et al. 2018). Under heat conditions, the invertase activity was found to balance the energy provision for pollen germination and tube growth (Jiang et al. 2020). In young tomato fruit, vacuolar and cellular invertase activity was higher in heat-tolerant than in heat-sensitive lines, which the authors interpreted as a contribution of invertases to heat tolerance via increasing sink strength and sugar signalling activity (Li et al. 2012). These few examples show that adjustment of photosynthetic CO_2 uptake and regulation of central carbohydrate metabolism play an essential role in plant temperature response and acclimation. Yet, the study of plant temperature response is challenged by the high diversity of molecular, biophysical and biochemical effects which need to be considered (Figure 1). This review aims to summarise and discuss plant temperature response with regard to photosynthetic CO_2 uptake and carbohydrate metabolism. Effects of heat and cold are summarised in separate chapters. A final outlook briefly suggests possible strategies for future studies to analyse and decipher plant metabolic regulations in a changing temperature regime.

2 | EFFECTS OF ELEVATED TEMPERATURE ON PLANT CARBOHYDRATE METABOLISM

A changing temperature regime has an immediate effect on the thermodynamic of enzyme reactions and membrane transport. Without

regulation, an increasing temperature would result in elevated enzymatic reaction rates due to thermodynamic constraints. This might, in particular, affect the balance between photosynthetic primary and secondary reactions, which potentially results in the generation of reactive oxygen species (ROS). Thus, fast sensing and signalling of heat, and significantly changing temperature in general, are crucial for the stabilisation of photosynthetic CO_2 uptake. Elevated temperature increases plasma membrane fluidity, leading to activation of Ca^{2+} channels and increased Ca^{2+} influx into the cell (Ranty et al. 2016; Sajid et al. 2018). Intracellular signals are then transduced by routes of calcium signalling, activation of kinases and phosphatases, ROS signalling, activation of transcriptions factors and cascades of phytohormonal control (Mittler et al. 2012; Saidi et al. 2010). This activates a regulatory network in part conserved among diverse groups of organisms (Richter et al. 2010). A central and conserved component of the heat response is an increased expression of heat shock proteins (HSPs) (Iba 2002). Together with heat stress factors (HSFs), which are central control proteins during heat stress response, HSPs establish and initiate signalling cascades which result in stabilised proteins and prevent overaccumulation of unfolded or damaged proteins (Qu et al. 2013). Also, for chloroplast function, HSPs play an essential role under heat stress and have been found to stabilise chloroplast development and function of PSII (Heckathorn et al. 1998; Zhong et al. 2013). Recently, thermomemory effects were also related to free calcium in the chloroplast, and it was shown that calcium-sensing receptor (CAS) proteins contribute to the maintenance of a thermopriming effect (Pollastri et al. 2021). This emphasises the role of chloroplasts and photosynthesis in heat response and tolerance mechanisms. Further evidence for an integration of light and temperature information has been provided by the finding that photoreceptors, like phytochrome B (phyB), act as thermosensors (Jung et al. 2016). Two interconnected branches downstream of phyB have been defined to control hypocotyl growth in response to light and temperature (Legris et al. 2017). Also, components of the circadian clock have been identified to function as thermosensors in plants. The evening complex member EARLY FLOWERING 3 (ELF3) was found to rapidly shift between active and inactive states via phase transition (Jung et al. 2020). The authors observed a correlation between length of a polyglutamine repeat, embedded within a predicted prion domain, and thermal responsiveness. Interestingly, ELF3 proteins of plants from hotter climates lacked such a prion domain and were not thermally responsive (Jung et al. 2020). This supplements the knowledge and understanding of the circadian clock's structure, regulation and function as a signalling hub and emphasises its central role in temperature response (Gil & Park 2019). The circadian clock has a significant regulatory effect on heat stress-responsive transcriptome in *Arabidopsis thaliana*, which also comprises the regulation of photosynthetic machinery (Blair et al. 2019). Thereby, clock-dependent regulation of photosynthesis directly connects temperature sensing and signalling with physiological output (Dodd et al. 2014). Further, depending on the severity and duration of heat exposure, elevated temperatures might have diverse effects on photosynthetic electron transport and rates of CO_2 assimilation. While moderate heat has only little effect on protein structure and function, higher temperatures, generally above 45°C, pose the risk of protein denaturation and irreversible damage of photosystem II (Yamori et al. 2014). Species-specific heat tolerance varies significantly and, thus, a temperature perceived as moderate or severe heat by plants cannot be generally defined. For example, comparison of critical temperature (T_{crit}) across more than 60 species from different thermal biomes across Australia revealed a temperature range between 40°C and 55°C (Zhu et al. 2018). Here, T_{crit} is a high temperature where minimal chlorophyll *a* fluorescence rises rapidly, which indicates disruption of photosystem II. The estimation of heat tolerance by applying a combination of electrolyte leakage and chlorophyll fluorescence measurement provided evidence for a broad range of basal heat tolerance and heat acclimation capacity across diverse species, including *Arabidopsis thaliana*, cereals and horticultural species (Ilik et al. 2018). Such plasticity of temperature tolerance promises to reveal diverse molecular and physiological mechanisms involved in heat stress response and acclimation. Simultaneously, phenotypic and molecular plasticity are challenging to interpret, and comparative systems biology studies become increasingly important to unravel specific and conserved mechanisms of plant heat tolerance (Pazhamala et al. 2021). Comparing C3, C4 and CAM photosynthesis might significantly promote the understanding of thermotolerance of photosynthetic CO_2 uptake and carbohydrate metabolism. The rate of photorespiration increases with temperature, while elevated concentration of atmospheric CO_2 has an opposing effect (Long 1991). Accordingly, elevated CO_2 was found to increase heat tolerance of photosynthesis in C_3 plants like *Pisum stativum*, *Triticum aestivum* and *Glycine max*, which might be due to a beneficial effect of reduced photorespiration under such conditions (Dan et al. 2008). Together with other studies, this indicates that photorespiration significantly contributes to plant stress tolerance (Dusenge et al. 2019).

Within the first hours of heat exposure, significant dynamics of regulation of carbon metabolism can be observed. For example, in soybean subjected to heat for 24 h, 15% of heat-induced proteins were related to carbon and carbohydrate metabolism, with a maximal upregulation of gene expression after 12 h (Ahsan et al. 2010). Remarkably, proteins associated with carbon assimilation and photosynthesis were downregulated during this period (Ahsan et al. 2010). In another study, more than 140 heat-responsive metabolites were identified, with 58 already increasing within the first 30 min of exposure to 40°C (Kaplan et al. 2004). Together with amino acids and organic acids, the amount of central carbohydrates increased (e.g. sucrose, raffinose and maltose). Cell wall monosaccharides also increased, which coincided with a significant increase in the thermotolerance of heat-treated plants (Kaplan et al. 2004). When the heat exposure is prolonged to several days, a decrease in biomass accumulation and reduced rates of net photosynthesis and carbon assimilation was observed in *Arabidopsis* (Prasch & Sonnewald 2013; Vasseur et al. 2011). Carbon depletion during the night and a differential expression of enzymes involved in metabolic pathways and photosynthesis indicated a high energy requirement of plants facing elevated temperatures (Sharmin et al. 2013; Vasseur et al. 2011). Regarding soluble sugars, more ambiguous findings have been reported for *Arabidopsis*. Some studies found an increase in hexoses (Atanasov et al. 2020; Prasch & Sonnewald 2013) and sucrose (Prasch & Sonnewald 2013), whereas other research showed a decrease in the combined pool of glucose, fructose and sucrose in response to

moderate heat (Vasseur et al. 2011). Invertase transcript abundance was also altered in some cases when cell wall invertase was strongly downregulated and cytosolic and vacuolar invertase were upregulated, which suggests alteration of sucrose degradation under heat (Prasch & Sonnewald 2013). Less significant but still detectable, the invertase enzyme activity also increased during heat exposure in natural accessions of *Arabidopsis thaliana* (Atanasov et al. 2020). While vacuolar invertase activity remained constant, the activity of neutral and cell wall invertase increased after 3 and 7 days of heat exposure (Atanasov et al. 2020). Maybe as a direct consequence, the concentration of hexoses (i.e. invertase reaction products) increased after 7 days at 32°C. Conversely, in wheat (*Triticum aestivum*), barley (*Hordeum vulgare*) and oat (*Avena sativa*) varieties, heat acclimation for 14 days at 30°C/27°C day/night temperature resulted in a decrease of hexose and sucrose concentrations (Janda et al. 2021). One explanation for this discrepancy might be a different period of heat acclimation (7 vs. 14 days). Additionally, *Arabidopsis* most probably does not reflect photosynthetic capacities and sugar metabolism of cereals as they might differ significantly in total metabolite amounts, sink-source capacities and also absolute heat tolerance (Ilik et al. 2018). Less ambiguously, starch amounts were observed to decrease in response to heat, which might hint toward a conserved redirection of photosynthetic assimilates from storage to stress-protective compounds (Atanasov et al. 2020; Vasseur et al. 2011). Finally, prolonged heat also resulted in a reduction of the membrane lipid content and an increase in lipid degradation at later stages of heat exposure, accounting for higher electrolyte leakage in heat-treated plants (Lee et al. 2007; Tang et al. 2016).

3 | LOW TEMPERATURE PERCEPTION AND REGULATION OF PHOTOSYNTHESIS AND CARBOHYDRATE METABOLISM

Like heat, low temperature also has an immediate effect on enzymatic activities and the integrity of cellular membrane systems. Based on the van't Hoff rule, (chemical) reaction rates are reduced by a factor of 2–3 per 10°C (Reyes et al. 2008; van't Hoff 1884). Thus, slowed consumption of reducing power by lowered reaction rates within the Calvin–Benson Cycle (CBC) might then result in reduced photosynthetic capacity (Savitch et al. 2001). In cold-stressed plants, the probability of reactive oxygen species (ROS) formation increases. To counteract, the activity of anti-oxidative enzymes increases as well (Huner et al. 1998; Mir et al. 2015; Wang et al. 2013). Hence, sensitive and fast perception of a (significant) temperature drop is essential to prevent irreversible tissue damage. Like perception of heat, the perception of low temperature comprises a cold-induced Ca^{2+} influx into the cell. Cold-induced Ca-signalling triggers cascades involving, e.g. CALCIUM/CALMODULIN-REGULATED RECEPTOR-LIKE KINASES (CRLK) and MITOGEN-ACTIVATED PROTEIN KINASES (MAPKs) (Ding et al. 2019; Guo et al. 2018). Differential phosphorylation and other post-translational modifications of diverse transcription factors induce significant transcriptomic changes (Barrero-Gil & Salinas 2013). Also, INDUCER OF CBF EXPRESSION 1 (ICE1), which is a MYC-type bHLH transcription factor and an important regulator of CBFs, is phosphorylated and activated under cold stress (Chinnusamy et al. 2003; Li et al. 2017; Liu & Zhou 2018). ICE1 induces the expression of *CBF* genes by direct binding to their promoters. The induction of the main C-repeat/dehydration-responsive element-binding factor (CBF/DREB1) regulon occurs within minutes after subjection to cold (Fowler & Thomashow 2002; Ritonga & Chen 2020). The ICE/CBF transcription factor network, together with many other CBF-independent regulators (e.g. MYBs and WRKYs), affects the transcription of *COLD-REGULATED* (*COR*) genes, which represents a key signalling pathway in plant cold response and formation of freezing tolerance (Fowler & Thomashow 2002; Jaglo-Ottosen et al. 1998; Ritonga & Chen 2020). About 10% of all *COR* genes are regulated by CBF1-3, also known as DREB1b/1c/1a (Park et al. 2015). Overexpression of CBF1 and CBF2 stimulated the accumulation of soluble sugars and proline, which are important for cold acclimation and freezing tolerance (Gilmour et al. 2004). Moreover, CBF1 modulates the accumulation of DELLA proteins, which are required for attaining freezing tolerance (Achard et al. 2008). DELLA proteins are stabilised by sucrose and induce anthocyanin synthesis by activating the PAP1/MYB75 transcription factor (Li et al. 2014). Transcription factors like PAP1/MYB75 and PAP2/MYB90 are cold-induced and are involved in natural variation of the regulation of flavonoid and anthocyanin metabolism, which contributes to freezing tolerance in *Arabidopsis thaliana* (Schulz et al. 2015; Teng et al. 2005). Previous analysis of *cbf1-3* loss-of-function mutants suggested that CBF2 and CBF3 play a more dominant role than CBF1 in directing cold response by *COR* gene regulation (Shi et al. 2017). The authors observed that more than 60% of *COR* genes were co-regulated by at least two CBFs, which indicates the complexity of the underlying transcriptional and regulatory networks. Further, the abundance of *COR78* transcript correlated with *Arabidopsis* freezing tolerance (Nagler et al. 2015), and increased with sucrose concentration in leaf epidermal cells, which directly connects CBF/DREB signalling to regulation of carbohydrate metabolism (Rekarte-Cowie et al. 2008). Together with COR15B, COR78 was predicted to interact with cold-inducible and ABA-inducible protein KIN1, which is a potential anti-freeze protein (Fürtauer et al. 2018). These observations, together with cold-induced flavonoid response, suggest a sensing and signalling network with feedback mechanisms connecting carbohydrates and secondary metabolism with the transcriptional and translational regulation of proteins with cryoprotective function. In combination with COR27 and COR28, which are negative regulators of freezing tolerance interacting with circadian clock components (Fowler & Thomashow 2002; Li et al. 2016; Rees et al. 2021), this signalling network integrates and combines circadian rhythm with diurnal light and temperature information.

To minimise potential damages resulting from low temperature under high excitation pressure, the composition of the photosynthetic apparatus is adjusted during cold acclimation. For example, evergreen plants tend to lower the abundance of light-harvesting complex proteins or increase the non-photochemical quenching (NPQ) capabilities to dissipate the excess of energy as heat (Huner et al. 1998). Winter cereals, like winter wheat and rye, can keep the primary quinone electron acceptor (Q_A) continuously oxidised, which is associated with

tolerance to photoinhibition (Huner et al. 1993). The sensitivity and recovery of photosynthetic activity during cold exposure correlate with the activity of enzymes of the central carbohydrate metabolism, e.g. several CBC enzymes and sucrose phosphate synthase (SPS) (Hurry et al. 1998; Nägele et al. 2012; Strand et al. 1999; Strand et al. 2003). When exposed to low but non-freezing temperatures, plant photosynthesis is rapidly inhibited due to reduced sucrose biosynthesis capacity (Hurry et al. 2002; Pollock & Lloyd 1987). A reduced rate of sucrose biosynthesis results in accumulation of triose phosphates, depletion of orthophosphate in the chloroplast and, finally, inhibition of the CBC (Leegood & Furbank 1986). A transiently lowered phosphate pool was found to trigger cold acclimation of leaves by increasing Rubisco and SPS expression (Hurry et al. 2000). Elevated SPS activity and the resulting higher capacity of sucrose biosynthesis, were further correlated with freezing tolerance and improved photosynthesis under low temperature (Nägele et al. 2012; Strand et al. 2003). Generally, as an early metabolic response to low temperature, soluble sugar concentration rapidly increases (Ristic & Ashworth 1993). Sugar accumulation correlates with freezing tolerance of natural accessions of *Arabidopsis thaliana*, which suggests a cryoprotective role (Hannah et al. 2006; Klotke et al. 2004). Also, in many other organisms with cold acclimation capacity, sugar accumulation correlated with freezing tolerance (Korn et al. 2008; Palonen et al. 2000; Sasaki et al. 1996). In alfalfa (*Medicago sativa*), short photoperiods improved freezing tolerance due to amplified sugar accumulation and induction of transcripts encoding biosynthesising enzymes (Bertrand et al. 2017). Yet, not only accumulation but also subcellular compartmentation of carbohydrates plays an essential role for cold stress response and acclimation. For example, raffinose, which amount positively correlates with cold acclimation capacities (Bertrand et al. 2017; Hannah et al. 2006; Kaplan et al. 2004; Smallwood & Bowles 2002), has been observed to be neither necessary nor sufficient for stabilisation of plasma membranes during freezing (Zuther et al. 2004). Instead, raffinose accumulation in the chloroplast was suggested to protect thylakoid membranes; hence stabilising photosynthetic capacity during cold and freezing (Knaupp et al. 2011). Sugar compartmentation has for long been known to play an important role in plants' cold response. For example, plastidial sucrose amount increased during (initial) cold acclimation in cabbage (*Brassica oleracea* L. var. *sabellica* L.) and decreased again during dehardening (Santarius & Milde 1977). Also, in *Arabidopsis*, sucrose was significantly accumulated in chloroplasts within the first 24 h of cold exposure, and the intensity of accumulation was correlated with freezing tolerance (Nägele & Heyer 2013). It was further hypothesised that plastidial sucrose accumulation might represent a fast and initial cold response, while raffinose accumulation represents a long-term response reaching peak values between 3 and 7 days of cold exposure (Nägele & Heyer 2013). While photosynthetic CO_2 assimilation drops during cold exposure (Nägele & Heyer 2013; Savitch et al. 2001), carbohydrate partitioning and regulation of export from source to sink tissue are essentially involved and can explain the significant increase of leaf carbohydrate amounts under such conditions (Lundmark et al. 2006). Further, vacuolar sucrose cleavage, catalysed by acidic invertase, stabilised photosynthesis of *Arabidopsis thaliana* under freezing conditions and the limitation of cytosolic hexose supply might be prevented by the vacuolar reaction (Weiszmann et al. 2018). In another study, the vacuolar sucrose amount was suggested to fully compensate for the effects of low monosaccharide amounts on frost tolerance (Vu et al. 2020). The authors observed that reduced vacuolar invertase activity had no significant effect on freezing tolerance quantified by electrolyte leakage assays. Thus, while the limitation of vacuolar sucrose cleavage seems to affect photosynthetic efficiency of *Arabidopsis thaliana* at freezing temperature, plasma membrane stability is not affected by the vacuolar release of monosaccharides. In tea plant (*Camellia sinensis* L.), overexpression of a vacuolar invertase gene, *CsINV5*, resulted in increased freezing tolerance (Qian et al. 2018). The authors observed an upregulation of a hexokinase gene in *CsINV5* overexpression lines, which potentially mediate glucose signalling to promote cold tolerance. Hexokinase plays a central role in sugar metabolism and signalling (Moore et al. 2003), and environmentally induced dynamics of (cytosolic) sugar phosphorylation are very likely to affect sugar phosphate exchange across the chloroplast envelope and photosynthesis (Herrmann et al. 2021; Küstner et al. 2019a; Küstner et al. 2019b; Weiszmann et al. 2018). Hexose phosphate concentration rapidly increases after cold exposure and is stabilised during cold acclimation at significantly higher levels than under ambient temperature (Gray & Heath 2005). This suggests a tight regulation of sugar phosphates in plant temperature response to sustain and stabilise the energy metabolism, which is essential to prevent limitation of leaf respiration (Talts et al. 2004). Together with the activity of SPS and invertases, hexokinase catalyses a cyclic sucrose breakdown and re-synthesis, frequently described as a *futile cycle* due to its seemingly wasteful ATP consumption. However, more and more evidence is provided for a stabilising function of this sucrose cycle to buffer carbohydrate metabolism against perturbations induced by changing temperature and environmental fluctuations in general (Atanasov et al. 2020; Brauner et al. 2015; Claeyssen et al. 2013; Geigenberger & Stitt 1991; Küstner et al. 2019b; Nägele et al. 2012). In summary, due to their central metabolic role as activated compounds, sugar phosphates together with sugar nucleotides are metabolic hubs regulating carbon distribution between biosynthesis of soluble intermediates, structural compounds and transitory starch (Domon et al. 2013; Figueroa et al. 2021; Geigenberger & Fernie 2014; Guy et al. 2008; Sharkey 2021; Somerville 2006; Stitt & Hurry 2002).

4 | RESPONSE OF STARCH METABOLISM TO DIFFERENT ENVIRONMENTAL TEMPERATURE REGIMES

Leaf transitory starch is synthesised within a pathway comprising multiple enzymes. Phosphoglucose isomerase (PGI) and phosphoglucomutase (PGM) catalyse the interconversion of fructose-6-phosphate (F6P) into glucose-1-phosphate (G1P), respectively. G1P, together with ATP, serves as substrate for ADP-glucose pyrophosphorylase (AGPase), which catalyses the biosynthesis of ADP-glucose and inorganic pyrophosphate (PP_i). AGPase is regulated by transcriptional and redox control, post-translational modification, sugar signals and allosteric regulation by metabolites (Geigenberger 2011; Tiessen et al. 2002). Starch synthases transfer

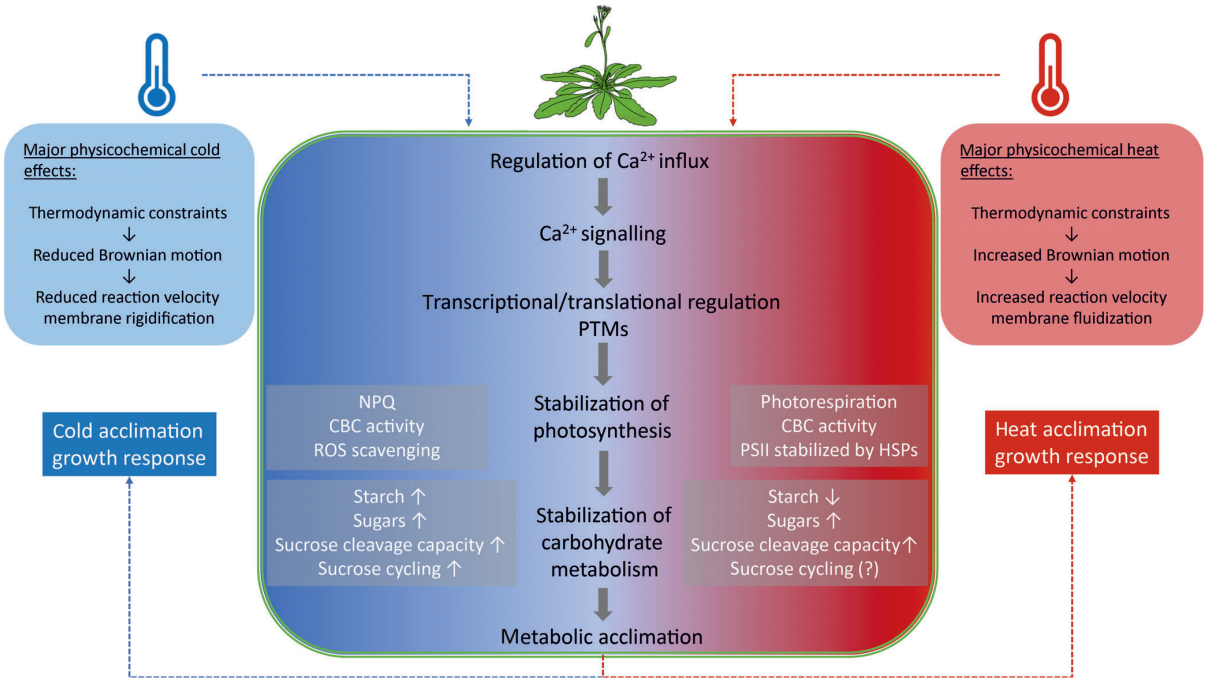

FIGURE 2 Central effects of high and low temperature on photosynthesis and carbohydrate metabolism. Heat and cold responses might differ significantly between plant species (C3 vs. C4 vs. CAM; annual vs. perennial vs. evergreen). Thus, only central and conserved effects are shown in this simplified and schematic overview. The role of sucrose cycling, involving SPS, HXK and INV activities, in heat acclimation still remains elusive but may represent a (conserved) temperature stress and acclimation response. CBC, Calvin–Benson cycle; NPQ, non-photochemical quenching; PSII, Photosystem II; ROS, reactive oxygen species; SPS, sucrose phosphate synthase

the glucose moiety from ADP-glucose to a growing alpha-1,4-glucan chain while branching enzymes and de-branching enzymes insert branch points and enable crystallisation (Ristic & Ashworth 1993; Sicher 2011; Yano et al. 2005). During the night, starch breakdown is catalysed by amylases and phosphorylases (Mahlow et al. 2016). During the light period, starch is continuously phosphorylated but, under ambient conditions, the phosphorylation rate is higher during starch breakdown (Ritte et al. 2004). Glucan, water dikinase and phosphoglucan, water dikinase catalyse the breakdown of starch granules into branched and linear glucans, which are substrates for beta-amylases catalysing the further breakdown into maltose units (Smith et al. 2005). Maltose is then exported to the cytosol, catalysed by the maltose transporter MEX1 (Monroe 2020; Nagler et al. 2015), where it is cleaved by glucosidases to supply the glucose pool.

Starch metabolism dynamically responds to a changing temperature regime. During and after cold acclimation, starch is diurnally synthesised and degraded, suggesting a tight regulation and temperature-induced adjustment of the involved pathways and enzyme activities (Espinoza et al. 2010; Nägele et al. 2012). AGPase activity increased during cold acclimation and was high in cold-developed leaves (Savitch et al. 1997; Strand et al. 1997). Following a slight initial increase, starch amount significantly drops during the first 24 h of low-temperature treatment, and it was suggested that starch hydrolysis contributes to the hexose supply during early cold response (Sicher 2011). Further, starch hydrolysis correlated with the increased expression of *BETA-AMYLASE 3* (*BAM3/BMY8*) and maltose concentration (Sicher 2011). Most of the plastidic amylase activity is explained by BAM1 and BAM3, yet both enzymes differ significantly in transcriptional regulation and temperature optima (Monroe et al. 2014). While *BAM3* transcription is cold-induced, BAM1 is induced by heat stress and has a temperature optimum approximately 10°C above the optimum of BAM3 (Monroe et al. 2014). Decreasing beta-amylase activity and the resulting depletion of plastidial maltose results in cold sensitivity of PSII (Kaplan & Guy 2005). Remarkably, ectopic expression of functional maltase enzymes in the chloroplast of *mex1* loss-of-function mutants of *Arabidopsis thaliana* improved frost tolerance (Cvetkovic et al. 2021). Also, *starch excess 1* (*sex1*) mutants, which are deficient in α-glucan water dikinase activity, were impaired in cold-induced hexose accumulation and freezing tolerance (Yano et al. 2005), which provides evidence for a crucial role of carbon supply via starch degradation for cold acclimation. Starch metabolism is regulated by the circadian clock, which ensures optimal carbon supply during a diurnal period (Graf & Smith 2011). Rhythmic accumulation of transcripts encoding circadian clock components is significantly affected by temperature (Gould et al. 2006), implying a significant effect of cold and heat on starch metabolism regulation. Further, maltose metabolism is regulated by the clock, daylength and temperature, and regulation of *BAM3* expression was suggested to adjust starch

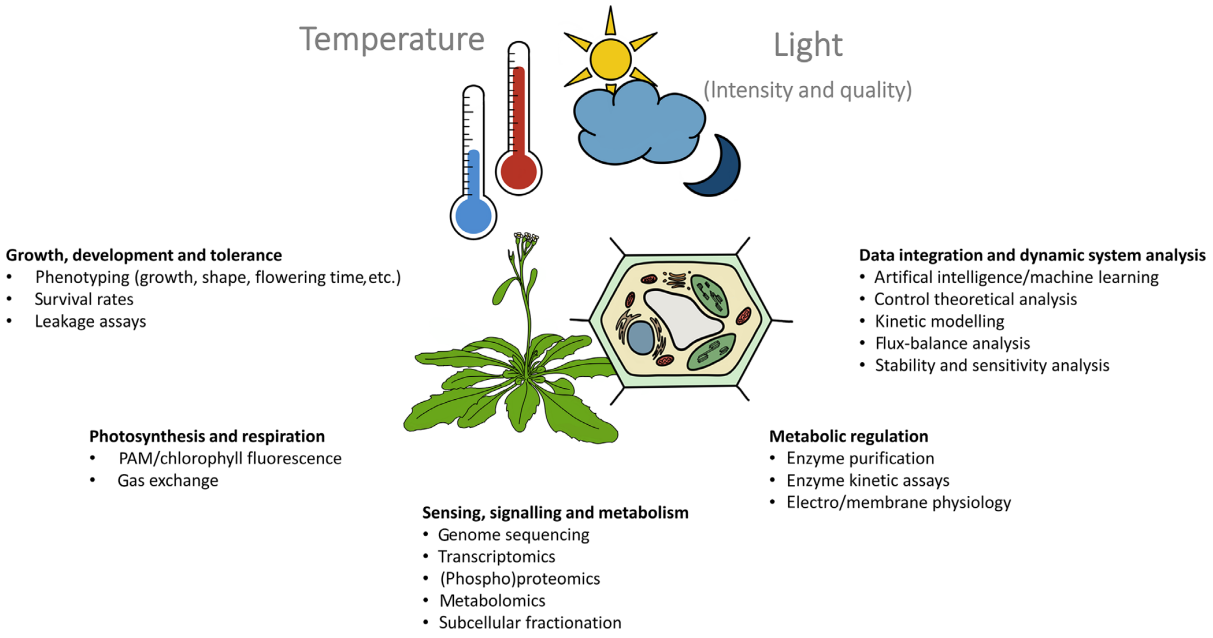

FIGURE 3 Deciphering plant–environment interactions to unravel temperature effects on plant growth and metabolism. Methodologies of phenotyping, tolerance quantification and molecular analysis are needed to advance the development of predictive models of plant metabolism in a changing temperature regime

breakdown to daylength (Lu & Sharkey 2006). Thus, under cold stress, induction of *BAM3* expression could explain the increased maltose amount (Espinoza et al. 2010; Lu & Sharkey 2006).

Following an initial decrease during the first hours of low-temperature stress, cold acclimation over days results in increased leaf starch amount (Klotke et al. 2004). Starch accumulation during cold acclimation varies across natural accessions of *Arabidopsis thaliana* (Guy et al. 2008; Hannah et al. 2006), and significant diurnal dynamics provide evidence for adjusted metabolic activity in biosynthesis and degradation pathways under low temperature (Nägele et al. 2012; Strand et al. 2003). Previous work has indicated that maintenance of circadian regulation of starch metabolism, and particularly breakdown, plays a key role in plants' cold acclimation (Espinoza et al. 2010). Accordingly, impaired starch breakdown was observed to increase sensitivity to freezing stress (Kaplan & Guy 2005). Further, natural accessions with lower freezing tolerance showed higher starch amount after cold acclimation than freezing tolerant accessions (Klotke et al. 2004; Nagler et al. 2015), indicating a more efficient reprogramming of carbon allocation into other metabolic pathways, growth or energy metabolism (Dong et al. 2018). Supported by computational simulations, recent experimental data suggest tightly regulated carbon allocation between starch and organic acids (fumarate) during cold acclimation (Herrmann et al. 2019b).

Heat significantly perturbs starch biosynthesis. In potato tubers, it was shown that decreased glycerate-3-phosphate limits the activity of AGPase and starch biosynthesis (Geigenberger et al. 1998). For wheat cultivars (*Triticum aestivum* L.), heat shock at 42°C for 2 h resulted in decreased transcript levels and enzyme activity of soluble starch synthase (Goswami et al. 2014). In maize (*Zea mays* L.), exposure to heat (33.5°C) was found to lengthen the period for grain filling and AGPase activity was affected (Wilhelm et al. 1999). Similarly, in chickpea (*Cicer arietinum* L.), starch deposition in grains was reduced due to reduced activity of AGPase and starch synthase (Awasthi et al. 2014). These findings point to conserved heat sensitivity of AGPase enzymes, limiting starch biosynthesis and storage compound metabolism under elevated temperature (Boehlein et al. 2019). Consistently, increasing heat stability of AGPase resulted in mitigation of yield losses (Hannah et al. 2017). Yet, other targets, like 6-phosphogluconate dehydrogenase of the oxidative pentose phosphate pathway, are promising candidates to engineer heat tolerance of starch synthesis and grain yield (Ribeiro et al. 2020).

Starch degradation affects growth regulation, respiration and energy metabolism (Brauner et al. 2014; Gibon et al. 2009; Lloyd & Kossmann 2015; Stitt & Zeeman 2012; Wienkoop et al. 2008). In sink-limited *Arabidopsis* plants, i.e. when grown under long-day or high irradiance, the rate of starch degradation was dependent on night temperature and accelerated by warming (Pilkington et al. 2015). BAMs play a central role in chloroplast starch degradation. In *Arabidopsis*, *BAM1/BMY7* expression was induced by heat and, like at low temperature, released maltose could act as a stabilising factor in the chloroplast (Kaplan & Guy 2004). In crops like wheat and rice (*Oryza sativa* L.), a high night temperature had a significant impact on yield and quality, but also affected photosynthesis and carbon gain during the light phase due to the negative impact on membrane integrity (Impa et al. 2021). Based on comprehensive data compilation and

analysis, Impa et al. (2021) suggested to combine experiments on night respiration, carbon balance, enzyme activities and starch protein balances in order to improve the estimation of high night temperature on crop yield. In rice, the transcription factor OsbZIP58 is involved in grain filling regulation under heat by promoting the expression of seed storage protein genes, genes of starch synthesis and by inhibiting starch hydrolysing enzymes (Xu et al. 2020). Heat-induced alternative splicing of *OsbZIP58* resulted in a truncated and less active form, which suggests the reduction of alternative splicing as a potential target for improving heat tolerance in rice (Xu et al. 2020). Conclusively, temperature-induced deregulation of starch biosynthesis and degradation significantly affects plant performance and yield. Further understanding of the involved regulatory molecular processes will promote the detailed understanding of plant–environment interactions, consequences of climate change and potential targets for biotechnological applications and engineering.

5 | FUTURE PERSPECTIVE AND CONCLUSION

A changing environmental temperature regime shapes plant development, ecology and evolution. Photosynthesis and carbohydrate metabolism are central processes that need to be tightly regulated and adjusted to a changing temperature in order to prevent irreversible cell and tissue damages. While many molecular components of plant temperature response have been unravelled to date, the assemblage of functional biochemical networks still remains a challenge and unveils many missing parts in the comprehensive plant–environment-puzzle (Kleine et al. 2021). Photosynthetic CO_2 fixation directly supplies the main carbon routes in a leaf, synthesising sucrose and starch that are dominant players in temperature stress response and acclimation (Figure 2). Although numerous pathways are involved in metabolising, transporting and interconverting, stabilisation of carbon gain (photosynthesis) and carbon loss (respiration) is central for plant survival and performance. Hence, to understand metabolic signatures and regulatory patterns, a very detailed insight into the compartmented regulation of carbohydrate metabolism is essential. Future studies might focus on combining controlled experiments in growth chambers with common garden experiments and studies in the field. Light intensity and quality significantly affect plant temperature response, and field experiments significantly differ from laboratory studies in both parameters. Experimental data on growth, development and temperature tolerance must be combined with molecular data on metabolism and metabolic regulation (Figure 3). The combination of phenotyping platforms with non-invasive photosynthesis measurements provides detailed information about growth in context of stress tolerance and acclimation. Finally, such studies should be combined with subcellular fractionation and resolution of plant metabolism to resolve the impact of temperature on regulatory circuits between carbohydrates and photosynthesis, which can be unravelled computationally by applying methods from the fields of artificial intelligence, control theory and kinetic modelling.

ACKNOWLEDGMENTS

We thank the members of Plant Development and Plant Evolutionary Cell Biology at LMU München for many fruitful discussions and advice. The authors declare that there is no conflict of interest. This work was supported by Deutsche Forschungsgemeinschaft (DFG), grants TR175/D03 and NA 1545/4-1.

Open access funding enabled and organized by Projekt DEAL.

CONFLICT OF INTEREST

The authors have declared no conflicts of interest for this article.

AUTHOR CONTRIBUTIONS

Charlotte Seydel and Anastasia Kitashova contributed equally to writing and illustrating this review. Lisa Fürtauer contributed to writing the paragraph on low temperature perception and regulation. Thomas Nägele conceived and wrote the review. All authors wrote and approved the review.

DATA AVAILABILITY STATEMENT

Data sharing is not applicable to this article as no new data were created or analysedanalyzed in this study.

ORCID

Charlotte Seydel https://orcid.org/0000-0001-9808-0720
Anastasia Kitashova https://orcid.org/0000-0002-4698-3255
Lisa Fürtauer https://orcid.org/0000-0001-5248-4105
Thomas Nägele https://orcid.org/0000-0002-5896-238X

REFERENCES

Achard, P., Gong, F., Cheminant, S., Alioua, M., Hedden, P. & Genschik, P. (2008) The cold-inducible CBF1 factor-dependent signaling pathway modulates the accumulation of the growth-repressing DELLA proteins via its effect on gibberellin metabolism. *Plant Cell*, 20(8), 2117–2129.

Ahsan, N., Donnart, T., Nouri, M.Z. & Komatsu, S. (2010) Tissue-specific defense and thermo-adaptive mechanisms of soybean seedlings under heat stress revealed by proteomic approach. *Journal of Proteome Research*, 9(8), 4189–4204.

Atanasov, V., Fürtauer, L. & Nägele, T. (2020) Indications for a central role of hexokinase activity in natural variation of heat acclimation in *Arabidopsis thaliana*. *Plants*, 9(7), 819.

Awasthi, R., Kaushal, N., Vadez, V., Turner, N.C., Berger, J., Siddique, K.H. M. et al. (2014) Individual and combined effects of transient drought and heat stress on carbon assimilation and seed filling in chickpea. *Functional Plant Biology*, 41(11), 1148–1167.

Barrero-Gil, J. & Salinas, J. (2013) Post-translational regulation of cold acclimation response. *Plant Science*, 205-206, 48–54.

Bertrand, A., Bipfubusa, M., Claessens, A., Rocher, S. & Castonguay, Y. (2017) Effect of photoperiod prior to cold acclimation on freezing tolerance and carbohydrate metabolism in alfalfa (*Medicago sativa* L.). *Plant Science*, 264, 122–128.

Blair, E.J., Bonnot, T., Hummel, M., Hay, E., Marzolino, J.M., Quijada, I.A. et al. (2019) Contribution of time of day and the circadian clock to the

heat stress responsive transcriptome in *Arabidopsis*. *Scientific Reports*, 9(1), 4814.

Boehlein, S.K., Liu, P., Webster, A., Ribeiro, C., Suzuki, M., Wu, S. et al. (2019) Effects of long-term exposure to elevated temperature on *Zea mays* endosperm development during grain fill. *The Plant Journal*, 99(1), 23–40.

Brauner, K., Hörmiller, I., Nägele, T. & Heyer, A.G. (2014) Exaggerated root respiration accounts for growth retardation in a starchless mutant of *Arabidopsis thaliana*. *The Plant Journal*, 79(1), 82–91.

Brauner, K., Stutz, S., Paul, M. & Heyer, A.G. (2015) Measuring whole plant CO2 exchange with the environment reveals opposing effects of the gin2–1 mutation in shoots and roots of *Arabidopsis thaliana*. *Plant Signaling & Behavior*, 10(1), e973822.

Chinnusamy, V., Ohta, M., Kanrar, S., Lee, B.-H., Hong, X., Agarwal, M. et al. (2003) ICE1: a regulator of cold-induced transcriptome and freezing tolerance in *Arabidopsis*. *Genes & Development*, 17(8), 1043–1054.

Claeyssen, É., Dorion, S., Clendenning, A., He, J.Z., Wally, O., Chen, J. et al. (2013) The futile cycling of hexose phosphates could account for the fact that hexokinase exerts a high control on glucose phosphorylation but not on glycolytic rate in transgenic potato (*Solanum tuberosum*) roots. *PLoS One*, 8(1), e53898.

Cvetkovic, J., Haferkamp, I., Rode, R., Keller, I., Pommerrenig, B., Trentmann, O. et al. (2021) Ectopic maltase alleviates dwarf phenotype and improves plant frost tolerance of maltose transporter mutants. *Plant Physiology*, 186(1), 315–329.

Dan, W., Heckathorn, S.A., Barua, D., Joshi, P., Hamilton, E.W. & LaCroix, J.J. (2008) Effects of elevated CO2 on the tolerance of photosynthesis to acute heat stress in C3, C4, and CAM species. *American Journal of Botany*, 95(2), 165–176.

Demmig-Adams, B., Stewart, J.J., Baker, C.R. & Adams, W.W. (2018) Optimization of photosynthetic productivity in contrasting environments by regulons controlling plant form and function. *International Journal of Molecular Sciences*, 19(3), 872.

Ding, Y., Shi, Y. & Yang, S. (2019) Advances and challenges in uncovering cold tolerance regulatory mechanisms in plants. *The New Phytologist*, 222(4), 1690–1704.

Ding, Y., Shi, Y. & Yang, S. (2020) Molecular regulation of plant responses to environmental temperatures. *Molecular Plant*, 13(4), 544–564.

Dodd, A.N., Kusakina, J., Hall, A., Gould, P.D. & Hanaoka, M. (2014) The circadian regulation of photosynthesis. *Photosynthesis Research*, 119(1–2), 181–190.

Domon, J.M., Baldwin, L., Acket, S., Caudeville, E., Arnoult, S., Zub, H. et al. (2013) Cell wall compositional modifications of *Miscanthus ecotypes* in response to cold acclimation. *Phytochemistry*, 85, 51–61.

Dong, S., Zhang, J. & Beckles, D.M. (2018) A pivotal role for starch in the reconfiguration of (14)C-partitioning and allocation in *Arabidopsis thaliana* under short-term abiotic stress. *Scientific Reports*, 8(1), 9314.

Dusenge, M.E., Duarte, A.G. & Way, D.A. (2019) Plant carbon metabolism and climate change: elevated CO_2 and temperature impacts on photosynthesis, photorespiration and respiration. *The New Phytologist*, 221(1), 32–49.

Espinoza, C., Degenkolbe, T., Caldana, C., Zuther, E., Leisse, A., Willmitzer, L. et al. (2010) Interaction with diurnal and circadian regulation results in dynamic metabolic and transcriptional changes during cold acclimation in Arabidopsis. *PLoS One*, 5(11), e14101.

Figueroa, C.M., Lunn, J.E. & Iglesias, A.A. (2021) Nucleotide-sugar metabolism in plants: the legacy of Luis F Leloir. *Journal of Experimental Botany*, 72(11), 4053–4067.

Fowler, S. & Thomashow, M.F. (2002) Arabidopsis transcriptome profiling indicates that multiple regulatory pathways are activated during cold acclimation in addition to the CBF cold response pathway. *Plant Cell*, 14(8), 1675–1690.

Fürtauer, L., Pschenitschnigg, A., Scharkosi, H., Weckwerth, W. & Nägele, T. (2018) Combined multivariate analysis and machine learning reveals a predictive module of metabolic stress response in *Arabidopsis thaliana*. *Molecular Omics*, 14(6), 437–449.

Gampe, D., Zscheischler, J., Reichstein, M., O'Sullivan, M., Smith, W.K., Sitch, S. et al. (2021) Increasing impact of warm droughts on northern ecosystem productivity over recent decades. *Nature Climate Change*, 11, 772–779. https://doi.org/10.1038/s41558-021-01112-8

Garcia-Molina, A., Kleine, T., Schneider, K., Muhlhaus, T., Lehmann, M. & Leister, D. (2020) Translational components contribute to acclimation responses to high light, heat, and cold in *Arabidopsis*. *iScience*, 23(7), 101331.

Gehan, M.A., Park, S., Gilmour, S.J., An, C., Lee, C.M. & Thomashow, M.F. (2015) Natural variation in the C-repeat binding factor cold response pathway correlates with local adaptation of *Arabidopsis* ecotypes. *The Plant Journal*, 84(4), 682–693.

Geigenberger, P. (2011) Regulation of starch biosynthesis in response to a fluctuating environment. *Plant Physiology*, 155(4), 1566–1577.

Geigenberger, P. & Fernie, A.R. (2014) Metabolic control of redox and redox control of metabolism in plants. *Antioxidants & Redox Signaling*, 21(9), 1389–1421.

Geigenberger, P., Geiger, M. & Stitt, M. (1998) High-temperature perturbation of starch synthesis is attributable to inhibition of ADP-glucose pyrophosphorylase by decreased levels of glycerate-3-phosphate in growing potato tubers. *Plant Physiology*, 117(4), 1307–1316.

Geigenberger, P. & Stitt, M. (1991) A futile cycle of sucrose synthesis and degradation is involved regulating partitioning between sucrose starch and respiration in cotyledons of germinating ricinus-communis l. seedlings when phloem transport is inhibited. *Planta*, 185, 81–90.

Gibon, Y., Pyl, E.T., Sulpice, R., Lunn, J.E., Hohne, M., Gunther, M. et al. (2009) Adjustment of growth, starch turnover, protein content and central metabolism to a decrease of the carbon supply when *Arabidopsis* is grown in very short photoperiods. *Plant, Cell & Environment*, 32(7), 859–874.

Gil, K.E. & Park, C.M. (2019) Thermal adaptation and plasticity of the plant circadian clock. *The New Phytologist*, 221(3), 1215–1229.

Gilmour, S.J., Fowler, S.G. & Thomashow, M.F. (2004) Arabidopsis transcriptional activators CBF1, CBF2, and CBF3 have matching functional activities. *Plant Molecular Biology*, 54(5), 767–781.

Gilmour, S.J., Zarka, D.G., Stockinger, E.J., Salazar, M.P., Houghton, J.M. & Thomashow, M.F. (1998) Low temperature regulation of the Arabidopsis CBF family of AP2 transcriptional activators as an early step in cold-induced COR gene expression. *The Plant Journal*, 16(4), 433–442.

Goswami, S., Kumar, R.R. & Rai, R.D. (2014) Heat-responsive microRNAs regulate the transcription factors and heat shock proteins in modulating thermo-stability of starch biosynthesis enzymes in wheat ("*Triticum aestivum*" L.) under the heat stress. Aust. *Australian Journal of Crop Science*, 8(5), 697–705.

Gould, P.D., Locke, J.C.W., Larue, C., Southern, M.M., Davis, S.J., Hanano, S. et al. (2006) The molecular basis of temperature compensation in the *Arabidopsis circadian* clock. *Plant Cell*, 18(5), 1177–1187.

Graf, A. & Smith, A.M. (2011) Starch and the clock: the dark side of plant productivity. *Trends in Plant Science*, 16(3), 169–175.

Gray, G.R. & Heath, D. (2005) A global reorganization of the metabolome in *Arabidopsis* during cold acclimation is revealed by metabolic fingerprinting. *Physiologia Plantarum*, 124(2), 236–248.

Guo, X., Liu, D. & Chong, K. (2018) Cold signaling in plants: insights into mechanisms and regulation. *Journal of Integrative Plant Biology*, 60(9), 745–756.

Guy, C., Kaplan, F., Kopka, J., Selbig, J. & Hincha, D.K. (2008) Metabolomics of temperature stress. *Physiologia Plantarum*, 132(2), 220–235.

Hannah, L.C., Shaw, J.R., Clancy, M.A., Georgelis, N. & Boehlein, S. K. (2017) A brittle-2 transgene increases maize yield by acting

in maternal tissues to increase seed number. *Plant Direct*, 1(6), e00029.

Hannah, M.A., Wiese, D., Freund, S., Fiehn, O., Heyer, A.G. & Hincha, D.K. (2006) Natural genetic variation of freezing tolerance in *Arabidopsis*. *Plant Physiology*, 142(1), 98–112.

Heckathorn, S.A., Downs, C.A., Sharkey, T.D. & Coleman, J.S. (1998) The small, methionine-rich chloroplast heat-shock protein protects photosystem II electron transport during heat stress. *Plant Physiology*, 116(1), 439–444.

Herrmann, H.A., Dyson, B.C., Miller, M.A.E., Schwartz, J.M. & Johnson, G. N. (2021) Metabolic flux from the chloroplast provides signals controlling photosynthetic acclimation to cold in *Arabidopsis thaliana*. *Plant, Cell & Environment*, 44(1), 171–185.

Herrmann, H.A., Dyson, B.C., Vass, L., Johnson, G.N. & Schwartz, J.M. (2019b) Flux sampling is a powerful tool to study metabolism under changing environmental conditions. *npj Systems Biology and Applications*, 5(1), 32.

Herrmann, H.A., Schwartz, J.M. & Johnson, G.N. (2019a) Metabolic acclimation-a key to enhancing photosynthesis in changing environments? *Journal of Experimental Botany*, 70(12), 3043–3056.

Huner, N.P.A., Gunnar, Ö. & Sarhan, F. (1998) Energy balance and acclimation to light and cold. *Trends in Plant Science*, 3(6), 224–230.

Huner, N.P.A., Öquist, G., Hurry, V.M., Krol, M., Falk, S. & Griffith, M. (1993) Photosynthesis, photoinhibition and low temperature acclimation in cold tolerant plants. *Photosynthesis Research*, 37, 19–39.

Hurry, V., Druart, N., Cavaco, A., Gardeström, P. & Strand, Å. (2002) Photosynthesis at low temperatures. In: Li, P.H. & Palva, E.T. (Eds.) *Plant cold hardiness: gene regulation and genetic engineering*. Boston, MA: Springer, pp. 161–179.

Hurry, V., Huner, N., Selstam, E., Gardestrom, P. & Oquist, G. (1998) *Photosynthesis at low growth temperatures*. Cambridge: Cambridge University Press, pp. 238–249.

Hurry, V., Strand, A., Furbank, R. & Stitt, M. (2000) The role of inorganic phosphate in the development of freezing tolerance and the acclimatization of photosynthesis to low temperature is revealed by the pho mutants of *Arabidopsis thaliana*. *The Plant Journal*, 24(3), 383–396.

Iba, K. (2002) Acclimative response to temperature stress in higher plants: approaches of gene engineering for temperature tolerance. *Annual Review of Plant Biology*, 53(1), 225–245.

Ilik, P., Spundova, M., Sicner, M., Melkovicova, H., Kucerova, Z., Krchnak, P. et al. (2018) Estimating heat tolerance of plants by ion leakage: a new method based on gradual heating. *The New Phytologist*, 218(3), 1278–1287.

Impa, S.M., Raju, B., Hein, N.T., Sandhu, J., Prasad, P.V.V., Walia, H. et al. (2021) High night temperature effects on wheat and rice: current status and way forward. *Plant, Cell & Environment*, 44(7), 2049–2065.

Jaglo-Ottosen, K.R., Gilmour, S.J., Zarka, D.G., Schabenberger, O. & Thomashow, M.F. (1998) Arabidopsis CBF1 overexpression induces COR genes and enhances freezing tolerance. *Science*, 280(5360), 104–106.

Janda, T., Tajti, J., Hamow, K.A., Marcek, T., Ivanovska, B., Szalai, G. et al. (2021) Acclimation of photosynthetic processes and metabolic responses to elevated temperatures in cereals. *Physiologia Plantarum*, 171(2), 217–231.

Jiang, N., Yu, P., Fu, W., Li, G., Feng, B., Chen, T. et al. (2020) Acid invertase confers heat tolerance in rice plants by maintaining energy homoeostasis of spikelets. *Plant, Cell & Environment*, 43(5), 1273–1287.

Jung, J.H., Barbosa, A.D., Hutin, S., Kumita, J.R., Gao, M., Derwort, D. et al. (2020) A prion-like domain in ELF3 functions as a thermosensor in *Arabidopsis*. *Nature*, 585(7824), 256–260.

Jung, J.H., Domijan, M., Klose, C., Biswas, S., Ezer, D., Gao, M. et al. (2016) Phytochromes function as thermosensors in *Arabidopsis*. *Science*, 354(6314), 886–889.

Kaplan, F. & Guy, C.L. (2004) Beta-amylase induction and the protective role of maltose during temperature shock. *Plant Physiology*, 135(3), 1674–1684.

Kaplan, F. & Guy, C.L. (2005) RNA interference of *Arabidopsis* beta-amylase8 prevents maltose accumulation upon cold shock and increases sensitivity of PSII photochemical efficiency to freezing stress. *The Plant Journal*, 44(5), 730–743.

Kaplan, F., Kopka, J., Haskell, D.W., Zhao, W., Schiller, K.C., Gatzke, N. et al. (2004) Exploring the temperature-stress metabolome of *Arabidopsis*. *Plant Physiology*, 136(4), 4159–4168.

Kleine, T., Nägele, T., Neuhaus, H.E., Schmitz-Linneweber, C., Fernie, A.R., Geigenberger, P. et al. (2021) Acclimation in plants: the green hub consortium. *The Plant Journal*, 106(1), 23–40.

Klotke, J., Kopka, J., Gatzke, N. & Heyer, A.G. (2004) Impact of soluble sugar concentrations on the acquisition of freezing tolerance in accessions of *Arabidopsis thaliana* with contrasting cold adaptation: evidence for a role of raffinose in cold acclimation. *Plant, Cell & Environment*, 27(11), 1395–1404.

Knaupp, M., Mishra, K.B., Nedbal, L. & Heyer, A.G. (2011) Evidence for a role of raffinose in stabilizing photosystem II during freeze-thaw cycles. *Planta*, 234(3), 477–486.

Korn, M., Peterek, S., Mock, H.-P., Heyer, A.G. & Hincha, D.K. (2008) Heterosis in the freezing tolerance, and sugar and flavonoid contents of crosses between *Arabidopsis thaliana* accessions of widely varying freezing tolerance. *Plant, Cell & Environment*, 31(6), 813–827.

Kurepin, L.V., Dahal, K.P., Savitch, L.V., Singh, J., Bode, R., Ivanov, A.G. et al. (2013) Role of CBFs as integrators of chloroplast redox, phytochrome and plant hormone signaling during cold acclimation. *International Journal of Molecular Sciences*, 14(6), 12729–12763.

Küstner, L., Fürtauer, L., Weckwerth, W., Nägele, T. & Heyer, A.G. (2019a) Subcellular dynamics of proteins and metabolites under abiotic stress reveal deferred response of the *Arabidopsis thaliana* hexokinase-1 mutant gin2-1 to high light. *The Plant Journal*, 100(3), 456–472.

Küstner, L., Nägele, T. & Heyer, A.G. (2019b) Mathematical modeling of diurnal patterns of carbon allocation to shoot and root in *Arabidopsis thaliana*. *npj Systems Biology and Applications*, 5(1), 4.

Lee, D.G., Ahsan, N., Lee, S.H., Kang, K.Y., Bahk, J.D., Lee, I.J. et al. (2007) A proteomic approach in analyzing heat-responsive proteins in rice leaves. *Proteomics*, 7(18), 3369–3383.

Leegood, R.C. & Furbank, R.T. (1986) Stimulation of photosynthesis by 2% oxygen at low temperatures is restored by phosphate. *Planta*, 168(1), 84–93.

Legris, M., Nieto, C., Sellaro, R., Prat, S. & Casal, J.J. (2017) Perception and signalling of light and temperature cues in plants. *The Plant Journal*, 90(4), 683–697.

Li, H., Ding, Y., Shi, Y., Zhang, X., Zhang, S., Gong, Z. et al. (2017) MPK3- and MPK6-mediated ICE1 phosphorylation negatively regulates ICE1 stability and freezing tolerance in *Arabidopsis*. *Developmental Cell*, 43(5), 630–642.

Li, X., Ma, D., Lu, S.X., Hu, X., Huang, R., Liang, T. et al. (2016) Blue light- and low temperature-regulated COR27 and COR28 play roles in the *Arabidopsis* circadian clock. *Plant Cell*, 28(11), 2755–2769.

Li, Y., van den Ende, W. & Rolland, F. (2014) Sucrose induction of anthocyanin biosynthesis is mediated by DELLA. *Molecular Plant*, 7(3), 570–572.

Li, Z., Palmer, W.M., Martin, A.P., Wang, R., Rainsford, F., Jin, Y. et al. (2012) High invertase activity in tomato reproductive organs correlates with enhanced sucrose import into, and heat tolerance of, young fruit. *Journal of Experimental Botany*, 63(3), 1155–1166.

Lippmann, R., Babben, S., Menger, A., Delker, C. & Quint, M. (2019) Development of wild and cultivated plants under global warming conditions. *Current Biology*, 29(24), R1326–R1338.

Liu, Y. & Zhou, J. (2018) Mapping kinase regulation of ICE1 in freezing tolerance. *Trends in Plant Science*, 23(2), 91–93.

Lloyd, J.R. & Kossmann, J. (2015) Transitory and storage starch metabolism: two sides of the same coin? *Current Opinion in Biotechnology*, 32, 143–148.

Lu, Y. & Sharkey, T.D. (2006) The importance of maltose in transitory starch breakdown. *Plant, Cell & Environment*, 29(3), 353–366.

Lundmark, M., Cavaco, A.M., Trevanion, S. & Hurry, V. (2006) Carbon partitioning and export in transgenic Arabidopsis thaliana with altered capacity for sucrose synthesis grown at low temperature: a role for metabolite transporters. *Plant, Cell & Environment*, 29(9), 1703–1714.

Long, S.P. (1991) Modification of the response of photosynthetic productivity to rising temperature by atmospheric CO_2 concentrations: Has its importance been underestimated?. *Plant, Cell & Environment*, 14(8), 729–739.

Mahlow, S., Orzechowski, S. & Fettke, J. (2016) Starch phosphorylation: insights and perspectives. *Cellular and Molecular Life Sciences*, 73(14), 2753–2764.

Mir, B.A., Mir, S.A., Khazir, J., Tonfack, L.B., Cowan, D.A., Vyas, D. et al. (2015) Cold stress affects antioxidative response and accumulation of medicinally important withanolides in *Withania somnifera* (L.) Dunal. *Industrial Crops and Products*, 74, 1008–1016.

Mittler, R., Finka, A. & Goloubinoff, P. (2012) How do plants feel the heat? *Trends in Biochemical Sciences*, 37(3), 118–125.

Monroe, J.D. (2020) Involvement of five catalytically active Arabidopsis beta-amylases in leaf starch metabolism and plant growth. *Plant Direct*, 4(2), e00199.

Monroe, J.D., Storm, A.R., Badley, E.M., Lehman, M.D., Platt, S.M., Saunders, L.K. et al. (2014) Beta-amylase1 and beta-amylase3 are plastidic starch hydrolases in Arabidopsis that seem to be adapted for different thermal, pH, and stress conditions. *Plant Physiology*, 166(4), 1748–1763.

Monroe, J.G., McGovern, C., Lasky, J.R., Grogan, K., Beck, J. & McKay, J.K. (2016) Adaptation to warmer climates by parallel functional evolution of CBF genes in *Arabidopsis thaliana*. *Molecular Ecology*, 25(15), 3632–3644.

Moore, B., Zhou, L., Rolland, F., Hall, Q., Cheng, W.H., Liu, Y.X. et al. (2003) Role of the Arabidopsis glucose sensor HXK1 in nutrient, light, and hormonal signaling. *Science*, 300(5617), 332–336.

Nägele, T. & Heyer, A.G. (2013) Approximating subcellular organisation of carbohydrate metabolism during cold acclimation in different natural accessions of *Arabidopsis thaliana*. *The New Phytologist*, 198(3), 777–787.

Nägele, T., Stutz, S., Hörmiller, I. & Heyer, A.G. (2012) Identification of a metabolic bottleneck for cold acclimation in *Arabidopsis thaliana*. *The Plant Journal*, 72(1), 102–114.

Nagler, M., Nukarinen, E., Weckwerth, W. & Nägele, T. (2015) Integrative molecular profiling indicates a central role of transitory starch breakdown in establishing a stable C/N homeostasis during cold acclimation in two natural accessions of *Arabidopsis thaliana*. *BMC Plant Biology*, 15(1), 284.

Pachauri RK, Allen MR, Barros VR, Broome J, Cramer W, Christ R, Church JA, Clarke L, Dahe Q, Dasgupta P (2014) Climate change 2014: synthesis report. Contribution of Working Groups I, II and III to the fifth assessment report of the Intergovernmental Panel on Climate Change.

Palonen, P., Buszard, D. & Donnelly, D. (2000) Changes in carbohydrates and freezing tolerance during cold acclimation of red raspberry cultivars grown in vitro and in vivo. *Physiologia Plantarum*, 110(3), 393–401.

Park, S., Lee, C.M., Doherty, C.J., Gilmour, S.J., Kim, Y. & Thomashow, M.F. (2015) Regulation of the Arabidopsis CBF regulon by a complex low-temperature regulatory network. *The Plant Journal*, 82(2), 193–207.

Pazhamala, L.T., Kudapa, H., Weckwerth, W., Millar, A.H. & Varshney, R.K. (2021) Systems biology for crop improvement. *Plant Genome*, 14(2), e20098.

Pilkington, S.M., Encke, B., Krohn, N., Hohne, M., Stitt, M. & Pyl, E.T. (2015) Relationship between starch degradation and carbon demand for maintenance and growth in *Arabidopsis thaliana* in different irradiance and temperature regimes. *Plant, Cell & Environment*, 38(1), 157–171.

Pollastri, S., Sukiran, N.A., Jacobs, B. & Knight, M.R. (2021) Chloroplast calcium signalling regulates thermomemory. *Journal of Plant Physiology*, 264, 153470.

Pollock, C.J. & Lloyd, E.J. (1987) The effect of low-temperature upon starch, sucrose and fructan synthesis in leaves. *Annals of Botany*, 60(2), 231–235.

Prasch, C.M. & Sonnewald, U. (2013) Simultaneous application of heat, drought, and virus to *Arabidopsis* plants reveals significant shifts in signaling networks. *Plant Physiology*, 162, 1849–1866.

Qian, W., Xiao, B., Wang, L., Hao, X., Yue, C., Cao, H. et al. (2018) CsINV5, a tea vacuolar invertase gene enhances cold tolerance in transgenic *Arabidopsis*. *BMC Plant Biology*, 18(1), 228.

Qu, A.L., Ding, Y.F., Jiang, Q. & Zhu, C. (2013) Molecular mechanisms of the plant heat stress response. *Biochemical and Biophysical Research Communications*, 432(2), 203–207.

Ranty, B., Aldon, D., Cotelle, V., Galaud, J.P., Thuleau, P. & Mazars, C. (2016) Calcium sensors as key hubs in plant responses to biotic and abiotic stresses. *Frontiers in Plant Science*, 7, 327.

Rees, H., Joynson, R., Brown, J.K.M. & Hall, A. (2021) Naturally occurring circadian rhythm variation associated with clock gene loci in Swedish Arabidopsis accessions. *Plant, Cell & Environment*, 44(3), 807–820.

Rekarte-Cowie, I., Ebshish, O.S., Mohamed, K.S. & Pearce, R.S. (2008) Sucrose helps regulate cold acclimation of *Arabidopsis thaliana*. *Journal of Experimental Botany*, 59(15), 4205–4217.

Reyes, B.A., Pendergast, J.S. & Yamazaki, S. (2008) Mammalian peripheral circadian oscillators are temperature compensated. *Journal of Biological Rhythms*, 23(1), 95–98.

Ribeiro, C., Hennen-Bierwagen, T.A., Myers, A.M., Cline, K. & Settles, A.M. (2020) Engineering 6-phosphogluconate dehydrogenase improves grain yield in heat-stressed maize. *Proceedings of the National Academy of Sciences*, 117(52), 33177–33185.

Richter, K., Haslbeck, M. & Buchner, J. (2010) The heat shock response: life on the verge of death. *Molecular Cell*, 40(2), 253–266.

Ristic, Z. & Ashworth, E.N. (1993) Changes in leaf ultrastructure and carbohydrates in *Arabidopsis thaliana* L. (Heyn) cv. Columbia during rapid cold acclimation. *Protoplasma*, 172, 111–123.

Ritonga, F.N. & Chen, S. (2020) Physiological and molecular mechanism involved in cold stress tolerance in plants. *Plants*, 9(5), 560.

Ritte, G., Scharf, A., Eckermann, N., Haebel, S. & Steup, M. (2004) Phosphorylation of transitory starch is increased during degradation. *Plant Physiology*, 135(4), 2068–2077.

Saidi, Y., Peter, M., Finka, A., Cicekli, C., Vigh, L. & Goloubinoff, P. (2010) Membrane lipid composition affects plant heat sensing and modulates Ca(2+)-dependent heat shock response. *Plant Signaling & Behavior*, 5(12), 1530–1533.

Sajid, M., Rashid, B., Ali, Q. & Husnain, T. (2018) Mechanisms of heat sensing and responses in plants. It is not all about Ca^{2+} ions. *Biologia Plantarum*, 62(3), 409–420.

Santarius, K.A. & Milde, H. (1977) Sugar compartmentation in frost-hardy and partially dehardened cabbage leaf cells. *Planta*, 136(2), 163–166.

Sasaki, H., Ichimura, K. & Oda, M. (1996) Changes in sugar content during cold acclimation and deacclimation of cabbage seedlings. *Annals of Botany*, 78(3), 365–369.

Savitch, L.V., Allard, G., Seki, M., Robert, L.S., Tinker, N.A., Huner, N.P.A. et al. (2005) The effect of overexpression of two brassica CBF/-DREB1-like transcription factors on photosynthetic capacity and freezing tolerance in *Brassica napus*. *Plant & Cell Physiology*, 46(9), 1525–1539.

Savitch, L.V., Barker-Astrom, J., Ivanov, A.G., Hurry, V., Oquist, G., Huner, N.P. et al. (2001) Cold acclimation of Arabidopsis thaliana results in incomplete recovery of photosynthetic capacity, associated with an increased reduction of the chloroplast stroma. *Planta*, 214(2), 295–303.

Savitch, L.V., Gray, G.R. & Huner, N.P.A. (1997) Feedback-limited photosynthesis and regulation of sucrose-starch accumulation during cold

acclimation and low-temperature stress in a spring and winter wheat. *Planta*, 201(1), 18–26.
Schulz, E., Tohge, T., Zuther, E., Fernie, A.R. & Hincha, D.K. (2015) Natural variation in flavonol and anthocyanin metabolism during cold acclimation in Arabidopsis thaliana accessions. *Plant, Cell & Environment*, 38(8), 1658–1672.
Sharkey, T.D. (2021) Pentose phosphate pathway reactions in photosynthesizing cells. *Cells*, 10(6), 1547.
Sharmin, S.A., Alam, I., Rahman, M.A., Kim, K.H., Kim, Y.G. & Lee, B.H. (2013) Mapping the leaf proteome of *Miscanthus sinensis* and its application to the identification of heat-responsive proteins. *Planta*, 238(3), 459–474.
Shi, Y., Huang, J., Sun, T., Wang, X., Zhu, C., Ai, Y. et al. (2017) The precise regulation of different COR genes by individual CBF transcription factors in *Arabidopsis thaliana*. *Journal of Integrative Plant Biology*, 59(2), 118–133.
Sicher, R. (2011) Carbon partitioning and the impact of starch deficiency on the initial response of Arabidopsis to chilling temperatures. *Plant Science*, 181(2), 167–176.
Smallwood, M. & Bowles, D.J. (2002) Plants in a cold climate. *Philosophical Transactions of the Royal Society of London. Series B, Biological Sciences*, 357(1423), 831–847.
Smith, A.M., Zeeman, S.C. & Smith, S.M. (2005) Starch degradation. *Annual Review of Plant Biology*, 56, 73–98.
Somerville, C. (2006) Cellulose synthesis in higher plants. *Annual Review of Cell and Developmental Biology*, 22(1), 53–78.
Stitt, M. & Hurry, V. (2002) A plant for all seasons: alterations in photosynthetic carbon metabolism during cold acclimation in *Arabidopsis*. *Current Opinion in Plant Biology*, 5(3), 199–206.
Stitt, M. & Zeeman, S.C. (2012) Starch turnover: pathways, regulation and role in growth. *Current Opinion in Plant Biology*, 15(3), 282–292.
Strand, A., Foyer, C.H., Gustafsson, P., Gardestrom, P. & Hurry, V. (2003) Altering flux through the sucrose biosynthesis pathway in transgenic *Arabidopsis thaliana* modifies photosynthetic acclimation at low temperatures and the development of freezing tolerance. *Plant, Cell & Environment*, 26(4), 523–535.
Strand, A., Hurry, V., Gustafsson, P. & Gardestrom, P. (1997) Development of *Arabidopsis thaliana* leaves at low temperatures releases the suppression of photosynthesis and photosynthetic gene expression despite the accumulation of soluble carbohydrates. *The Plant Journal*, 12(3), 605–614.
Strand, Å., Hurry, V., Henkes, S., Huner, N., Gustafsson, P., Gardeström, P. et al. (1999) Acclimation of *Arabidopsis* leaves developing at low temperatures. Increasing cytoplasmic volume accompanies increased activities of enzymes in the calvin cycle and in the sucrose-biosynthesis pathway. *Plant Physiology*, 119, 1387–1397.
Talts, P., Parnik, T., Gardestrom, P. & Keerberg, O. (2004) Respiratory acclimation in *Arabidopsis thaliana* leaves at low temperature. *Journal of Plant Physiology*, 161(5), 573–579.
Tang, T., Liu, P., Zheng, G. & Li, W. (2016) Two phases of response to long-term moderate heat: variation in thermotolerance between *Arabidopsis thaliana* and its relative *Arabis paniculata*. *Phytochemistry*, 122, 81–90.
Teng, S., Keurentjes, J., Bentsink, L., Koornneef, M. & Smeekens, S. (2005) Sucrose-specific induction of anthocyanin biosynthesis in *Arabidopsis* requires the MYB75/PAP1 gene. *Plant Physiology*, 139(4), 1840–1852.
Thomashow, M.F. (2010) Molecular basis of plant cold acclimation: insights gained from studying the CBF cold response pathway. *Plant Physiology*, 154(2), 571–577.
Thuiller, W., Lavorel, S., Araujo, M.B., Sykes, M.T. & Prentice, I.C. (2005) Climate change threats to plant diversity in Europe. *Proceedings of the National Academy of Sciences*, 102(23), 8245–8250.
Tiessen, A., Hendriks, J.H., Stitt, M., Branscheid, A., Gibon, Y., Farre, E.M. et al. (2002) Starch synthesis in potato tubers is regulated by post-translational redox modification of ADP-glucose pyrophosphorylase: a novel regulatory mechanism linking starch synthesis to the sucrose supply. *Plant Cell*, 14(9), 2191–2213.
van't Hoff, M.J.H. (1884) Etudes de dynamique chimique. *Recueil des Travaux Chimiques des Pays-Bas*, 3(10), 333–336.
Vasseur, F., Pantin, F. & Vile, D. (2011) Changes in light intensity reveal a major role for carbon balance in Arabidopsis responses to high temperature. *Plant, Cell & Environment*, 34(9), 1563–1576.
Vu, D.P., Martins Rodrigues, C., Jung, B., Meissner, G., Klemens, P.A.W., Holtgrawe, D. et al. (2020) Vacuolar sucrose homeostasis is critical for plant development, seed properties, and night-time survival in *Arabidopsis*. *Journal of Experimental Botany*, 71(16), 4930–4943.
Wang, X., Fang, G., Li, Y., Ding, M., Gong, H. & Li, Y. (2013) Differential antioxidant responses to cold stress in cell suspension cultures of two subspecies of rice. *Plant Cell, Tissue and Organ Culture*, 113(2), 353–361.
Weiszmann, J., Fürtauer, L., Weckwerth, W. & Nägele, T. (2018) Vacuolar sucrose cleavage prevents limitation of cytosolic carbohydrate metabolism and stabilizes photosynthesis under abiotic stress. *The FEBS Journal*, 285(21), 4082–4098.
Wienkoop, S., Morgenthal, K., Wolschin, F., Scholz, M., Selbig, J. & Weckwerth, W. (2008) Integration of metabolomic and proteomic phenotypes: analysis of data covariance dissects starch and RFO metabolism from low and high temperature compensation response in *Arabidopsis thaliana*. *Molecular & Cellular Proteomics*, 7(9), 1725–1736.
Wilczek, A.M., Cooper, M.D., Korves, T.M. & Schmitt, J. (2014) Lagging adaptation to warming climate in *Arabidopsis thaliana*. *Proceedings of the National Academy of Sciences of the United States of America*, 111(22), 7906–7913.
Wilhelm, E.P., Mullen, R.E., Keeling, P.L. & Singletary, G.W. (1999) Heat stress during grain filling in maize: effects on kernel growth and metabolism. *Crop Science*, 39(6), 1733–1741.
Xu, H., Li, X., Zhang, H., Wang, L., Zhu, Z., Gao, J. et al. (2020) High temperature inhibits the accumulation of storage materials by inducing alternative splicing of OsbZIP58 during filling stage in rice. *Plant, Cell & Environment*, 43(8), 1879–1896.
Yamori, W., Hikosaka, K. & Way, D.A. (2014) Temperature response of photosynthesis in C3, C4, and CAM plants: temperature acclimation and temperature adaptation. *Photosynthesis Research*, 119(1–2), 101–117.
Yano, R., Nakamura, M., Yoneyama, T. & Nishida, I. (2005) Starch-related alpha-glucan/water dikinase is involved in the cold-induced development of freezing tolerance in *Arabidopsis*. *Plant Physiology*, 138(2), 837–846.
Zhong, L., Zhou, W., Wang, H., Ding, S., Lu, Q., Wen, X. et al. (2013) Chloroplast small heat shock protein HSP21 interacts with plastid nucleoid protein pTAC5 and is essential for chloroplast development in *Arabidopsis* under heat stress. *Plant Cell*, 25(8), 2925–2943.
Zhu, L., Bloomfield, K.J., Hocart, C.H., Egerton, J.J.G., O'Sullivan, O.S., Penillard, A. et al. (2018) Plasticity of photosynthetic heat tolerance in plants adapted to thermally contrasting biomes. *Plant, Cell & Environment*, 41(6), 1251–1262.
Zuther, E., Buchel, K., Hundertmark, M., Stitt, M., Hincha, D.K. & Heyer, A. G. (2004) The role of raffinose in the cold acclimation response of Arabidopsis thaliana. *FEBS Letters*, 576(1–2), 169–173.

How to cite this article: Seydel, C., Kitashova, A., Fürtauer, L. & Nägele, T. (2022) Temperature-induced dynamics of plant carbohydrate metabolism. *Physiologia Plantarum*, 174(1), e13602. Available from: https://doi.org/10.1111/ppl.13602

4. Discussion

Plants need to efficiently adapt to dynamic environmental conditions. Already five minutes of heat stress has been found to be memorised by *Arabidopsis*, hinting towards a tightly regulated network of stress perception and reactions (Oyoshi et al., 2020). In temperate zones, temperatures can fluctuate considerably during the day, but also over the course of the whole year. Regulation of metabolism was shown to play an important role in stabilising temperature tolerance. The impact of temperature on the carbohydrate metabolism has been studied extensively over the last decades, and it has become clear that the response to environmental changes within and between compartmentalised plant cells is highly dynamic (Kaplan et al., 2004; Hannah et al., 2006; Ahsan et al., 2010; Nägele et al., 2012; Prasch & Sonnewald, 2013; Hurry, 2017; Weiszmann et al., 2018; Atanasov et al., 2020; Seydel et al., 2022b; Hernandez et al., 2023; Kitashova et al., 2023).

Heat can impact signalling pathways, photosynthesis and the primary carbohydrate metabolism (Seydel et al., 2022a). Metabolic pathways are regulated in response to heat, some transiently, some lasting over a longer period of time, and often already within the first 30 minutes of heat exposure (Kaplan et al., 2004). But it always depends on the duration of the heat exposure and the actual temperature, how the plant reacts. When collecting data from various studies, it becomes clear that the individual heat response is likely tailored to the specific heat conditions, as findings vary and sometimes contradict. An accumulation of sucrose seems to coincide with heat treatment in many cases, whereas the response of hexoses is not described as uniformly. The enzymatic activities reported for heat treatment differ as well. Invertases were reported to increase in their activity, but in another study, their transcription was reported to be regulated depending on the isoform (Seydel et al., 2022a). The collection of metabolic reactions to heat showcases a responsive and flexible system, which is, however, not yet understood in its entirety (Seydel et al., 2022a). Based on these observations, the aim of this thesis was to derive a mechanistic understanding of how the metabolic, photosynthetic and ultrastructural heat response results in elevated thermotolerance.

4.1. Balance modelling using Fourier polynomials reveals a central role of sucrose biosynthesis in stabilising carbohydrate metabolism under elevated temperature

Describing biological systems by mathematical means can be a challenge, especially when attempting to capture highly dynamic processes in a sound mathematical framework. There are

several approaches to distil biological systems into mathematical models, and they all depend on the questions that are asked about the system (Schaber et al., 2009). Here, balance modelling was chosen to capture the dynamic changes induced by transient temperature increase for several temperatures, timepoints and genotypes. The general assumption of the balance model utilised in this study (see Figure 3) is based on the direct connection of net photosynthesis (NPS), which creates a carbon pool in the plant, and the interconversion of carbon into starch and soluble sugars (Seydel et al., 2022a). This way, the fluxes in the observed system could be quantified. Balance modelling critically depends on the assumption of input and consuming

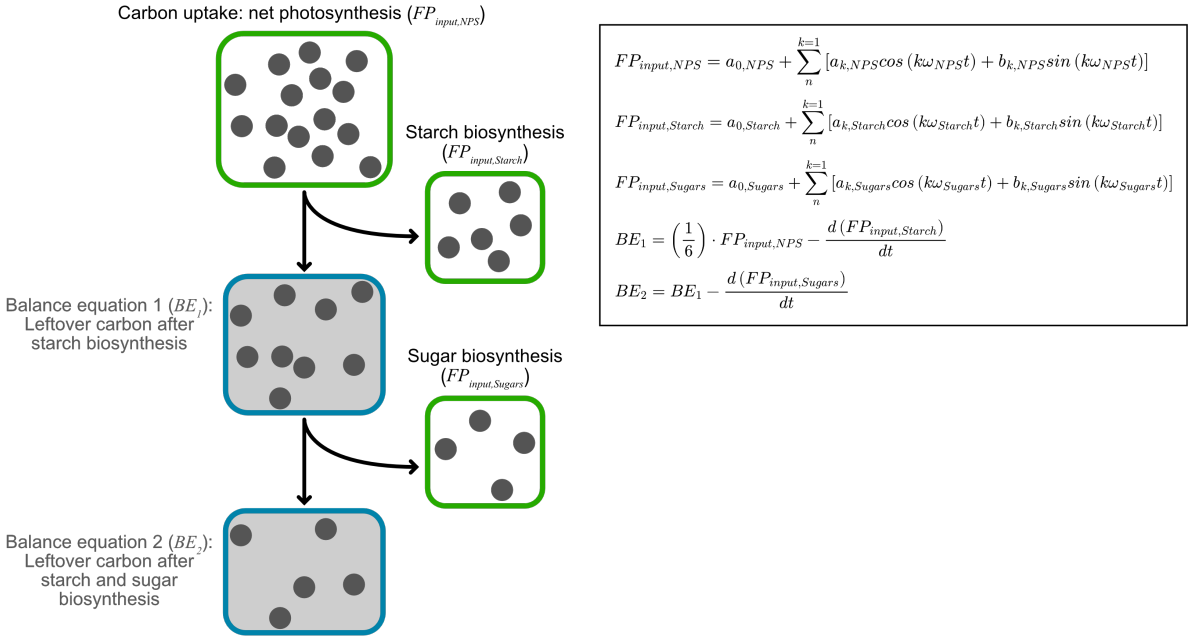

Figure 3. Depiction of the balance model developed in Seydel et al. (2022a). The grey dots represent carbon in C6 equivalents, the green boxes show the Fourier polynomial input functions that were determined with experimental data, the blue boxes represent the balance equations developed to level the input functions. Carbon is accumulated by photosynthesis ($FP_{input,NPS}$) and funneled into starch bioynthesis ($FP_{input,Starch}$) or used otherwise (BE_1). This leftover carbon is used either for sugar biosynthesis ($FP_{input,Sugars}$) or for processes further downstream (BE_2).

functions within the model. In plants, photosynthetic CO_2 assimilation determines growth and metabolism. Hence, to estimate heat effects on carbon metabolism, experimentally determined CO_2 assimilation rates were interpolated using Fourier polynomials. The mathematical function needs to fit the experimental data as representatively as possible. This can be quite challenging, especially when highly dynamic processes are concerned. In this study, NPS was measured over time for different conditions. Thus, the changing amount of assimilated carbon needed to be described depending on the time of day and on the transient temperature change. In natural sciences and engineering, Fourier polynomials are used to describe periodic systems. The rhythms that define the natural environment on Earth, such as the day-night cycle, the tides or

seasonal rhythm, are prime examples of periodic processes. But also on a smaller scale, biological systems can be described by Fourier analysis, for example, the expression of housekeeping genes in a time series (Dong et al., 2011) or the oscillatory nature of body movement that strains tissue (Wang et al., 1997). As the data produced in this study mirrors a periodic rhythm, Fourier polynomials were used to depict this dynamic process in a time-continuous manner. The Fourier polynomials were fitted to the experimental NPS data ($FP_{input,NPS}$), as well as starch and sugar rates ($FP_{input,Starch}$, $FP_{input,Sugars}$). The balance equations BE_1 and BE_2 were deduced from the Fourier polynomials, and this way, the whole mathematical framework could be analysed. The comparison of the integrals, as well as amplitude and frequency of the derivatives of the input functions and balance equations, yielded further insight into the dynamics of metabolic regulation, and genotypes and temperature treatments could be distinguished.

In *pgm1*, a disturbed CO_2 assimilation rate and photosynthesis, as well as a distinct pattern of sugar accumulation, all showed the impact of heat on the mutant's carbon fluxes. The derivatives of BE_1 and BE_2 of *pgm1* were exhibiting more fluctuations than those of the natural accession Columbia-0 (Col-0) and *spsa1* upon heat exposure, especially during the 32°C and 36°C treatment, suggesting a less robust metabolic homeostasis due to deficiencies in starch biosynthesis. With the loss of the stabilising function of starch on the metabolism, the whole process from carbon uptake to its conversion into chemical energy is impaired. The net carbon gain, illustrated by the integrals of $FP_{input,NPS}$, BE_1 and BE_2 also was considerably lowered in *pgm1* compared to Col-0, also under control conditions. This indicates that *pgm1* retains less carbon than Col-0, even though at 36°C and 40°C, the CO_2 assimilation did not differ too much from that of Col-0. Even the significant decrease of maximum quantum yield of PSII (F_v/F_m) during 40°C treatment does not hint towards critical damage in PSII, as F_v/F_m lay between 0.76 and 0.78, which is still within physiological range, eg. when compared to the values measured in cotton plants (Law & Crafts-Brandner, 1999). Even though the integral of $FP_{input,NPS}$ of *pgm1* still bears some resemblance to Col-0 in control and heat, the integrals of BE_1 and BE_2 are deviating considerably from Col-0. This fits the starch and sugar measurements, which deviated from the wild type as well. If all the carbon that can not be stored in the form of starch were instead stored in the form of sugars, the integral of BE_2, illustrating the net carbon gain during the light period, would show similar or more stabilised dynamics as the integral of BE_1. But the BE_2 integral displayed a severe drop in carbon gain, implying a loss of carbon after starch biosynthesis. Hence, it is assumed that the disturbance of the metabolic system due to low starch assimilation is not entirely balanced by increased sugar synthesis. It was found that instead of funnelling all assimilated carbon into sugar biosynthesis, *pgm1* exports excess carbon to the roots where it is respired (Brauner et al., 2014). Such an efflux of carbon would account for the differing dynamics of the integrals of BE_2 and thus the lowered net carbon gain. Ac-

cording to the trend of the integrals of BE_2, this effect might be exacerbated in the heat, at least for 32°C and 36°C. In *spsa1*, the derivatives and integrals of the balance equations showed an opposed trend. The reduced SPS activity was not destabilising the metabolism; it rather led to a more stable rate of net carbon gain throughout the process from CO_2 assimilation over starch biosynthesis to sugar biosynthesis, as illustrated by the integrals. Even a severe heat wave was not impacting the carbon gain over the light period, demonstrating an improved stability of the metabolic process in *spsa1*.

Reconstructing the flux of the carbon through the plant can reveal important details about certain metabolic processes and create a basis for new focal points of metabolic research. A balance-based modelling approach could prove valuable in crop species, where understanding the carbon flux under adverse conditions can help predict and improve yield. For balance analysis, the data required for the construction of a large network model is readily available, as it can encompass genomics, transcriptomics, proteomics, and metabolomics datasets (Sweetlove et al., 2025). The plethora of available omics datasets enabled the development of genome-scale metabolic models (GEMs), which can be important tools in metabolic engineering, especially in crop plants (Mangaravite et al., 2025). Those GEMs are often developed employing flux balance analysis, as a kinetic modelling approach would not be feasible for the amount of data fed into the model (Sweetlove et al., 2025). The dependence of the rice metabolic network on photon flux, for example, was described in a genome-scale balance modelling approach, which used only a few kinetic constraints in combination with a mostly stochiometric model. The model realistically reproduced physiological behaviour and predicted organelle interactions based solely on balancing mass and energy (Poolman et al., 2013). For potato leaves, a GEM was developed to include not only the primary, but also the secondary and lipid metabolism to quantify the trade-off between growth and defence against biotic stresses. The authors found that when the growth rate was reduced, the flux through secondary metabolism pathways increased. Trade-offs like this were characterised by their specific metabolic flux signature, and predicted metabolite flux-sums were in line with experimental findings (Zrimec et al., 2025). Another approach would be to experimentally resolve and depict source and sink tissues in a model to analyse the balancing of carbon between those tissues under adverse conditions. This can reveal possible approaches for crop enhancement. In maize, metabolic bottlenecks could be identified in a GEM encompassing leaves, roots, stalk and kernels, and a beneficial effect of inoculation with arbuscular mycorrhizal fungi during heat treatment was accurately predicted (Chowdhury et al., 2023). Current advances like this show that, independent of the specific modelling approach, the mathematical representation and prediction of metabolic networks is critical for a deeper mechanistic understanding of metabolism.

4.1.1. The importance of sucrose and sucrose phosphate synthase for metabolic stabilisation

Approximately 90% of plant biomass is built up of carbohydrates originating from sucrose (Ruan, 2014). Sucrose is a non-reducing sugar with a broad array of functions in the plant. In many species, and also in *Arabidopsis*, it is the most abundant transport sugar and plays central roles in signalling cascades and acclimation processes (Huber & Huber, 1996; Stitt et al., 2010; Nägele et al., 2012; Ruan, 2014; Herrmann et al., 2019; Kitashova et al., 2021). In photosynthetically active tissue, it is synthesised in the cytosol from F6P and UDPG by the sequential enzymatic reactions of SPS and SPP. Degradation into hexoses can take place in several compartments of the cell via the different isoforms of invertase located in the cytosol, vacuole, chloroplast and the apoplast (see Figure 2; Vargas et al. (2008); Ruan (2014)). This creates a sucrose cycle in the cell, enabling the plant to flexibly and finely regulate compartmental sugar concentration, albeit under energy consumption. For further use in other parts of the plant, sucrose is loaded into the phloem in the source tissue and transported to carbon sinks (Geigenberger & Stitt, 1991; Ruan, 2014).

In cold, it was found that increased SPS activity could facilitate the acclimation process and a shift of sucrose cleavage capacity to the vacuole contributed to stabilisation of photosynthesis and the carbohydrate metabolism (Strand et al., 2003; Hoermiller et al., 2017; Weiszmann et al., 2018). During transient heat exposure, an inverse effect of SPS activity could be shown: a lowered activity of SPS (30% - 50% of the wild type) in the mutant *spsa1* resulted in stabilised photosynthesis and generally less perturbation of metabolism by transient heat, whereas a lowered PGM activity in *pgm1* resulted in higher heat susceptibility and a less stabilised metabolism (Seydel et al., 2022a). Under control conditions, *spsa1* exhibited a slightly higher CO_2 assimilation than Col-0 and the starch-deficient mutant *pgm1*. In Col-0 and *pgm1*, the Fourier series fit to the experimental data of CO_2 uptake showed a deviation from control with the onset of heat, whereas for *spsa1*, the Fourier series of heat-treated samples stayed much closer to the control values. This indicates a strong impact of the reduced SPS activity on the assimilation of CO_2.

Compared to the wild type, photosynthesis in the *spsa1* mutant was found to be stabilised after 4 hours of heat exposure. F_v/F_m was found to be not affected as severely by transient heat exposure as in the wild type and *pgm1*. Even though F_v/F_m dropped slightly during the 40°C treatment and rose again during recovery, those dynamics were dampened and not significant in *spsa1* compared to the more pronounced dynamics in Col-0 and especially *pgm1*. An opposing trend could be seen in the electron transport rate (ETR), which showed a significant increase during heat treatment in *spsa1*, whereas it did not increase in Col-0 or *pgm1*. These

observations hinted towards a stabilisation of the photosynthetic process in *spsa1*, which was also corroborated by the NPS rates and the increased rate of starch accumulation. This trend was illustrated by the integrals of the Fourier polynomials FP_{NPS}, BE_1 and BE_2, representing the total sum of net carbon gain during the light period. As soon as the transient heat set in, the integrals of Fourier polynomials from heat-treated Col-0 and *pgm1* samples deviated from the control, suggesting a lowered amount of carbon that is funnelled from NPS to starch and sugar biosynthesis. For *spsa1*, on the other hand, there was no reduction in the sum of net carbon gain with the onset of heat. The reduction in SPS activity resulted in a stable CO_2 uptake and constant, unimpeded conversion into carbohydrates. The impact of this effect could also be detected in stabilised growth after prolonged heat treatment in *spsa1*. As the transpiration rates did not change significantly, but the ETR was elevated in our measurements, an improvement in the photosynthetic machinery could be the reason for this stabilisation. This could be achieved, for example, by synthesising more proteins that take part in the photosynthetic process. However, to verify this, a more detailed analysis of the proteins of the photosynthetic machinery would be needed.

It could be assumed that the reduction of SPS activity is taken as a signal for a lower sucrose supply in the plant, so the capacity for photosynthetic energy acquisition is increased to balance this metabolic deficit. The increased stability in the *spsa1* mutants also occurred at the level of carbohydrate synthesis, as they accumulated more sucrose than Col-0 during the 40°C treatment and also showed slightly increased starch levels compared to Col-0. Thus, it is assumed the cause for a stabilised carbohydrate metabolism is not the perception of a lowered amount of sucrose in the cells, but rather the perception of the lowered SPS activity. In Col-0, treatment with 40°C led to an accumulation of sugars, which was also continued in the recovery period after alleviation of the heat stress, whereas treatment with 36°C only resulted in an increase in sugar levels during the recovery period, and 32°C did not change sugar dynamics considerably. As it resulted in the most distinct change in metabolism, especially the 40°C treatment, is discussed below. In the cold, an increase in sucrose levels was shown to be beneficial for acclimation (Hincha et al., 1996), and here, sucrose seems to accumulate in response to heat, suggesting a similar role. The accumulation of sugars could be achieved by increased enzymatic reaction rates in biosynthesis or by a suppression of interconversion and/or export to carbon sinks. Either explanation could result in a stabilisation of leaf sugar levels in the face of newly encountered stress and thus higher probability of an increased energy demand of the cells. In *spsa1*, the sugar levels followed the same trend as in Col-0, except for sucrose, which accumulated to a higher level. In this case, the increase in sucrose levels could not arise from an increased activity of SPS, as the reduction of enzymatic activity in the mutant was quantified. Hence, a hindrance of sucrose export to the sinks as reason for a stronger accumulation of

sucrose in the source tissue is proposed.

In *spsa1*, the ETR is increased and sucrose accumulates to levels higher than in Col-0. If the cell could sense that a desirable level of sucrose is reached, the export to the sinks would be unblocked at some point. However, this was not observed during the heat wave analysed here. This could imply that the cell is not sensing sucrose levels directly, but rather the activity of the enzyme responsible for sucrose synthesis. This proposed "blindness" for a compound has been described in plants before. Mutants deficient in spliceosomal complex components showed the symptoms of nitrogen deficiency despite not experiencing nitrogen starvation (Araguirang et al., 2024). Even though the trend of increased sucrose levels was only detectable in 40°C treated plants, the stabilisation of carbon gain was visible in the integrals of the Fourier polynomials for all temperature treatments. This stresses the importance of sucrose metabolism for growth stabilisation during stressful conditions. Its profound impact on carbon balancing within the plant remains a topic of interest for further research. To test the hypothesis presented here, more components of the carbohydrate metabolism should be analysed in this experimental setup, such as enzymatic reaction rates and carbon allocation on a subcellular and an organ level.

4.2. Ultrastructural data can support and contextualise metabolic measurements

The carbohydrate metabolism of plants is compartmentalised, which poses challenges for its experimental analysis. Non-aqueous fractionation (NAF) represents an experimental technique which has been proven useful and suitable to efficiently quench and fractionate subcellular compartments (Gerhardt & Heldt, 1984; Szecowka et al., 2013; Fürtauer et al., 2016; Hernandez et al., 2023). The analysis of compartment-specific amounts of metabolites can shed light on redistribution processes and their role in maintaining metabolic homeostasis (Weiszmann et al., 2018). However, the actual concentration of metabolites in the various compartments can also hold important information. Transport processes often depend on concentration gradients, and the spatial distribution and availability of compounds can be crucial for enzymatic reactions (Lunn, 2007; Linka & Weber, 2010).

The concentration of metabolites in the compartments cannot be determined with NAF alone. For measuring metabolite concentrations correctly, the volume of the respective compartment is needed. Thus, following the establishment of the NAF procedure for plant tissue (Gerhardt & Heldt, 1984), Winter and colleagues generated datasets of barley and spinach to aid analysis by approximating volume ratios of the respective compartments. They achieved this by measuring area ratios in transmission electron microscopy (TEM) images and estimating volume ratios

by linear regression analysis (Winter et al., 1993, 1994). Recently, an estimation of volumetric data for *Arabidopsis* was provided by concatenation of volume data from different sources (Tolleter et al., 2024). It combined data from 2D TEM approaches (Winter et al., 1994; Armstrong et al., 2006; Koffler et al., 2013) with data acquired by confocal fluorescence microscopy and volume electron microscopy (vEM) workflows (Armstrong et al., 2006; Bouchekhima et al., 2009; Crumpton-Taylor et al., 2012). Those results were adjusted to fit the same frame of reference, as they were originating from different studies with different experimental setups and for some compartments even a different plant species (Tolleter et al., 2024). In this work, the compartmental volume ratios of leaf mesophyll cells from each condition were determined from serial block-face scanning electron microscopy (SBF-SEM) datasets (Seydel et al., 2025). As the growth and acclimation conditions matched those of the NAF experiment, a close fit of volume and metabolite data could be assumed. The trend of spinach and *Arabidopsis* volume ratios from those approaches reveals similar findings: the vacuole occupies the largest fraction of a leaf mesophyll cell, between 79% and 84%, the chloroplasts 9% to 16% and the cytosol between 2.4% and 3.4%. The data generated in this work also matches those volume proportions. The most distinct differences were the vacuole and the chloroplast volume proportions. The 2D analysis in spinach calculated a slightly lower vacuolar percentage of 79% compared to approximately 83% in our study, whereas the cytosol and chloroplast values were close to our observations (Winter et al., 1994). In the concatenated *Arabidopsis* dataset, the volume percentage of the chloroplasts was lower (9.4%) compared to our data (14%), whereas cytosol and vacuole showed quite similar values (Tolleter et al., 2024). The commonalities between those datasets could hint towards a rather conserved volume ratio of compartments within mesophyll cells in general. But as there was no distinguishing between palisade and spongy mesophyll cells in this study, there might be smaller differences between those cell types that were missed. It should also be noted that, depending on the environmental conditions, the actual volumes of the cells differed substantially. In this study, cells were shown to shrink during prolonged heat exposure, which was also described before (Wahid et al., 2012). Especially when datasets of different temperatures become available, it could be assessed whether the cell size change is a more general heat stress response, independent of the exact temperature, or can be connected to specific temperatures and acclimation capacity.

This decrease in cell size may also have repercussions for the actual volumes of the single organelles, which were not quantified separately. It was reported in several studies that chloroplasts and mitochondria can swell during heat exposure (Rizhsky et al., 2004; Zhang et al., 2010; Grigorova et al., 2012; Zhang et al., 2014; Zou et al., 2017). This would, together with the observed decrease in cell size, influence the functioning of cellular processes. An increase in organelle volume and a decrease in cell volume brings the compartments of the cell closer

together. This vicinity could facilitate intracellular transport processes and lipid exchange by direct membrane contact or vesicle transport (Shomo et al., 2024). The image data in this study was segmented with the help of a deep learning assisted workflow. It utilised a variant of U-Net, a fully convolutional neural network, which is specially designed to generate several precise labels from one dataset with few training images (Ronneberger et al., 2015). This approach, however, is specially suited for semantic segmentation, i.e. assigning a label to each pixel, defining its value, but not tracking the individual structures, eg. separate chloroplasts (Alom et al., 2019). Hence, information about individual organelle size is limited. However, the existing labels could be reevaluated, and tracking of the individual organelles can be achieved by hand or with the help of machine learning based approaches for microscopic image annotation and tracking (Archit et al., 2025).

4.2.1. Implications of sugar concentrations for transport processes

Combining subcellular volume data obtained from SBF-SEM with the subcellular sugar amounts obtained from NAF, calculation of sugar concentrations for the three compartments, chloroplast, cytosol, and vacuole was possible. This way, not only sugar distribution between the compartments could be analysed, but also concentrations and concentration gradients, drawing conclusions for transport mechanisms and other concentration-dependent processes. Also, the change of subcellular sugar distribution in the plants that were acclimated for 7 days to 34°C was analysed. Sugar concentrations are not always highest in the vacuole, even though it is the foremost storage compartment of the cell and thus contains the highest amount of sugars (Aluri & Büttner, 2007; Pommerrenig et al., 2018). On the contrary, only glucose concentration under control conditions was highest in the vacuole by a small margin, whereas sucrose and fructose exhibited the highest concentrations in the cytosol. Heat acclimation resulted in an increase in cytosolic glucose concentration, reversing the concentration gradient. In addition to the concentration gradient of the respective sugar, the high concentration of H^+ in the vacuole not only generates an acidic environment, but also exerts a proton motive force, which can be utilised for active transport of sugars (Hedrich et al., 2015; Pommerrenig et al., 2018).

Several vacuolar sugar transporters are described in *Arabidopsis*, rice, apple and other species (Zhu et al., 2025). The importers are translocating sugars from the cytosol into the vacuole by H^+ coupled antiport, utilising the high vacuolar H^+ concentration. The two importers currently described for *Arabidopsis* are Tonoplast Sugar Transporter 1 (TST1), which imports glucose and sucrose, and Vacuolar Glucose Transporter 1 (VGT1), which imports glucose (Aluri & Büttner, 2007; Keller & Neuhaus, 2025). Glucose was found to exhibit a concentration gradient from the vacuole to the cytosol under control conditions, which would necessitate import of

glucose against a concentration gradient with TST1 and VGT1. The active import of sucrose with TST1, however, seems less crucial during standard conditions or heat exposure, as the concentration gradient did not change under those conditions. Nonetheless, an increase in vacuolar sucrose levels was observed, which necessitates an import mechanism. The members of the Sugars Will Eventually be Exported Transporter (SWEET) family of sugar transporters are functioning as uniporters without utilising the proton motive force. Thus, they can translocate sugars along their concentration gradient (Zhu et al., 2025), which grants additional flexibility to the transport processes between cytosol and vacuole and presents a suitable candidate for the import of sucrose into the vacuole during heat.

Glucose and fructose were accumulating in the cytosol during heat acclimation. Export of sugars from the vacuole is achieved mostly as H^+ coupled symport by the Early Response to Dehydration Like 4 and 6 (ERDL4, ERDL6) transporters for fructose and glucose, respectively, and Sucrose transporter 4 (SUC4), which transports sucrose (Keller & Neuhaus, 2025). Only Early Response to Dehydration Six-Like1 (ESL1) has been described to export glucose by facilitated diffusion, and its directionality depends on the substrate concentration gradient (Yamada et al., 2010). This would imply that this transporter is probably active under control conditions, but not when the concentration gradient is reversed during heat. The ERDL4 and SUC4 facilitated sugar export by H^+ coupled symport fits to the concentration gradients in our study, as export of fructose and sucrose from the vacuole might need to be carried out against the cytosolic concentration gradient. ERDL6 might gain importance as an active glucose exporter during heat, when the concentration gradient of glucose is reversed. Many of the transporters mentioned here are crucial for sugar metabolism, as loss-of-function mutations often result in drastically changed total leaf sugar amount or developmental impediments (Wormit et al., 2006; Aluri & Büttner, 2007; Poschet et al., 2011; Zhu et al., 2025). Also, the extensive regulatory network influencing some of those transporters paints a complex picture. Some are mainly stress-induced (Yamada et al., 2010; Slawinski et al., 2021), others are influenced by the presence of certain sugars or by a combination of various environmental and metabolic stimuli (Wormit et al., 2006). However, it is difficult to accurately test vacuolar sugar transporters for their specific function (Zhu et al., 2025), which emphasises the benefit of utilising subcellular metabolite and ultrastructure data for interpretation of those results. One example is the description of the Senescence-Associated Sugar Transporter 1 (SAST1). SAST1 is mainly induced upon abscisic acid accumulation, a phytohormone associated with senescence and wounding (Keller & Neuhaus, 2025). It was observed to transport glucose and sucrose from the cytosol to the vacuole, and it was suggested this transport occurs against a concentration gradient, thus probably utilising the proton gradient of the vacuole (Cheng et al., 2024). Those assumptions might need to be reevaluated, as glucose and sucrose displayed differing concentration gradients in our study, which opens

up questions for the exact functioning of the described transporter. Especially as glucose was observed to change its concentration gradient over the tonoplast due to temperature changes, subcellular sugar concentrations might play an important role in the analysis of sugar transport in the future.

4.2.2. Adjustment of sucrose metabolism is crucial for acclimation to elevated temperature

An optimal acclimation capacity at 34°C was assumed due to the lowest index of injury in the electrolyte leakage assay. Even though F_v/F_m dropped significantly for heat-treated plants, the values of 32°C to 36°C were still within physiologically functional range, as discussed earlier (see chapter 4.1). Additionally, NPS rates did not significantly change at 34°C compared to control conditions. Thus, sufficient acclimation capacity of *Arabidopsis* was assumed at 34°C, as just minor constraints on the photosynthetic process occurred at that temperature. It was discussed that heat exposure leads to the dissociation of the oxygen evolving complex from PSII, causing destabilisation of the electron flow from the oxygen evolving complex towards PSII (Sun & Guo, 2016). Additionally, the equilibrium of light absorption between PSI and PSII can be affected by heat (Allakhverdiev et al., 2008). High temperatures necessitate an increase in electron transport capacity, because the cyclic electron flow around PSI can compensate for increased proton leakiness of the thylakoid membranes, enabling a continuation of ATP synthesis (Yamori et al., 2014). Especially for the temperatures analysed in this study, a cause for the slightly reduced photosynthetic capacity could also be a decrease in the Rubisco activation state. During elevated temperatures, the rate of Rubisco inactivation rises. But due to the heat lability of Rubisco activase, the rate of Rubisco reactivation is not sufficient to maintain this pace, leading to a reduction in active Rubisco amounts (Yamori et al., 2014). This could explain the slightly lowered maximum quantum yield of PSII observed here. In literature, a disordering of thylakoid membranes and de-stacking was observed from 35°C to 40°C (Gounaris et al., 1983, 1984), whereas in this study, no severe chloroplast phenotype in plants that were treated with up to 38°C could be observed. The thylakoids remained organised in grana stacks, and only a few isolated stroma thylakoids were not arranged completely parallel at higher temperatures. It has to be noted, however, that the chloroplasts observed by Gounaris et al. (1983, 1984) were subjected to the heat treatment after isolation from the tissue, whereas in this study, the whole tissue of heat-acclimated plants was observed. This could have repercussions for the severity of observed damages, because the intact plant with its various protection mechanisms could buffer the severity of the heat, and the plants observed in this study are assumed to have acclimated well to the elevated temperature. Nonetheless, the observed changes in photosynthetic performance can be connected to a slight phenotype of the chloroplasts. The most distinct indicator

of heat treatment in chloroplast ultrastructure is the increase of plastoglobule size, which can be attributed to heat-induced chloroplast senescence (Staehelin, 1986; Zhang et al., 2014; Arzac et al., 2022). This size change implies accumulation of various compounds that play important roles in chloroplast maintenance (Bréhélin & Kessler, 2008; Arzac et al., 2022).

The carbohydrate metabolism and subcellular sugar dynamics were analysed under the premise of optimal acclimation to get a better mechanistic understanding of the acclimation process. The treatment with 34°C for 7 days led to an increase of sucrose amounts in the vacuole, and a simultaneous decrease in cytosolic and plastidial amounts. Thus, it was assumed that sucrose was exported from the plastid to the vacuole. In contrast to heat acclimation, in the cold, plastidial sucrose was shown to increase (Nägele & Heyer, 2013) and was hypothesised to partake in stabilisation of the thylakoid membranes during cold, albeit not as efficiently as raffinose or other raffinose family oligosaccharides (RFOs) (Knaupp et al., 2011). This is based on the *in vitro* observation that sucrose and RFOs can protect liposomes from lipid fusion, which can occur during drying and rehydration, but also during cold treatment (Hincha et al., 2003). In this study, plants were well watered and acclimated to a moderately increased temperature. The photosynthetic performance itself was not detrimentally affected at 34°C, so it was assumed that in well-acclimated plants, sucrose is not needed in high amounts in the plastid for protection of thylakoid membranes. This is in accord with the microscopic data, which shows no damage to the thylakoid membranes at 34°C. The missing prevention of lipid fusion could also be an additional reason why plastoglobules increase in size in our study. However, as plastoglobules are involved in chloroplast senescence, lipid metabolism, thylakoid maintenance, and accumulation of antioxidant compounds like tocopherol, an increase in size or number during elevated temperature is well-grounded in research (Bréhélin & Kessler, 2008; Arzac et al., 2022).

An accumulation of sucrose in the vacuole was accompanied by a simultaneous increase in vacuolar glucose and fructose amounts, as well as an increase in vacuolar invertase activity. This indicates elevated sucrose cleavage activity in the vacuole, coupled to a high influx of sucrose, leading to consistently high levels of sucrose despite high cleavage rates. Also, significantly elevated levels of glucose and non-significantly elevated levels of fructose were found in the cytosol, but no marked increase in cytosolic invertase activity. Invertase activity was rather shown to be stabilised at levels also measured under control conditions, suggesting a regulatory effect maintaining cytosolic invertase activity. However, for analysis of invertase activity, the concentration of glucose and fructose in the cytosol needs to be taken into account, because invertases are inhibited by their reaction products glucose and fructose (Sturm, 1999). If hexoses accumulate in the cytosol, a compartment of rather small volume, concentration increases already with low amounts of the respective sugar. Our simulations showed a strong inhibitory effect of measured hexose concentrations on cytosolic invertase, reducing sucrose cleavage in this com-

partment considerably. In the large vacuole, on the other hand, a much higher amount of hexoses is needed to reach a critical concentration to result in inhibition of invertase. Thus, sucrose cleavage might be mainly conducted in the vacuole and the resulting hexoses are transported back into the cytosol, where they accumulate to high concentrations. For cold acclimation, it was hypothesised that a shift of sucrose cleavage capacity from the cytosol into the vacuole could contribute to a stabilisation of photosynthesis and metabolism (Weiszmann et al., 2018). Accordingly, the shift of sucrose to the vacuole coupled to an increase in vacuolar invertase reaction rates might support this hypothesis for heat acclimation as well. It has been reported that due to oxidative stress, sucrose is accumulated in the vacuole (Kohli et al., 2019), so this might be a common response to abiotic stress in general. In a scenario of a short heat wave described earlier (Seydel et al., 2022a) (4.1.1), sucrose was shown to accumulate in the leaves after 4h exposure to 40°C. It is hypothesised that this accumulation is due to a throttled export of sucrose to the sinks. To limit the export of sucrose, it must be prevented from entering the phloem. It was shown that specifically cytosolic sucrose concentration is impacting the rate of phloem loading and thus the concentration of sucrose in the roots (Brauner et al., 2014). Hence, it is assumed that sequestering the sucrose into the vacuole can prevent export of the sucrose into the sinks. This might also be an explanation for the observed transport of sucrose into the vacuole in the acclimated plants. But in contrast to the transient heat exposure, in this case, the sucrose concentration in the whole leaf did not increase; for 34°C, they even decreased slightly below control values. This could show a more refined sucrose distribution due to the acclimation process. As a shock response, export of sucrose is limited to a degree that ultimately leads to accumulation of sucrose in the source tissue. When heat exposure is prolonged and the plant is acclimated, the sucrose can be redistributed in the cell and to the sinks more efficiently. In addition, plants in the 34°C acclimation period also started inducing their inflorescence. This could constitute another sink for the sugars in the plant.

The cytosolic sugar amounts are also of importance for the cellular energy homeostasis. It was hypothesised that cytosolic invertase can influence mitochondrial hexokinase by either regulation of sucrose concentration or glucose production (Rolland et al., 2006; Li et al., 2007; Bolouri-Moghaddam et al., 2010; Xiang et al., 2011). This would connect cytosolic sugar levels with energy production in the mitochondria. Mitochondrial hexokinase plays an important role in maintaining the mitochondrial electron transport chain, as well as influencing the production of ROS there (Camacho-Pereira et al., 2009), and it is a source of ADP in the mitochondria, which is consumed by oxidative phosphorylation to produce ATP (Xiang et al., 2011). An increase in cytosolic hexose concentrations could thus lead to an increased flux into glycolysis and production of pyruvate. But also a decreased SPS activity could contribute to increasing the flux of carbon into pyruvate, as it converts hexose phosphates into sucrose, and a lowered activity

could lead to increased levels of hexose phosphates which in turn are a substrate for glycolysis. Supporting this idea, it was reported that a combination of heat and drought treatment led to an increase in transcripts of hexokinase and fructokinase, which would result in an increase in F6P, the direct substrate for the TCA cycle (Rizhsky et al., 2004). Even though no reduction in SPS activity was observed, the activity of SPS in the cytosol during heat acclimation was stabilised, suggesting regulatory effects. In theory, when assuming temperature dependence of SPS activity according to the results calculated by Kitashova et al. (2023) for the range of 4°C to 22°C, higher activity of SPS during elevated temperatures would be expected. However, the stabilisation of SPS activity at control levels during heat acclimation supports the hypothesis about increasing flux into glycolysis by enabling accumulation of hexose phosphates. During a heat wave, a lowered SPS activity in the mutant *spsa1* led to stabilised metabolism and CO_2 assimilation. This observation would be fitting for the hypothesis presented here: During a fast onset heat wave, the Col-0 plants have not yet regulated their enzymatic activities to ensure a high input into glycolysis. The *spsa1* mutant, on the other hand, can already utilise the reduced SPS activity with the onset of the heat and can maintain a high influx into glycolysis, leading to a more stable energy supply for the cell. Mitochondrial respiration is not limited at the observed temperatures, as it declines only between 50°C and 60°C, after reaching its optimum shortly before (Scafaro et al., 2021). Hence, regulating the enzymes responsible for providing substrate for glycolysis, and by this the TCA cycle, could have a major regulatory impact on the rate of respiration. An additional factor to consider is ROS production. Under control conditions, the electron transport chain (ETC) in the mitochondria is a major source of ROS, but the damage is limited by antioxidant compounds in the mitochondria. Under adverse conditions, leading to higher ROS production, defence systems might be overwhelmed and ROS could accumulate (Jacoby et al., 2012). Also, several complexes of the ETC are known to produce superoxide when the reduction state of the ETC is increasing, which can be caused by increased input or reduced activity (Møller et al., 2021). Thus, regulation of the cytosolic sugar concentration would be an instance to ensure limited ROS production and an acceptable balance between photosynthesis and respiration. However, as optimal acclimation is assumed, the impact of ROS production in the mitochondria might be just a minor factor influencing sugar balance in the cytosol.

In addition to its role as precursor for glycolysis, glucose was shown to have an impact on heat tolerance (Sharma et al., 2019; Wang et al., 2025). *Arabidopsis* seedlings that were grown on glucose-rich medium exhibited higher thermotolerance due to transcriptional regulation by glucose (Sharma et al., 2019). In tomato, external application of glucose led to high apoplastic glucose concentration, resulting in increased thermotolerance due to glucose signalling (Wang et al., 2024). A glucose G protein signalling pathway was shown to contribute to thermotoler-

ance and thermomemory regulation by increasing photosynthesis and photorespiration (Wang et al., 2024). However, it is unclear which concentrations of glucose are required and present in the apoplast for this. This further stresses the apparent complexity of the carbohydrate metabolism and its influence on processes like signalling, organic acid, protein and lipid production. The connectivity of the described processes adds another layer of intricacy to the network that this work aimed to elucidate a little further.

4.3. Conclusion and future perspectives

Future studies might resolve the interplay between cytosolic sugar concentrations and mitochondrial hexokinase function, as well as the consequences for the energy balance within the cell. The mitochondrial part of the proposed heat response, as well as the metabolic interplay between source and sink tissue, emerged as topics for future research projects. With the techniques at our disposal, such as NAF coupled to mass spectrometry analysis (Fürtauer et al., 2019), or hydroponics growth for root analysis (Brauner et al., 2014), we can further contribute towards resolving the metabolic plant heat response. In addition, new discoveries emerge, such as the stark metabolic difference between old and young leaves of an *Arabidopsis* leaf rosette (Brodsky et al., 2025). This discovery opens up many new directions for future research and illustrates that with every new insight into a system, new questions will come forward.

The dataset of subcellular volume ratios that is presented here can support future studies in the model organism *Arabidopsis thaliana* by providing realistic estimations of subcellular architecture and volumetrics. Especially for determining enzymatic reaction kinetics, it was shown that exact sugar concentrations are crucial to accurately simulate inhibitory effects as well as substrate availability. Fourier polynomials illustrated non-linear dynamics and were utilised to develop a balance model that could track the carbon flux during a heat wave. This approach can be used for further research, especially concerning highly dynamic environments.

The carbohydrate metabolism is an important factor in plant heat response. It is crucial for plants to maintain the process of generating energy from light, even under adverse conditions. In summary, a model of metabolic regulation is proposed that contributes to acclimation to elevated temperatures in *Arabidopsis thaliana*. A change in subcellular sugar concentrations and a stabilisation in cytosolic enzyme activities is hypothesised to establish and maintain a balance between photosynthetic input and carbon flux through the system. Especially, the central role of sucrose metabolism for short and long term heat response was demonstrated.

This research and future findings will contribute to tackling the mounting challenges posed by progressing climate change. The knowledge of sucrose metabolism and its role in plant heat

response can be utilised to ultimately retain food security in the face of diminishing crop yields. Findings like those presented here can guide metabolic engineering efforts and give directions to further projects, both in fundamental and applied research.

5. Supplements

Supplementary Table I. Exemplary temperature data from Munich, Germany from 26. to 31. July 2020. Data source: https://www.timeanddate.com/weather/germany/munich/historic?month=7&year=2020, accessed 25.03.2022

Day	Time	Temperature
2020-07-26	00:20	15°C
2020-07-26	00:50	16°C
2020-07-26	01:20	15°C
2020-07-26	01:50	15°C
2020-07-26	02:50	15°C
2020-07-26	03:20	14°C
2020-07-26	03:50	16°C
2020-07-26	04:20	16°C
2020-07-26	04:50	15°C
2020-07-26	05:20	15°C
2020-07-26	05:50	16°C
2020-07-26	06:20	16°C
2020-07-26	06:50	16°C
2020-07-26	07:20	17°C
2020-07-26	07:50	17°C
2020-07-26	08:20	17°C
2020-07-26	08:50	16°C
2020-07-26	09:20	16°C
2020-07-26	09:50	16°C
2020-07-26	10:20	17°C
2020-07-26	10:50	17°C
2020-07-26	11:20	18°C
2020-07-26	11:50	19°C
2020-07-26	12:20	20°C
2020-07-26	12:50	20°C
2020-07-26	13:20	21°C
2020-07-26	13:50	22°C
2020-07-26	14:20	23°C
2020-07-26	14:50	23°C
2020-07-26	15:20	24°C
2020-07-26	16:20	24°C
2020-07-26	16:50	23°C
2020-07-26	17:20	21°C
2020-07-26	17:50	21°C
2020-07-26	18:20	20°C
2020-07-26	18:50	19°C
2020-07-26	19:20	20°C
2020-07-26	19:50	19°C
2020-07-26	20:20	18°C
2020-07-26	20:50	18°C
2020-07-26	21:20	17°C
2020-07-26	21:50	16°C
2020-07-26	22:20	16°C
2020-07-26	22:50	15°C
2020-07-26	23:20	14°C
2020-07-26	23:50	15°C
2020-07-27	00:20	14°C
2020-07-27	00:50	14°C
2020-07-27	01:20	14°C
2020-07-27	01:50	14°C

Day	Time	Temperature
2020-07-27	02:20	13°C
2020-07-27	02:50	13°C

Day	Time	Temperature
2020-07-27	03:20	13°C
2020-07-27	03:50	12°C
2020-07-27	04:20	11°C
2020-07-27	04:50	11°C
2020-07-27	05:20	10°C
2020-07-27	05:50	10°C
2020-07-27	06:20	10°C
2020-07-27	06:50	12°C
2020-07-27	07:20	14°C
2020-07-27	07:50	16°C
2020-07-27	08:20	18°C
2020-07-27	08:50	19°C
2020-07-27	09:20	19°C
2020-07-27	10:20	21°C
2020-07-27	10:50	22°C
2020-07-27	11:20	22°C
2020-07-27	11:50	23°C
2020-07-27	12:20	23°C
2020-07-27	12:50	24°C
2020-07-27	13:20	25°C
2020-07-27	13:50	25°C
2020-07-27	14:20	25°C
2020-07-27	14:50	26°C
2020-07-27	15:20	26°C
2020-07-27	15:50	27°C
2020-07-27	16:20	27°C
2020-07-27	16:50	27°C
2020-07-27	17:20	27°C

Day	Time	Temperature
2020-07-27	17:50	27°C
2020-07-27	18:20	28°C
2020-07-27	18:50	27°C
2020-07-27	19:20	26°C
2020-07-27	19:50	25°C
2020-07-27	20:20	25°C
2020-07-27	20:50	24°C
2020-07-27	21:20	20°C
2020-07-27	22:20	19°C
2020-07-27	22:50	20°C
2020-07-27	23:20	20°C
2020-07-27	23:50	18°C
2020-07-28	00:20	18°C
2020-07-28	00:50	16°C
2020-07-28	01:20	17°C
2020-07-28	01:50	16°C
2020-07-28	02:20	17°C
2020-07-28	02:50	16°C
2020-07-28	03:20	17°C
2020-07-28	03:50	17°C
2020-07-28	04:20	16°C
2020-07-28	04:50	17°C
2020-07-28	05:20	15°C
2020-07-28	05:50	15°C
2020-07-28	06:20	16°C
2020-07-28	06:50	18°C
2020-07-28	07:20	21°C
2020-07-28	07:50	23°C

Day	Time	Temperature
2020-07-28	08:20	24°C
2020-07-28	08:50	25°C
2020-07-28	09:20	25°C
2020-07-28	10:20	27°C
2020-07-28	10:50	27°C
2020-07-28	11:20	27°C
2020-07-28	11:50	28°C
2020-07-28	12:20	28°C
2020-07-28	12:50	29°C
2020-07-28	13:20	29°C
2020-07-28	13:50	29°C
2020-07-28	14:20	29°C
2020-07-28	14:50	29°C
2020-07-28	15:20	28°C
2020-07-28	15:50	28°C
2020-07-28	16:20	27°C
2020-07-28	16:50	26°C
2020-07-28	17:20	25°C
2020-07-28	17:50	23°C
2020-07-28	18:20	24°C
2020-07-28	18:50	24°C
2020-07-28	19:20	24°C
2020-07-28	19:50	23°C
2020-07-28	20:20	22°C
2020-07-28	20:50	20°C
2020-07-28	21:20	20°C
2020-07-28	21:50	19°C
2020-07-28	22:20	19°C

Day	Time	Temperature
2020-07-28	22:50	19°C
2020-07-28	23:20	18°C
2020-07-28	23:50	19°C
2020-07-29	00:20	19°C
2020-07-29	00:50	19°C
2020-07-29	01:20	19°C
2020-07-29	01:50	18°C
2020-07-29	02:20	19°C
2020-07-29	02:50	16°C
2020-07-29	03:20	15°C
2020-07-29	03:50	16°C
2020-07-29	04:20	16°C
2020-07-29	04:50	16°C
2020-07-29	05:20	15°C
2020-07-29	05:50	15°C
2020-07-29	06:20	16°C
2020-07-29	06:50	16°C
2020-07-29	07:20	17°C
2020-07-29	07:50	18°C
2020-07-29	08:20	18°C
2020-07-29	08:50	19°C
2020-07-29	09:20	19°C
2020-07-29	09:50	20°C
2020-07-29	10:20	20°C
2020-07-29	10:50	21°C
2020-07-29	11:20	21°C
2020-07-29	11:50	22°C
2020-07-29	12:20	22°C

Day	Time	Temperature
2020-07-29	12:50	23°C
2020-07-29	13:20	23°C
2020-07-29	13:50	24°C
2020-07-29	14:20	24°C
2020-07-29	14:50	24°C
2020-07-29	15:20	25°C
2020-07-29	15:50	25°C
2020-07-29	16:20	24°C
2020-07-29	16:50	24°C
2020-07-29	17:20	24°C
2020-07-29	17:50	25°C
2020-07-29	18:20	25°C
2020-07-29	18:50	25°C
2020-07-29	19:20	25°C
2020-07-29	19:50	24°C
2020-07-29	20:20	23°C
2020-07-29	20:50	22°C
2020-07-29	21:20	19°C
2020-07-29	21:50	18°C
2020-07-29	22:20	16°C
2020-07-29	22:50	16°C
2020-07-29	23:20	17°C
2020-07-30	00:20	14°C
2020-07-30	00:50	14°C
2020-07-30	01:20	15°C
2020-07-30	01:50	15°C
2020-07-30	02:20	14°C
2020-07-30	02:50	14°C
2020-07-30	03:20	14°C
2020-07-30	03:50	13°C
2020-07-30	04:20	14°C
2020-07-30	04:50	13°C
2020-07-30	05:20	13°C
2020-07-30	05:50	13°C
2020-07-30	06:20	12°C
2020-07-30	06:50	14°C
2020-07-30	07:20	17°C
2020-07-30	07:50	18°C
2020-07-30	08:20	18°C
2020-07-30	08:50	19°C
2020-07-30	09:20	21°C
2020-07-30	09:50	22°C
2020-07-30	10:20	23°C
2020-07-30	10:50	23°C
2020-07-30	11:20	24°C
2020-07-30	11:50	25°C
2020-07-30	12:20	26°C
2020-07-30	12:50	26°C
2020-07-30	13:20	27°C
2020-07-30	13:50	27°C
2020-07-30	14:20	27°C
2020-07-30	14:50	27°C
2020-07-30	15:20	27°C
2020-07-30	15:50	28°C
2020-07-30	16:20	28°C
2020-07-30	16:50	29°C

Day	Time	Temperature
2020-07-30	17:20	29°C
2020-07-30	17:50	28°C
2020-07-30	18:20	28°C
2020-07-30	18:50	28°C
2020-07-30	19:20	27°C
2020-07-30	19:50	27°C
2020-07-30	20:20	26°C
2020-07-30	20:50	23°C
2020-07-30	21:20	22°C
2020-07-30	21:50	18°C
2020-07-30	22:20	18°C
2020-07-30	22:50	17°C
2020-07-30	23:20	16°C
2020-07-30	00:20	16°C
2020-07-30	00:50	17°C
2020-07-30	01:20	17°C
2020-07-30	01:50	17°C
2020-07-30	02:50	16°C
2020-07-30	03:20	16°C
2020-07-30	03:50	15°C
2020-07-30	04:20	14°C
2020-07-30	04:50	14°C
2020-07-30	05:20	15°C
2020-07-30	05:50	15°C
2020-07-30	06:20	16°C
2020-07-30	06:50	17°C
2020-07-30	07:20	18°C
2020-07-30	07:50	20°C

Day	Time	Temperature
2020-07-30	08:20	21°C
2020-07-30	08:50	22°C
2020-07-30	09:20	24°C
2020-07-30	10:20	25°C
2020-07-30	10:50	26°C
2020-07-30	11:20	27°C
2020-07-30	11:50	27°C
2020-07-30	12:20	28°C
2020-07-30	12:50	28°C
2020-07-30	13:20	29°C
2020-07-30	13:50	30°C
2020-07-30	14:20	30°C
2020-07-30	14:50	30°C
2020-07-30	15:20	30°C
2020-07-30	15:50	30°C
2020-07-30	16:20	31°C
2020-07-30	16:50	30°C
2020-07-30	17:20	30°C
2020-07-30	17:50	31°C
2020-07-30	18:20	31°C
2020-07-30	18:50	30°C
2020-07-30	19:20	30°C
2020-07-30	19:50	29°C
2020-07-30	20:20	27°C
2020-07-30	20:50	26°C
2020-07-30	21:20	23°C
2020-07-30	21:50	21°C
2020-07-30	22:20	20°C

Day	Time	Temperature
2020-07-30	22:50	20°C
2020-07-30	23:20	20°C
2020-07-30	23:50	19°C
2020-07-31	00:20	19°C
2020-07-31	00:50	19°C
2020-07-31	01:20	19°C
2020-07-31	01:50	18°C
2020-07-31	02:20	19°C
2020-07-31	02:50	16°C
2020-07-31	03:20	15°C
2020-07-31	03:50	16°C
2020-07-31	04:20	16°C
2020-07-31	04:50	16°C
2020-07-31	05:20	15°C
2020-07-31	05:50	15°C
2020-07-31	06:20	16°C
2020-07-31	06:50	17°C
2020-07-31	07:20	18°C
2020-07-31	07:50	20°C
2020-07-31	08:20	21°C
2020-07-31	08:50	22°C
2020-07-31	09:20	24°C
2020-07-31	10:20	25°C
2020-07-31	10:50	26°C
2020-07-31	11:20	27°C
2020-07-31	11:50	27°C
2020-07-31	12:20	28°C
2020-07-31	12:50	28°C
2020-07-31	13:20	29°C
2020-07-31	13:50	30°C
2020-07-31	14:20	30°C
2020-07-31	14:50	30°C
2020-07-31	15:20	30°C
2020-07-31	15:50	30°C
2020-07-31	16:20	31°C
2020-07-31	16:50	30°C
2020-07-31	17:20	30°C
2020-07-31	17:50	31°C
2020-07-31	18:20	31°C
2020-07-31	18:50	30°C
2020-07-31	19:20	30°C
2020-07-31	19:50	29°C
2020-07-31	20:20	27°C
2020-07-31	20:50	26°C
2020-07-31	21:20	23°C
2020-07-31	21:50	21°C
2020-07-31	22:20	20°C
2020-07-31	22:50	20°C
2020-07-31	23:20	20°C
2020-07-31	23:50	19°C

Bibliography

Adler, S. O., Kitashova, A., Bulovic, A., Nagele, T., & Klipp, E. (2025). Plant cold acclimation and its impact on sensitivity of carbohydrate metabolism. NPJ Syst Biol Appl, 11(1), 28.

Ahsan, N., Donnart, T., Nouri, M. Z., & Komatsu, S. (2010). Tissue-specific defense and thermo-adaptive mechanisms of soybean seedlings under heat stress revealed by proteomic approach. J Proteome Res, 9(8), 4189–204.

Ali, S., Rizwan, M., Arif, M. S., Ahmad, R., Hasanuzzaman, M., Ali, B., & Hussain, A. (2020). Approaches in enhancing thermotolerance in plants: An updated review. Journal of Plant Growth Regulation, 39(1), 456–480.

Allakhverdiev, S. I., Kreslavski, V. D., Klimov, V. V., Los, D. A., Carpentier, R., & Mohanty, P. (2008). Heat stress: an overview of molecular responses in photosynthesis. Photosynth Res, 98(1-3), 541–50.

Alom, M. Z., Taha, T. M., Yakopcic, C., Westberg, S., Sidike, P., Nasrin, M. S., Hasan, M., Van Essen, B. C., Awwal, A. A. S., & Asari, V. K. (2019). A state-of-the-art survey on deep learning theory and architectures. Electronics, 8(3).

Aluri, S., & Büttner, M. (2007). Identification and functional expression of the arabidopsis thaliana vacuolar glucose transporter 1 and its role in seed germination and flowering. PNAS, 104(7), 2537–2542.

Araguirang, G. E., Venn, B., Kelber, N. M., Feil, R., Lunn, J., Kleine, T., Leister, D., Muhlhaus, T., & Richter, A. S. (2024). Spliceosomal complex components are critical for adjusting the c:n balance during high-light acclimation. Plant J, 119(1), 153–175.

Archit, A., Freckmann, L., Nair, S., Khalid, N., Hilt, P., Rajashekar, V., Freitag, M., Teuber, C., Spitzner, M., Tapia Contreras, C., Buckley, G., von Haaren, S., Gupta, S., Grade, M., Wirth, M., Schneider, G., Dengel, A., Ahmed, S., & Pape, C. (2025). Segment anything for microscopy. Nat Methods, 22(3), 579–591.

Arkin, A., Ross, J., & McAdams, H. H. (1998). Stochastic kinetic analysis of developmental pathway bifurcation in phage λ-infected escherichia coli cells. Genetics, 149, 1633–1648.

Armstrong, A. F., Logan, D. C., Tobin, A. K., O'Toole, P., & Atkin, O. K. (2006). Heterogeneity of plant mitochondrial responses underpinning respiratory acclimation to the cold in arabidopsis thaliana leaves. Plant Cell Environ, 29(5), 940–9.

Arrivault, S., Guenther, M., Florian, A., Encke, B., Feil, R., Vosloh, D., Lunn, J. E., Sulpice, R., Fernie, A. R., Stitt, M., & Schulze, W. X. (2014). Dissecting the subcellular compartmentation of proteins and metabolites in arabidopsis leaves using non-aqueous fractionation. Mol Cell Proteomics, 13(9), 2246–59.

Arzac, M. I., Fernandez-Marin, B., & Garcia-Plazaola, J. I. (2022). More than just lipid balls: quantitative analysis of plastoglobule attributes and their stress-related responses. Planta, 255(3), 62.

Ashraf, M., & Harris, P. J. C. (2013). Photosynthesis under stressful environments: An overview. Photosynthetica, 51(2), 163–190.

Atanasov, V., Fürtauer, L., & Nägele, T. (2020). Indications for a central role of hexokinase activity in natural variation of heat acclimation in arabidopsis thaliana. Plants (Basel), 9(7).

Awasthi, R., Kaushal, N., Vadez, V., Turner, N. C., Berger, J., Siddique, K. H. M., & Nayyar, H. (2014). Individual and combined effects of transient drought and heat stress on carbon assimilation and seed filling in chickpea. Funct Plant Biol, 41(11), 1148–1167.

Barkan, A. (2011). Expression of plastid genes: organelle-specific elaborations on a prokaryotic scaffold. Plant Physiol, 155(4), 1520–32.

Basler, G., Fernie, A. R., & Nikoloski, Z. (2018). Advances in metabolic flux analysis toward genome-scale profiling of higher organisms. Biosci Rep, 38(6).

Bolouri-Moghaddam, M. R., Le Roy, K., Xiang, L., Rolland, F., & Van den Ende, W. (2010). Sugar signalling and antioxidant network connections in plant cells. FEBS J, 277(9), 2022–37.

Bouchekhima, A. N., Frigerio, L., & Kirkilionis, M. (2009). Geometric quantification of the plant endoplasmic reticulum. J Microsc, 234(2), 158–72.

Brauner, K., Hörmiller, I., Nägele, T., & Heyer, A. G. (2014). Exaggerated root respiration accounts for growth retardation in a starchless mutant ofarabidopsis thaliana. The Plant Journal, 79(1), 82–91.

Brodsky, V., Kerscher, A., Urban, M., & Nägele, T. (2025). Acclimation of carbon metabolism to a changing environment across a leaf rosette of arabidopsis thaliana. Plant Stress, 17.

Bräutigam, K., Dietzel, L., & Pfannschmidt, T. (2007). Plastid-nucleus communication: anterograde and retrograde signalling in the development and function of plastids, vol. 19 of Topics in Current Genetics, (pp. 409–455). Berlin, Heidelberg: Springer.

Bréhélin, C., & Kessler, F. (2008). The plastoglobule: A bag full of lipid biochemistry tricks. Photochemistry and Photobiology, 84, 1388–1394.

Bukhov, N. G., Samson, G., & Carpentier, R. (2000). Nonphotosynthetic reduction of the intersystem electron transport chain of chloroplasts following heat stress. steady-state rate. Photochemistry and Photobiology, 72(3), 351–357.

Bukhov, N. G., Wiese, C., Neimanis, S., & Heber, U. (1999). Heat sensitivity of chloroplasts and leaves: Leakage of protons from thylakoids and reversible activation of cyclic electron transport. Photosynthesis Research, 59, 81–93.

Camacho-Pereira, J., Meyer, L. E., Machado, L. B., Oliveira, M. F., & Galina, A. (2009). Reactive oxygen species production by potato tuber mitochondria is modulated by mitochondrially bound hexokinase activity. Plant Physiol, 149(2), 1099–110.

Cheng, J., Arystanbek Kyzy, M., Heide, A., Khan, A., Lehmann, M., Schroder, L., Nagele, T., Pommerrenig, B., Keller, I., & Neuhaus, H. E. (2024). Senescence-associated sugar transporter1 affects developmental master regulators and controls senescence in arabidopsis. Plant Physiol, 196(4), 2749–2767.

Cheung, C. Y., Poolman, M. G., Fell, D. A., Ratcliffe, R. G., & Sweetlove, L. J. (2014). A diel flux balance model captures interactions between light and dark metabolism during day-night cycles in c3 and crassulacean acid metabolism leaves. Plant Physiol, 165(2), 917–929.

Chowdhury, N. B., Simons-Senftle, M., Decouard, B., Quillere, I., Rigault, M., Sajeevan, K. A., Acharya, B., Chowdhury, R., Hirel, B., Dellagi, A., Maranas, C., & Saha, R. (2023). A multi-organ maize metabolic model connects temperature stress with energy production and reducing power generation. iScience, 26(12), 108400.

Cook, A. M., Rezende, E. L., Petrou, K., & Leigh, A. (2024). Beyond a single temperature threshold: Applying a cumulative thermal stress framework to plant heat tolerance. Ecol Lett, 27(3), e14416.

Crafts-Brandner, S. J., & Salvucci, M. E. (2000). Rubisco activase constrains the photosynthetic potential of leaves at high temperature and co2. Proc Natl Acad Sci U S A, 97(24), 13430–5.

Crafts-Brandner, S. J., van de Loo, F. J., & Salvucci, M. E. (1997). The two forms of ribulose-1,5-bisphosphate carboxylase/oxygenase activase differ in sensitivity to elevated temperature. Plant Physiol., 114, 439–444.

Crumpton-Taylor, M., Grandison, S., Png, K. M., Bushby, A. J., & Smith, A. M. (2012). Control of starch granule numbers in arabidopsis chloroplasts. Plant Physiol, 158(2), 905–16.

Distéfano, A. M., Bauer, V., Cascallares, M., López, G. A., Fiol, D. F., Zabaleta, E., & Pagnussat, G. C. (2024). Heat stress in plants: sensing, signalling and ferroptosis. J Exp Bot.

Dong, B., Zhang, P., Chen, X., Liu, L., Wang, Y., He, S., & Chen, R. (2011). Predicting housekeeping genes based on fourier analysis. PLoS One, 6(6), e21012.

Fang, X., Sastry, A., Mih, N., Kim, D., Tan, J., Yurkovich, J. T., Lloyd, C. J., Gao, Y., Yang, L., & Palsson, B. O. (2017). Global transcriptional regulatory network for escherichia coli robustly connects gene expression to transcription factor activities. Proc Natl Acad Sci U S A, 114(38), 10286–10291.

Firmansyah, & Argosubekti, N. (2020). A review of heat stress signaling in plants. IOP Conference Series: Earth and Environmental Science, 484(1).

Fürtauer, L., Küstner, L., Weckwerth, W., Heyer, A. G., & Nägele, T. (2019). Resolving subcellular plant metabolism. Plant J, 100(3), 438–455.

Fürtauer, L., Weckwerth, W., & Nägele, T. (2016). A benchtop fractionation procedure for subcellular analysis of the plant metabolome. Front Plant Sci, 7, 1912.

Gampe, D., Zscheischler, J., Reichstein, M., O'Sullivan, M., Smith, W. K., Sitch, S., & Buermann, W. (2021). Increasing impact of warm droughts on northern ecosystem productivity over recent decades. Nature Climate Change, 11(9), 772–779.

Garcia-Molina, A., Kleine, T., Schneider, K., Muhlhaus, T., Lehmann, M., & Leister, D. (2020). Translational components contribute to acclimation responses to high light, heat, and cold in arabidopsis. iScience, 23(7), 101331.

Geigenberger, P., Geiger, M., & Stitt, M. (1998). High-temperature perturbation of starch synthesis is attributable to inhibition of adp-glucose pyrophosphorylase by decreased levels of glycerate-3-phosphate in growing potato tubers. Plant Physiol., 117, 1307–1316.

Geigenberger, P., & Stitt, M. (1991). A "futile" cycle of sucrose synthesis and degradation is involved in regulating partitioning between sucrose, starch and respiration in cotyledons of germinating ricinus communis l. seedlings when phloem transport is inhibited. Planta, 185, 81–90.

Gerhardt, R., & Heldt, H. W. (1984). Measurement of subcellular metabolite levels in leaves by fractionation of freeze-stopped material in nonaqueous media. Plant Physiol., 75, 542–547.

Gounaris, K., Brain, A. P. R., Quinn, P. J., & Williams, W. P. (1983). Structural and functional changes associated with heat-induced phase-separations of non-bilayer lipids in chloroplast thylakoid membranes. FEBS Letters, 153(1), 47–52.

Gounaris, K., Brain, A. P. R., Quinn, P. J., & Williams, W. P. (1984). Structural reoganisation of chloroplast thylakoid membranes in response to heat-stress. Biochimica at Biophysica Acta, 766, 198–208.

Grigorova, B., Vassileva, V., Klimchuk, D., Vaseva, I., Demirevska, K., & Feller, U. (2012). Drought, high temperature, and their combination affect ultrastructure of chloroplasts and mitochondria in wheat (triticum aestivuml.) leaves. Journal of Plant Interactions, 7(3), 204–213.

Hannah, M. A., Wiese, D., Freund, S., Fiehn, O., Heyer, A. G., & Hincha, D. K. (2006). Natural genetic variation of freezing tolerance in arabidopsis. Plant Physiol, 142(1), 98–112.

Havaux, M. (1996). Short-term responses of photosystem i to heat stress. Photosynthesis Research, 47, 85–97.

Hedrich, R., Sauer, N., & Neuhaus, H. E. (2015). Sugar transport across the plant vacuolar membrane: nature and regulation of carrier proteins. Curr Opin Plant Biol, 25, 63–70.

Hernandez, J. S., Dziubek, D., Schröder, L., Seydel, C., Kitashova, A., Brodsky, V., & Nägele, T. (2023). Natural variation of temperature acclimation of arabidopsis thaliana. Physiol Plant, 175(6), e14106.

Hernandez, J. S., & Nägele, T. (2022). The trade-off function of photorespiration in a changing environment. in silico Plants, 5, 1–12.

Herrmann, H. A., Schwartz, J. M., & Johnson, G. N. (2019). Metabolic acclimation-a key to enhancing photosynthesis in changing environments? J Exp Bot, 70(12), 3043–3056.

Hincha, D. K., Sonnewald, U., Willmitzer, L., & Schmitt, J. M. (1996). The role of sugar accumulation in leaf frost hardiness — investigations with transgenic tobacco expressing a bacterial pyrophosphatase or a yeast invertase gene. Journal of Plant Physiology, 147(5), 604–610.

Hincha, D. K., Zuther, E., & Heyer, A. G. (2003). The preservation of liposomes by raffinose family oligosaccharides during drying is mediated by effects on fusion and lipid phase transitions. Biochim Biophys Acta, 1612(2), 172–7.

Hoermiller, I. I., Nägele, T., Augustin, H., Stutz, S., Weckwerth, W., & Heyer, A. G. (2017). Subcellular reprogramming of metabolism during cold acclimation in arabidopsis thaliana. Plant Cell Environ, 40(5), 602–610.

Huber, S. C., & Huber, J. L. (1996). ¡huber1996.pdf¿. Annu. Rev. Plant Physiol. Plant Mol. Biol., 47, 431–444.

Hurry, V. (2017). Metabolic reprogramming in response to cold stress is like real estate, it's all about location. Plant Cell Environ, 40(5), 599–601.

IPCC (2023). Climate Change 2023: Synthesis Report. Contribution of Working Groups I, II and III to the Sixth Assessment Report of the Intergovernmental Panel on Climate Change. Geneva, Switzerland.

Jacoby, R. P., Li, L., Huang, S., Pong Lee, C., Millar, A. H., & Taylor, N. L. (2012). Mitochondrial composition, function and stress response in plants. J Integr Plant Biol, 54(11), 887–906.

Jagadish, S. V. K. (2020). Heat stress during flowering in cereals - effects and adaptation strategies. New Phytol, 226(6), 1567–1572.

Janda, T., Tajti, J., Hamow, K. A., Marcek, T., Ivanovska, B., Szalai, G., Pal, M., Zalewska, E. D., & Darko, E. (2021). Acclimation of photosynthetic processes and metabolic responses to elevated temperatures in cereals. Physiol Plant, 171(2), 217–231.

Jiang, Z., Verhoeven, A., Li, Y., Geertsma, R., Sasidharan, R., & van Zanten, M. (2024). Deciphering acclimation to sublethal combined and sequential abiotic stresses in arabidopsis thaliana. Plant Physiol.

Jung, J.-H., Doomijan, M., Klose, C., Biswas, S., Ezer, D., Gao, M., Khattak, A. K., Box, M. S., Charoensawan, V., Cortijo, S., Kumar, M., Grant, A., Locke, J. C. W., Schäfer, E., Jaeger, K. E., & Wigge, P. A. (2016). Phytochromes function as thermosensors in arabidopsis. Science, 354(6314), 886–889.

Kadereit, J. W., Körner, C., Nick, P., & Sonnewald, U. (2021). Strasburger - Lehrbuch der Pflanzenwissenschaften. Berlin, Heidelberg: Springer Spektrum, 38 ed.

Kaplan, F., Kopka, J., Haskell, D. W., Zhao, W., Schiller, K. C., Gatzke, N., Sung, D. Y., & Guy, C. L. (2004). Exploring the temperature-stress metabolome of arabidopsis. Plant Physiol, 136(4), 4159–68.

Keller, I., & Neuhaus, H. E. (2025). Humboldt review: Function and characterization of sugar transport across plant membranes: History and perspectives. J Plant Physiol, 314, 154600.

Kirchhoff, H. (2013). Architectural switches in plant thylakoid membranes. Photosynth Res, 116(2-3), 481–7.

Kitashova, A., Adler, S. O., Richter, A. S., Eberlein, S., Dziubek, D., Klipp, E., & Nagele, T. (2023). Limitation of sucrose biosynthesis shapes carbon partitioning during plant cold acclimation. Plant Cell Environ, 46, 464–478.

Kitashova, A., Lehmann, M., Schwenkert, S., Munch, M., Leister, D., & Nagele, T. (2024). Insights into physiological roles of flavonoids in plant cold acclimation. Plant J, 120(5), 2269–2285.

Kitashova, A., Schneider, K., Fürtauer, L., Schröder, L., Scheibenbogen, T., Fürtauer, S., & Nägele, T. (2021). Impaired chloroplast positioning affects photosynthetic capacity and regulation of the central carbohydrate metabolism during cold acclimation. Photosynth Res, 147(1), 49–60.

Kleine, T., Nägele, T., Neuhaus, H. E., Schmitz-Linneweber, C., Fernie, A. R., Geigenberger, P., Grimm, B., Kaufmann, K., Klipp, E., Meurer, J., Mohlmann, T., Muhlhaus, T., Naranjo, B., Nickelsen, J., Richter, A., Ruwe, H., Schroda, M., Schwenkert, S., Trentmann, O., Willmund, F., Zoschke, R., & Leister, D. (2021). Acclimation in plants - the green hub consortium. Plant J, 106(1), 23–40.

Knaupp, M., Mishra, K. B., Nedbal, L., & Heyer, A. G. (2011). Evidence for a role of raffinose in stabilizing photosystem ii during freeze-thaw cycles. Planta, 234(3), 477–86.

Koffler, B. E., Bloem, E., Zellnig, G., & Zechmann, B. (2013). High resolution imaging of subcellular glutathione concentrations by quantitative immunoelectron microscopy in different leaf areas of arabidopsis. Micron, 45, 119–28.

Kohli, S. K., Khanna, K., Bhardwaj, R., Abd Allah, E. F., Ahmad, P., & Corpas, F. J. (2019). Assessment of subcellular ros and no metabolism in higher plants: Multifunctional signaling molecules. Antioxidants (Basel), 8(12).

Koini, M. A., Alvey, L., Allen, T., Tilley, C. A., Harberd, N. P., Whitelam, G. C., & Franklin, K. A. (2009). High temperature-mediated adaptations in plant architecture require the bhlh transcription factor pif4. Curr Biol, 19(5), 408–13.

Kottek, M., Grieser, J., Beck, C., Rudolph, B., & Rubel, F. (2006). World map of the köppen-geiger climate classification updated. Meteorologische Zeitschrift, 15(3), 259–263.

Kumar, A., Li, C., & Portis, J., A. R. (2009). Arabidopsis thaliana expressing a thermostable chimeric rubisco activase exhibits enhanced growth and higher rates of photosynthesis at moderately high temperatures. Photosynth Res, 100(3), 143–53.

Kumar, L., Chhogyel, N., Gopalakrishnan, T., Hasan, M. K., Jayasinghe, S. L., Kariyawasam, C. S., Kogo, B. K., & Ratnayake, S. (2022). Climate change and future of agri-food production, (pp. 49–79).

Kumar, S. V., Lucyshyn, D., Jaeger, K. E., Alos, E., Alvey, E., Harberd, N. P., & Wigge, P. A. (2012). Transcription factor pif4 controls the thermosensory activation of flowering. Nature, 484(7393), 242–245.

Law, D. R., & Crafts-Brandner, S. J. (1999). Inhibition and acclimation of photosynthesis to heat stress is closely correlated with activation of ribulose-1,5-bisphosphate carboxylase/oxygenase. Plant Physiology, 120, 173–181.

Leloir, L. F., & Cardini, C. E. (1955). The biosynthesis of sucrose phosphate. Journal of Biological Chemistry, 214(1), 157–165.

Li, Y., Smith, C., Corke, F., Zheng, L., Merali, Z., Ryden, P., Derbyshire, P., Waldron, K., & Bevan, M. W. (2007). Signaling from an altered cell wall to the nucleus mediates sugar-responsive growth and development in arabidopsis thaliana. Plant Cell, 19(8), 2500–15.

Li, Z., Palmer, W. M., Martin, A. P., Wang, R., Rainsford, F., Jin, Y., Patrick, J. W., Yang, Y., & Ruan, Y. L. (2012). High invertase activity in tomato reproductive organs correlates with enhanced sucrose import into, and heat tolerance of, young fruit. J Exp Bot, 63(3), 1155–66.

Linka, N., & Weber, A. P. (2010). Intracellular metabolite transporters in plants. Mol Plant, 3(1), 21–53.

Lippmann, R., Babben, S., Menger, A., Delker, C., & Quint, M. (2019). Development of wild and cultivated plants under global warming conditions. Curr Biol, 29(24), R1326–R1338.

Long, S. P. (1991). Modification of the response of photosynthetic productivity to rising temperature by atmospheric co2 concentrations: Has its importance been underestimated? Plant, Cell and Environment, 14, 729–739.

Lopatkin, A. J., & Collins, J. J. (2020). Predictive biology: modelling, understanding and harnessing microbial complexity. Nat Rev Microbiol, 18(9), 507–520.

Lunn, J. E. (2007). Compartmentation in plant metabolism. J Exp Bot, 58(1), 35–47.

Ma, D., Li, X., Guo, Y., Chu, J., Fang, S., Yan, C., Noel, J. P., & Liu, H. (2016). Cryptochrome 1 interacts with pif4 to regulate high temperature-mediated hypocotyl elongation in response to blue light. Proc Natl Acad Sci U S A, 113(1), 224–9.

Mangaravite, E., Vinson, C. C., de Almeida, E. L. M., & Williams, T. C. R. (2025). Genome-scale metabolic models in plant stress physiology: implications for future climate resilience. Plant Physiol, 199(2).

Mittler, R., Finka, A., & Goloubinoff, P. (2012). How do plants feel the heat? Trends Biochem Sci, 37(3), 118–25.

Morelli, R., Russo-Volpe, S., Bruno, N., & La Scalzo, R. (2003). Fenton-dependent damage to carbohydrates: Free radical scavenging activity of some simple sugars. Journal of Agricultural and Food Chemistry, 51(25), 7418–7425.

Møller, I. M., Rasmusson, A. G., & Van Aken, O. (2021). Plant mitochondria - past, present and future. Plant J, 108(4), 912–959.

Neuner, G., & Buchner, O. (2023). The dose makes the poison: The longer the heat lasts, the lower the temperature for functional impairment and damage. Environmental and Experimental Botany, 212.

Nägele, T. (2022). Metabolic regulation of subcellular sucrose cleavage inferred from quantitative analysis of metabolic functions. Quantitative Plant Biology, 3.

Nägele, T., Fürtauer, L., Nagler, M., Weiszmann, J., & Weckwerth, W. (2016). A strategy for functional interpretation of metabolomic time series data in context of metabolic network information. Front Mol Biosci, 3, 6.

Nägele, T., Henkel, S., Hörmiller, I., Sauter, T., Sawodny, O., Ederer, M., & Heyer, A. G. (2010). Mathematical modeling of the central carbohydrate metabolism in arabidopsis reveals a substantial regulatory influence of vacuolar invertase on whole plant carbon metabolism. Plant Physiol, 153(1), 260–72.

Nägele, T., & Heyer, A. G. (2013). Approximating subcellular organisation of carbohydrate metabolism during cold acclimation in different natural accessions of arabidopsis thaliana. New Phytol, 198(3), 777–787.

Nägele, T., Stutz, S., Hörmiller, I., & Heyer, A. G. (2012). Identification of a metabolic bottleneck for cold acclimation in arabidopsis thaliana. Plant J, 72(1), 102–14.

Nägele, T., & Weckwerth, W. (2012). Mathematical modeling of plant metabolism-from reconstruction to prediction. Metabolites, 2(3), 553–66.

Olas, J. J., Apelt, F., Annunziata, M. G., John, S., Richard, S. I., Gupta, S., Kragler, F., Balazadeh, S., & Mueller-Roeber, B. (2021). Primary carbohydrate metabolism genes participate in heat-stress memory at the shoot apical meristem of arabidopsis thaliana. Mol Plant, 14(9), 1508–1524.

Oyoshi, K., Katano, K., Yunose, M., & Suzuki, N. (2020). Memory of 5-min heat stress in arabidopsis thaliana. Plant Signal Behav, 15(8), 1778919.

Patzke, K., Prananingrum, P., Klemens, P. A. W., Trentmann, O., Rodrigues, C. M., Keller, I., Fernie, A. R., Geigenberger, P., Bolter, B., Lehmann, M., Schmitz-Esser, S., Pommerrenig, B., Haferkamp, I., & Neuhaus, H. E. (2019). The plastidic sugar transporter psut influences flowering and affects cold responses. Plant Physiol, 179(2), 569–587.

Paul, P., Mesihovic, A., Chaturvedi, P., Ghatak, A., Weckwerth, W., Bohmer, M., & Schleiff, E. (2020). Structural and functional heat stress responses of chloroplasts of arabidopsis thaliana. Genes (Basel), 11(6).

Pogson, B. J., Woo, N. S., Forster, B., & Small, I. D. (2008). Plastid signalling to the nucleus and beyond. Trends Plant Sci, 13(11), 602–9.

Pommerrenig, B., Ludewig, F., Cvetkovic, J., Trentmann, O., Klemens, P. A. W., & Neuhaus, H. E. (2018). In concert: Orchestrated changes in carbohydrate homeostasis are critical for plant abiotic stress tolerance. Plant Cell Physiol, 59(7), 1290–1299.

Poolman, M. G., Kundu, S., Shaw, R., & Fell, D. A. (2013). Responses to light intensity in a genome-scale model of rice metabolism. Plant Physiol, 162(2), 1060–72.

Poschet, G., Hannich, B., Raab, S., Jungkunz, I., Klemens, P. A., Krueger, S., Wic, S., Neuhaus, H. E., & Buttner, M. (2011). A novel arabidopsis vacuolar glucose exporter is involved in cellular sugar homeostasis and affects the composition of seed storage compounds. Plant Physiol, 157(4), 1664–76.

Poulet, A., Arganda-Carreras, I., Legland, D., Probst, A. V., Andrey, P., & Tatout, C. (2015). Nucleusj: an imagej plugin for quantifying 3d images of interphase nuclei. Bioinformatics, 31(7), 1144–6.

Prasch, C. M., & Sonnewald, U. (2013). Simultaneous application of heat, drought, and virus to arabidopsis plants reveals significant shifts in signaling networks. Plant Physiology, 162, 1849–1866.

Rao, X., & Liu, W. (2025). A guide to metabolic network modeling for plant biology. Plants (Basel), 14(3).

Reichelt, N., Korte, A., Krischke, M., Mueller, M. J., & Maag, D. (2023). Natural variation of warm temperature-induced raffinose accumulation identifies trehalose-6-phosphate synthase 1 as a modulator of thermotolerance. Plant Cell Environ, 46(11), 3392–3404.

Rhoads, D. M. (2011). Plant Mitochondrial Retrograde Regulation, vol. 1, chap. Chapter 16, (pp. 411–437). New York: Springer.

Ries, F., Gorlt, J., Kaiser, S., Scherer, V., Seydel, C., Nguyen, S., Klingl, A., Legen, J., Schmitz-Linneweber, C., Plaggenborg, H., Ng, J. Z. Y., Wiens, D., Hochberg, G. K. A., Raschle, M., Mohlmann, T., Scheuring, D., & Willmund, F. (2025). A truncated variant of the ribosome-associated trigger factor specifically contributes to plant chloroplast ribosome biogenesis. Nat Commun, 16(1), 629.

Rizhsky, L., Liang, H., Shuman, J., Shulaev, V., Davletova, S., & Mittler, R. (2004). When defense pathways collide. the response of arabidopsis to a combination of drought and heat stress. Plant Physiol, 134(4), 1683–96.

Rohwer, J. M. (2012). Kinetic modelling of plant metabolic pathways. J Exp Bot, 63(6), 2275–92.

Rolland, F., Baena-Gonzalez, E., & Sheen, J. (2006). Sugar sensing and signaling in plants: conserved and novel mechanisms. Annu Rev Plant Biol, 57, 675–709.

Ronneberger, O., Fischer, P., & Brox, T. (2015). U-Net: Convolutional Networks for Biomedical Image Segmentation, (pp. 234–241). Springer International Publishing.

Ruan, Y. L. (2014). Sucrose metabolism: gateway to diverse carbon use and sugar signaling. Annu Rev Plant Biol, 65, 33–67.

Ruelland, E., & Zachowski, A. (2010). How plants sense temperature. Environmental and Experimental Botany, 69(3), 225–232.

Salvucci, M., & Crafts-Brandner, S. J. (2004). Inhibition of photosynthesis by heat stress: the activation state of rubisco as a limiting factor in photosynthesis. Physiologica Plantarum, 120, 179–186.

Samtani, H., Sharma, A., Khurana, J. P., & Khurana, P. (2022). Thermosensing in plants: Deciphering the mechanisms involved in heat sensing and their role in thermoresponse and thermotolerance. Environmental and Experimental Botany, 203.

Scafaro, A. P., Fan, Y., Posch, B. C., Garcia, A., Coast, O., & Atkin, O. K. (2021). Responses of leaf respiration to heatwaves. Plant Cell Environ, 44(7), 2090–2101.

Schaber, J., Liebermeister, W., & Klipp, E. (2009). Nested uncertainties in biochemical models. IET Systems Biology, 3(1).

Seydel, C., Biener, J., Brodsky, V., Eberlein, S., & Nägele, T. (2022a). Predicting plant growth response under fluctuating temperature by carbon balance modelling. Commun Biol, 5(1), 164.

Seydel, C., Heß, M., Schröder, L., Klingl, A., & Nägele, T. (2025). Subcellular plant carbohydrate metabolism under elevated temperature. Plant Physiol.

Seydel, C., Kitashova, A., Fürtauer, L., & Nägele, T. (2022b). Temperature-induced dynamics of plant carbohydrate metabolism. Physiol Plant, 174(1), e13602.

Sharkey, T. D. (2005). Effects of moderate heat stress on photosynthesis: importance of thylakoid reactions, rubisco deactivation, reactive oxygen species, and thermotolerance provided by isoprene. Plant, Cell and Environment, 28, 269–277.

Sharma, A., Kumar, V., Shahzad, B., Ramakrishnan, M., Singh Sidhu, G. P., Bali, A. S., Handa, N., Kapoor, D., Yadav, P., Khanna, K., Bakshi, P., Rehman, A., Kohli, S. K., Khan, E. A., Parihar, R. D., Yuan, H., Thukral, A. K., Bhardwaj, R., & Zheng, B. (2020). Photosynthetic response of plants under different abiotic stresses: A review. Journal of Plant Growth Regulation, 39(2), 509–531.

Sharma, M., Banday, Z. Z., Shukla, B. N., & Laxmi, A. (2019). Glucose-regulated hlp1 acts as a key molecule in governing thermomemory. Plant Physiol, 180(2), 1081–1100.

Sharmin, S. A., Alam, I., Rahman, M. A., Kim, K. H., Kim, Y. G., & Lee, B. H. (2013). Mapping the leaf proteome of miscanthus sinensis and its application to the identification of heat-responsive proteins. Planta, 238(3), 459–74.

Shaw, R., & Cheung, C. Y. M. (2018). A dynamic multi-tissue flux balance model captures carbon and nitrogen metabolism and optimal resource partitioning during arabidopsis growth. Front Plant Sci, 9, 884.

Shomo, Z. D., Li, F., Smith, C. N., Edmonds, S. R., & Roston, R. L. (2024). From sensing to acclimation: The role of membrane lipid remodeling in plant responses to low temperatures. Plant Physiol, 196(3), 1737–1757.

Simons, M., Saha, R., Amiour, N., Kumar, A., Guillard, L., Clement, G., Miquel, M., Li, Z., Mouille, G., Lea, P. J., Hirel, B., & Maranas, C. D. (2014). Assessing the metabolic impact of nitrogen availability using a compartmentalized maize leaf genome-scale model. Plant Physiol, 166(3), 1659–74.

Slawinski, L., Israel, A., Paillot, C., Thibault, F., Cordaux, R., Atanassova, R., Dedaldechamp, F., & Laloi, M. (2021). Early response to dehydration six-like transporter family: Early origin in streptophytes and evolution in land plants. Front Plant Sci, 12, 681929.

Staehelin, L. A. (1986). Chloroplast Structure and Supramolecular Organization of Photosynthetic Membranes, chap. 1. Berlin Heidelberg: Springer-Verlag.

Stitt, M., Lilley, R. M., Gerhardt, R., & Heldt, H. W. (1989). Metabolite levels in specific cells and subcellular compartments of plant leaves. Methods in Enzymology, 174, 518–552.

Stitt, M., Lunn, J., & Usadel, B. (2010). Arabidopsis and primary photosynthetic metabolism - more than the icing on the cake. Plant J, 61(6), 1067–91.

Strand, A., Foyer, C. H., Gustafsson, P., GardestrÖM, P., & Hurry, V. (2003). Altering flux through the sucrose biosynthesis pathway in transgenic arabidopsis thaliana modifies photosynthetic acclimation at low temperatures and the development of freezing tolerance. Plant, Cell and Environment, 26(4), 523–535.

Sturm, A. (1999). Invertases. primary structures, functions, and roles in plant development and sucrose partitioning. Plant Physiology, 121, 1–7.

Sun, A. Z., & Guo, F. Q. (2016). Chloroplast retrograde regulation of heat stress responses in plants. Front Plant Sci, 7, 398.

Sweetlove, L. J., & Ratcliffe, R. G. (2011). Flux-balance modeling of plant metabolism. Front Plant Sci, 2, 38.

Sweetlove, L. J., Ratcliffe, R. G., & Fernie, A. R. (2025). Non-canonical plant metabolism. Nature Plants, 11(4), 696–708.

Szecowka, M., Heise, R., Tohge, T., Nunes-Nesi, A., Vosloh, D., Huege, J., Feil, R., Lunn, J., Nikoloski, Z., Stitt, M., Fernie, A. R., & Arrivault, S. (2013). Metabolic fluxes in an illuminated arabidopsis rosette. Plant Cell, 25(2), 694–714.

Thuiller, W., Lavorel, S., Araújo, M. B., Sykes, M. T., & Prentice, I. C. (2005). Climate change threats to plant diversity in europe. PNAS, 102(23), 8245–8250.

Tolleter, D., Smith, E. N., Dupont-Thibert, C., Uwizeye, C., Vile, D., Gloaguen, P., Falconet, D., Finazzi, G., Vandenbrouck, Y., & Curien, G. (2024). The arabidopsis leaf quantitative atlas: a cellular and subcellular mapping through unified data integration. Quantitative Plant Biology, 5.

Töpfer, N. (2021). Environment-coupled models of leaf metabolism. Biochem Soc Trans, 49(1), 119–129.

van Zanten, M., Voesenek, L. A., Peeters, A. J., & Millenaar, F. F. (2009). Hormone- and light-mediated regulation of heat-induced differential petiole growth in arabidopsis. Plant Physiol, 151(3), 1446–58.

Vargas, W. A., Pontis, H. G., & Salerno, G. L. (2008). New insights on sucrose metabolism: evidence for an active a/n-inv in chloroplasts uncovers a novel component of the intracellular carbon trafficking. Planta, 227(4), 795–807.

Vasseur, F., Pantin, F., & Vile, D. (2011). Changes in light intensity reveal a major role for carbon balance in arabidopsis responses to high temperature. Plant Cell Environ, 34(9), 1563–76.

Vicente, A. M., Manavski, N., Rohn, P. T., Schmid, L. M., Garcia-Molina, A., Leister, D., Seydel, C., Bellin, L., Mohlmann, T., Ammann, G., Kaiser, S., & Meurer, J. (2023). The plant cytosolic m(6)a rna methylome stabilizes photosynthesis in the cold. Plant Commun, 4(6), 100634.

Vile, D., Pervent, M., Belluau, M., Vasseur, F., Bresson, J., Muller, B., Granier, C., & Simonneau, T. (2012). Arabidopsis growth under prolonged high temperature and water deficit: independent or interactive effects? Plant Cell Environ, 35(4), 702–18.

Wahid, A., Farooq, M., Hussain, I., Rasheed, R., & Galani, S. (2012). Responses and Management of Heat Stress in Plants, chap. Chapter 6, (pp. 135–157).

Wahid, A., Gelani, S., Ashraf, M., & Foolad, M. (2007). Heat tolerance in plants: An overview. Environmental and Experimental Botany, 61(3), 199–223.

Wan, H., Wu, L., Yang, Y., Zhou, G., & Ruan, Y. L. (2018). Evolution of sucrose metabolism: The dichotomy of invertases and beyond. Trends Plant Sci, 23(2), 163–177.

Wang, D., Heckathorn, S. A., Barua, D., Joshi, P., Hamilton, E. W., & Lacroix, J. J. (2008). Effects of elevated co2 on the tolerance of photosynthesis to acute heat stress in c3, c4, and cam species. Am J Bot, 95(2), 165–76.

Wang, J., Kawocha, M. A., Liu, T., Liu, T., Guo, J., Hu, S., Liu, Y., Liu, S., Chen, L., Nie, B., & Song, B. (2025). Tonoplast sugar transporter sttst1 mediates vacuolar sugar partitioning and abiotic stress tolerance in potato. Plant Physiol Biochem, 229(Pt C), 110549.

Wang, J., Luo, Q., Liang, X., Liu, H., Wu, C., Fang, H., Zhang, X., Ding, S., Yu, J., & Shi, K. (2024). Glucose-g protein signaling plays a crucial role in tomato resilience to high temperature and elevated co2. Plant Physiol, 195(2), 1025–1037.

Wang, L., Bert, J. L., Okazawa, M., Paré, P. D., & Pinder, K. L. (1997). Fast fourier transform analysis of dynamic data: sine wave stress-strain analysis of biological tissue. Phys. Med. Biol., 42, 537–547.

Weiszmann, J., Furtauer, L., Weckwerth, W., & Nagele, T. (2018). Vacuolar sucrose cleavage prevents limitation of cytosolic carbohydrate metabolism and stabilizes photosynthesis under abiotic stress. FEBS J, 285(21), 4082–4098.

Wilczek, A. M., Cooper, M. D., Korves, T. M., & Schmitt, J. (2014). Lagging adaptation to warming climate in arabidopsis thaliana. Proc Natl Acad Sci U S A, 111(22), 7906–13.

Winter, H., Robinson, D. G., & Heldt, H. W. (1993). Subcellular volumes and metabolite concentrations in barley leaves. Planta, 191(2), 180–190.

Winter, H., Robinson, D. G., & Heldt, H. W. (1994). Subcellular volumes and metabolite concentrations in spinach leaves. Planta, 193, 530–535.

Wormit, A., Trentmann, O., Feifer, I., Lohr, C., Tjaden, J., Meyer, S., Schmidt, U., Martinoia, E., & Neuhaus, H. E. (2006). Molecular identification and physiological characterization of a novel monosaccharide transporter from arabidopsis involved in vacuolar sugar transport. Plant Cell, 18(12), 3476–90.

Wuyts, N., Palauqui, J.-C., Conejero, G., Verdeil, J.-L., Granier, C., & Massonnet, C. (2010). High-contrast three-dimensionalimaging of the arabidopsis leaf enables the analysis of cell dimensions in the epidermis and mesophyll. Plant Methods, 6(17).

Xalxo, R., Yadu, B., Chandra, J., Chandrakar, V., & Keshavkant, S. (2020). Alteration in Carbohydrate Metabolism Modulates Thermotolerance of Plant under Heat Stress, (pp. 77–115).

Xiang, L., Le Roy, K., Bolouri-Moghaddam, M. R., Vanhaecke, M., Lammens, W., Rolland, F., & Van den Ende, W. (2011). Exploring the neutral invertase-oxidative stress defence connection in arabidopsis thaliana. J Exp Bot, 62(11), 3849–62.

Yamada, K., Osakabe, Y., Mizoi, J., Nakashima, K., Fujita, Y., Shinozaki, K., & Yamaguchi-Shinozaki, K. (2010). Functional analysis of an arabidopsis thaliana abiotic stress-inducible facilitated diffusion transporter for monosaccharides. J Biol Chem, 285(2), 1138–46.

Yamori, W., Hikosaka, K., & Way, D. A. (2014). Temperature response of photosynthesis in c3, c4, and cam plants: temperature acclimation and temperature adaptation. Photosynth Res, 119(1-2), 101–17.

Zepner, L., Karrasch, P., Wiemann, F., & Bernard, L. (2020). Climatecharts.net – an interactive climate analysis web platform. International Journal of Digital Earth, 14(3), 338–356.

Zhang, J., Jiang, X. D., Li, T. L., & Cao, X. J. (2014). Photosynthesis and ultrastructure of photosynthetic apparatus in tomato leaves under elevated temperature. Photosynthetica, 52(3), 430–436.

Zhang, R., Wise, R. R., Struck, K. R., & Sharkey, T. D. (2010). Moderate heat stress of arabidopsis thaliana leaves causes chloroplast swelling and plastoglobule formation. Photosynth Res, 105(2), 123–34.

Zhu, L., Bloomfield, K. J., Hocart, C. H., Egerton, J. J. G., O'Sullivan, O. S., Penillard, A., Weerasinghe, L. K., & Atkin, O. K. (2018). Plasticity of photosynthetic heat tolerance in plants adapted to thermally contrasting biomes. Plant Cell Environ, 41(6), 1251–1262.

Zhu, L., Lan, J., Zhao, T., Li, M., & Ruan, Y. L. (2025). How vacuolar sugar transporters evolve and control cellular sugar homeostasis, organ development and crop yield. Nat Plants, 11(6), 1102–1115.

Zou, M., Yuan, L., Zhu, S., Liu, S., Ge, J., & Wang, C. (2017). Effects of heat stress on photosynthetic characteristics and chloroplast ultrastructure of a heat-sensitive and heat-tolerant cultivar of wucai (brassica campestris l.). Acta Physiologiae Plantarum, 39(1).

Zrimec, J., Correa, S., Zagorscak, M., Petek, M., Bleker, C., Stare, K., Schuy, C., Sonnewald, S., Gruden, K., & Nikoloski, Z. (2025). Evaluating plant growth-defense trade-offs by modeling the interaction between primary and secondary metabolism. Proc Natl Acad Sci U S A, 122(32), e2502160122.

Acknowledgements

This thesis could only exist due to the many people who were with me throughout the process. I am extremely grateful that I came all this way and even more so that I had the luck of not being alone.

I want to express my deepest gratitude to my doctoral supervisor, Prof. Dr. Thomas Nägele. Without his support and constant engagement, this thesis would not have been possible. I knew I could always rely on you - on a technical and on a personal level. Your support was constant and palpable, especially in the last months of the thesis. Your enthusiasm is a gift and I will always endeavour to keep up the excitement for science that you amplified in me.

My thanks also go to Prof. Dr. Andreas Klingl, who welcomed me into his lab and helped me with his expertise in the field of electron microscopy. He always gave me free rein to work at my own pace but was there if I needed help. Thank you for the support and opportunity over the last years. I never regretted coming to your lab and will always be thankful for the introduction into the marvellous world of electron microscopy.

Further, I want to express my gratitude to the members of the examination committee for taking the time to evaluate my work. Additionally, I want to thank Prof. Dr. Martin Heß, who helped me greatly in my thesis with the acquisition of the SBF-SEM datasets and Prof. Dr. Christof Osman, who was part of my thesis advisory committee. In the last months, I was additionally supported by Ulrike Zendel and Prof. Dr. Herwig Stibor, who took great care of my colleagues and me, and I am immensely grateful for this.

Without the endless support of Jennifer Grünert, I would have never succeeded with my work. She was always there, be it in the lab, where she taught me so much, or during our lunch breaks, all by ourselves or in large groups. I am so grateful to have such a funny, caring and capable colleague by my side.

I was also greatly supported by Cornelia Niemann and Dr. Katja Schneider, who shared a lot of their knowledge with me. Conny and Jenny taught me everything I know about sample preparation, whereas Katja showed me the ”Witze, Tipps und Tricks” of working with our TEM. The three of you encouraged me, made me feel at home in our group, and always were the perfect crowd for culinary excellence. Thank you!

I also want to thank my colleagues of AG Klingl, Julia Buchner, Andrea Cheradil and Isabella Gantner, for creating a happy and relaxed working environment. Special thanks go to Julia Buchner, who is a great office neighbour and who supported me with her expertise from day one. Also the temporary members of the group always contributed to the affectionate working

environment, I will not name all of you, but you were also part of this. Many thanks also go to my colleagues, old and new, from AG Nägele. Special thanks go to Dr. Lisa Fürtauer and Laura Schröder for teaching me NAF and showing me the ropes of the ”upstairs” lab, and to Dr. Anastasia Kitashova, Dr. Jakob Hernandez, Vladimir Brodsky, Bianca Süling and Sophia Bagshaw for the nice time we had in and out of the lab. I also want to thank Dr. Matthias Ostermeier and Nicolas Wendler, as they also did their part in making my days much more fun.

Outside of university, I was held and supported by a tight network of family and friends. I owe my passion for biology to my family, especially to my grandparents Armin and Ursula Kurth, who always took me for walks in the forest and educated me along the way, to my mother, Brigitte Seydel, who never fails to share her deep love and reverence for nature with me, and to my father Fabian Seydel, who instilled the love and fascination for natural science in me. Many thanks go to my siblings, parents and friends for always cheering me on, and who delved into fantastic worlds with me so I could start every day with a new dose of creativity and motivation.

Lastly, I want to thank the most important person in my life. My husband Philipp was there for me throughout the whole process. I could always be sure of his unwavering support and love. There is no need for more words here.